IEEE Recommended Practice for Inertial Sensor Test Equipment, Instrumentation, Data Acquisition, and Analysis

IEEE Aerospace and Electronic Systems Society

Sponsored by the
Gyro and Accelerometer Panel

1554™

IEEE
3 Park Avenue
New York, NY 10016-5997, USA

28 November 2005

IEEE Std 1554™-2005

Recognized as an
American National Standard (ANSI)

IEEE Std 1554™-2005

IEEE Recommended Practice for Inertial Sensor Test Equipment, Instrumentation, Data Acquisition, and Analysis

Sponsor

Gyro Accelerometer Panel Committee
of the
IEEE Aerospace and Electronic Systems Society

Approved 5 October 2005

American National Standards Institute

Approved 9 June 2005

IEEE-SA Standards Board

Abstract: Test equipment, data acquisition equipment, instrumentation, test facilities, and data analysis techniques used in inertial sensor testing are described in this recommended practice.
Keywords: data acquisition, data analysis techniques, gyro and accelerometer testing, inertial sensor testing, instrumentation, test equipment

The Institute of Electrical and Electronics Engineers, Inc.
3 Park Avenue, New York, NY 10016-5997, USA

Print: ISBN 0-7381-4738-9 SH95347
PDF: ISBN 0-7381-4739-7 SS95347

IEEE Standards documents are developed within the IEEE Societies and the Standards Coordinating Committees of the IEEE Standards Association (IEEE-SA) Standards Board. The IEEE develops its standards through a consensus development process, approved by the American National Standards Institute, which brings together volunteers representing varied viewpoints and interests to achieve the final product. Volunteers are not necessarily members of the Institute and serve without compensation. While the IEEE administers the process and establishes rules to promote fairness in the consensus development process, the IEEE does not independently evaluate, test, or verify the accuracy of any of the information contained in its standards.

Use of an IEEE Standard is wholly voluntary. The IEEE disclaims liability for any personal injury, property or other damage, of any nature whatsoever, whether special, indirect, consequential, or compensatory, directly or indirectly resulting from the publication, use of, or reliance upon this, or any other IEEE Standard document.

The IEEE does not warrant or represent the accuracy or content of the material contained herein, and expressly disclaims any express or implied warranty, including any implied warranty of merchantability or fitness for a specific purpose, or that the use of the material contained herein is free from patent infringement. IEEE Standards documents are supplied "**AS IS**."

The existence of an IEEE Standard does not imply that there are no other ways to produce, test, measure, purchase, market, or provide other goods and services related to the scope of the IEEE Standard. Furthermore, the viewpoint expressed at the time a standard is approved and issued is subject to change brought about through developments in the state of the art and comments received from users of the standard. Every IEEE Standard is subjected to review at least every five years for revision or reaffirmation. When a document is more than five years old and has not been reaffirmed, it is reasonable to conclude that its contents, although still of some value, do not wholly reflect the present state of the art. Users are cautioned to check to determine that they have the latest edition of any IEEE Standard.

In publishing and making this document available, the IEEE is not suggesting or rendering professional or other services for, or on behalf of, any person or entity. Nor is the IEEE undertaking to perform any duty owed by any other person or entity to another. Any person utilizing this, and any other IEEE Standards document, should rely upon the advice of a competent professional in determining the exercise of reasonable care in any given circumstances.

Interpretations: Occasionally questions may arise regarding the meaning of portions of standards as they relate to specific applications. When the need for interpretations is brought to the attention of IEEE, the Institute will initiate action to prepare appropriate responses. Since IEEE Standards represent a consensus of concerned interests, it is important to ensure that any interpretation has also received the concurrence of a balance of interests. For this reason, IEEE and the members of its societies and Standards Coordinating Committees are not able to provide an instant response to interpretation requests except in those cases where the matter has previously received formal consideration. At lectures, symposia, seminars, or educational courses, an individual presenting information on IEEE standards shall make it clear that his or her views should be considered the personal views of that individual rather than the formal position, explanation, or interpretation of the IEEE.

Comments for revision of IEEE Standards are welcome from any interested party, regardless of membership affiliation with IEEE. Suggestions for changes in documents should be in the form of a proposed change of text, together with appropriate supporting comments. Comments on standards and requests for interpretations should be addressed to:

Secretary, IEEE-SA Standards Board

445 Hoes Lane

Piscataway, NJ 08854

USA

NOTE—Attention is called to the possibility that implementation of this standard may require use of subject matter covered by patent rights. By publication of this standard, no position is taken with respect to the existence or validity of any patent rights in connection therewith. The IEEE shall not be responsible for identifying patents for which a license may be required by an IEEE standard or for conducting inquiries into the legal validity or scope of those patents that are brought to its attention.

Introduction

This introduction is not part of IEEE Std 1554-2005, IEEE Recommended Practice for Inertial Sensor Test Equipment, Instrumentation, Data Acquisition, and Analysis.

This document gives recommended practices for gyroscope and accelerometer testing and test data analysis. General and sensor specific equipment and instrumentation are described, including mounting fixtures, dividing heads and rotary test tables, vibration and shock machines, centrifuges, radiation test facilities, and thermal and other environmental chambers. Inertial sensor readouts, test control, data acquisition, filtering, and analysis are discussed. Analysis procedures include plotting, least-square polynomial and other fits, power spectral density and Allan variance noise analysis, and performance model parameter calibration estimation.

This recommended practice represents a consensus of manufacturers and users in industry, government agencies, and other interested groups. When necessary, the needs of the inertial sensor community have been given preference over general technical usage.

This recommended practice was prepared by the Gyro and Accelerometer Panel of the Aerospace Electronics System Society of the Institute of Electrical and Electronic Engineers. This document represents a group effort on a large scale. A total of 81 individuals attended 31 meetings of the Gyro and Accelerometer Panel while this standard was in preparation.

Notice to users

Errata

Errata, if any, for this and all other standards can be accessed at the following URL: http://standards.ieee.org/reading/ieee/updates/errata/index.html. Users are encouraged to check this URL for errata periodically.

Interpretations

Current interpretations can be accessed at the following URL: http://standards.ieee.org/reading/ieee/interp/index.html.

Patents

Attention is called to the possibility that implementation of this standard may require use of subject matter covered by patent rights. By publication of this standard, no position is taken with respect to the existence or validity of any patent rights in connection therewith. The IEEE shall not be responsible for identifying patents or patent applications for which a license may be required to implement an IEEE standard or for conducting inquiries into the legal validity or scope of those patents that are brought to its attention.

Participants

At the time this recommended practice was completed, the Gyro and Accelerometer Working Group had the following membership:

Randall Curey, *Chair*

Michael E. Ash
Cleon H. Barker
Stephen F. Becka
Sid Bennett
Stephen Bongiovanni
Pierre Bouniol
Tim Buck
Herbert T. Califano
A. T. Campbell
George W. Erickson
Yuri Filatov
Thomas A. Fuhrman
Kerry N. Green
Yoshiaki Hirobe
Tommy Ichinose
Jean-François Kieffer
Takashi Kunimi
Greg Lepore
Dmitri Loukianov
Bryan Lovitt
Jean Martel
Robert Moore
Harold D. Morris
Bart Morrow, Jr.
Charles Pearce
Rex B. Peters
Arkadii Sinelnikov
David Rozelle
Vladimir Skvortzov
Daniel Tazartes
Mohammad Tehrani
Leroy O. Thielman
Angelo Truncale
David J. Winkel
Bruce R. Youmans

The following individuals also contributed to the development of this recommended practice.

Jacques P. Govignon
Duane E. Larsen
Joseph A. Miola
Richard Spencer

The following members of the individual balloting committee voted on this guide. Balloters may have voted for approval, disapproval, or abstention.

Michael Ash
Cleon H. Barker
Sid Bennett
Keith Chow
Robert Correllus
Randall Curey
Robert Dahlgren
Jean-François Kieffer
Vladimir Skvortzov
Daniel Tazartes
Leroy O. Thielman
Bruce R. Youmans

When the IEEE-SA Standards Board approved this guide on 9 June 2005, it had the following membership:

Steve M. Mills, *Chair*
Richard H. Hulett, *Vice Chair*
Judith Gorman, *Secretary*

Mark D. Bowman
Dennis B. Brophy
Joseph Bruder
Richard Cox
Bob Davis
Julian Forster*
Joanna N. Guenin
Mark S. Halpin
Raymond Hapeman
William B. Hopf
Lowell G. Johnson
Herman Koch
Joseph L. Koepfinger*
David J. Law
Daleep C. Mohla
Paul Nikolich
T. W. Olsen
Glenn Parsons
Ronald C. Petersen
Gary S. Robinson
Frank Stone
Malcolm V. Thaden
Richard L. Townsend
Joe D. Watson
Howard L. Wolfman

*Member Emeritus

Also included are the following nonvoting IEEE-SA Standards Board liaisons:

Satish K. Aggarwal, *NRC Representative*
Richard DeBlasio, *DOE Representative*
Alan H. Cookson, *NIST Representative*

Jennie Steinhagen
IEEE Standards Project Editor

Contents

IEEE Recommended Practice for Inertial Sensor Test Equipment, Instrumentation, Data Acquisition, and Analysis

1. Overview

1.1 Scope

Recommended practices for gyroscope and accelerometer testing are discussed, ranging from the equipment and instrumentation employed to the way that tests are carried out and data are acquired and analyzed.

Normative references are given in Clause 2, and a bibliography is given in Annex A. Test planning is described in Clause 3. General equipment and sensor-specific equipment for testing gyroscopes and accelerometers are described in Clause 4 and Clause 5. Mounting fixtures, test piers, accelerometer dividing heads, and gyroscope rate tables are discussed in Clause 6, Clause 7, Clause 8, and Clause 9. Three-axis tables for inertial sensor assembly (ISA) testing are described in 9.4.

Vibration and shock equipment, centrifuges, and environmental chambers are described in Clause 10, Clause 11, and Clause 12. Nuclear radiation facilities are discussed in Clause 13. Special readout instrumentation required in gyroscope and accelerometer testing is discussed in Clause 14, Clause 15, Clause 16, and Clause 17. Such instrumentation includes counter and frequency readouts, analog-to-digital (A/D) conversion readouts, temperature monitoring, and other monitoring and commanding functions over various types of interfaces and buses.

Computer data acquisition, control, filtering, and storage are described in Clause 18. The analysis of test data is discussed in Clause 19. Such analysis includes the plotting of data channels versus time and other data channels, least-squares fits of polynomials and other models to data, power spectral density (PSD) and Allan variance noise analysis, and regression analysis and parameter estimation.

Geophysics instrumentation is discussed in Clause 20 because inertial sensors are tested on the earth, which provides seismic, tilt, and other disturbances, but also provides the fundamental gravity and earth rotation inputs against which sensor parameters (such as scale factor) are calibrated. Therefore, the acceleration due to gravity at a test site and the site latitude and longitude must be accurately determined.

The calibration of test site coordinates and gravity acceleration, the calibration of test station electrical and other equipment, and fundamental time and frequency references are discussed in Clause 21.

1.2 Purpose

This recommended practice is intended for people who test inertial sensors and analyze the results from such testing. The general and specialized test equipment employed in such testing is described, and recommendations are made on techniques for acquisition, filtering, storage, and analysis of the test data in keeping with modern practice.

2. Normative references

The following referenced documents are indispensable for the application of this recommended practice. For dated references, only the edition cited applies. For undated references, the latest edition of the referenced document (including any amendments or corrigenda) applies. In the event of any conflict, the recommended practices of this document shall have precedence over the documents listed in this clause.

2.1 IEEE standards

IEEE/ASTM SI 10, Standard for Use of the International System of Units (SI): The Modern Metric System.[1]

IEEE Std 260.1™, American National Standard Letter Symbols for Units of Measurement (SI Units, Customary Inch-Pound Units, and Certain Other Units). [2]

IEEE Std 292™, IEEE Specification Format for Single-Degree-of-Freedom Spring-Restrained Rate Gyros.

IEEE Std 293™, IEEE Test Procedure for Single-Degree-of-Freedom Spring-Restrained Gyros.

IEEE Std 315™, IEEE Standard Graphic Symbols for Electrical and Electronics Diagrams.

IEEE Std 517™, IEEE Standard Specification Format Guide and Test Procedure for Single-Degree-of-Freedom Rate-Integrating Gyros.

IEEE Std 528™, IEEE Standard for Inertial Sensor Terminology.

IEEE Std 529™, IEEE Supplement for Strapdown Applications to IEEE Standard Specification Format Guide and Test Procedure for Single-Degree-of-Freedom Rate-Integrating Gyros.

IEEE Std 647™, IEEE Standard Specification Format Guide and Test Procedure for Single-Axis Laser Gyros.

IEEE Std 671™, IEEE Standard Specification Format Guide and Test Procedure for Nongyroscopic Inertial Angular Sensors: Jerk, Acceleration, Velocity, and Displacement.

IEEE Std 813™, IEEE Specification Format Guide and Test Procedure for Two-Degree-of-Freedom Dynamically Tuned Gyros.

IEEE Std 836™, IEEE Recommended Practice for Precision Centrifuge Testing of Linear Accelerometers.

IEEE Std 952™, IEEE Standard Specification Format Guide and Test Procedure for Single-Axis Interferometric Fiber Optic Gyros.

[1]IEEE publications are available from the Institute of Electrical and Electronic Engineers, 445 Hoes Lane, Piscataway, NJ 08854, USA (http://www.standards.ieee.org).
[2]The IEEE standards or products referred to in this clause are trademarks of the Institute of Electrical and Electronics Engineers, Inc.

IEEE Std 1293™-1998, IEEE Standard Specification Format Guide and Test Procedures for Linear, Single-Axis, Non-Gyroscopic Accelerometers.

IEEE Std 1431™, IEEE Standard Specification Format Guide and Test Procedure for Coriolis Vibratory Gyros.

2.2 ISO standards

ISO 8568, Mechanical Shock — Testing machines — Characteristics and performance.[3]

ISO 16063 series, Methods for the calibration of vibration and shock transducers.

2.3 Nuclear radiation test standards

ASTM F 744M, Standard Test Method for Measuring Dose Rate Threshold for Upset of Digital Integrated Circuits (Metric).[4]

ASTM F 773M, Standard Practice for Measuring Dose Rate Response of Linear Integrated Circuits (Metric).

ASTM F 980M, Standard Guide for Measurement of Rapid Annealing of Neutron-Induced Displacement Damage in Silicon Semiconductor Devices (Metric).

ASTM F 1190, Standard Guide for Neutron Irradiation of Unbiased Electronic Components.

ASTM F 1192M, Standard Guide for the Measurement of Single Event Phenomena (SEP) Induced by Heavy Ion Irradiation of Semiconductor Devices (Metric).

ASTM F1262M-95, Standard Guide for Transient Radiation Upset Threshold of Digital Integrated Circuits.

ASTM F 1892, Standard Guide for Ionizing Radiation (Total Dose) Effects Testing of Semiconductor Devices.

ASTM F 1893, Standard Guide for Measurement of Ionizing Dose-Rate Burnout of Semiconductor Devices.

EIA JESD 57, Test Procedures for the Measurement of Single-Event Effects in Semiconductor Devices from Heavy Ion Irradiation.[5]

MIL-STD-750, Test Method Standard for Semiconductor Devices.[6]

MIL-STD-883E, Test Method Standard for Microcircuits.

[3]ISO publications are available from the ISO Central Secretariat, Case Postale 56, 1 rue de Varembé, CH-1211, Genève 20, Switzerland/ Suisse (http://www.iso.ch/). ISO publications are also available in the United States from the Sales Department, American National Standards Institute, 25 West 43rd Street, 4th Floor, New York, NY 10036, USA (http://www.ansi.org/).
[4]ASTM publications are available from the American Society for Testing and Materials, 100 Barr Harbor Drive, West Conshohocken, PA 19428-2959, USA (http://www.astm.org/).
[5]EIA publications are available from Global Engineering Documents, 15 Inverness Way East, Englewood, Colorado 80112, USA (http://global.ihs.com/).
[6]MIL publications are available from Customer Service, Defense Printing Service, 700 Robbins Ave., Bldg. 4D, Philadelphia, PA 19111-5094.

3. Test planning

3.1 Classification of tests

The inspection and testing of inertial sensors can be classified into the following categories:

a) *Characterization tests* and *evaluation tests*, performed on a device that is under development. *Requalification tests* to verify design changes. *Development tests* to design improved test methodologies and test equipment.

b) *Acceptance tests*, performed on production or repaired sensors submitted for acceptance under contract in environments expected to be encountered in the intended application.

c) *Diagnostic tests* and/or *anomaly investigation*, performed on devices that pass acceptance test procedures (ATP), but subsequently exhibit nontypical performance.

d) *Calibration tests*, such as for scale factor, bias, and misalignments, can be performed during acceptance testing and throughout the lifetime of the sensor at the inertial-navigation-system level as well as the individual-sensor level. Some parameters, such as temperature sensitivities and model nonlinearities, require factory calibration and may have to be valid for the lifetime of the sensor. Calibration of model parameters to be used in an inertial navigation mission is accomplished before a mission by estimating the parameters from data collected when the sensor is provided with known inputs, such as from tumbling in the earth's gravity field, slewing about various axes, or from vibration or centrifuge tests. Parameter calibration can also be accomplished during a mission using external aids to the inertial navigation system, such as from a radio navigation receiver or a star tracker, or during periods of zero velocity update when it is known that the inertial navigation system is stationary.

e) *Qualification tests*, performed on samples submitted for qualification as a satisfactory product. Qualification test environments may be more severe than environments used in acceptance testing because the purpose of qualification testing is to demonstrate design margin. Sensors that have undergone qualification testing are usually not considered mission-worthy.

f) *Reliability tests* and *life tests*, performed to demonstrate the level of reliability and mean time before failure (MTBF) and to assure the ability to maintain, with a certain confidence level, the required reliability. Accelerated reliability and life testing may involve environments more severe than environments encountered in operational use.

g) *Analysis*, a process used in lieu of or in addition to testing to verify compliance with specifications. The technique typically includes interpretation or interpolation/ extrapolation of analytical or empirical data under defined conditions or reasoning to show theoretical compliance with requirements.

3.2 Calibrated parameter characteristics

The variation in a gyroscope's angular rate bias or in an accelerometer's acceleration bias can be due to systematic effects, such as trend (due to such things as stress relaxation and magnetic decay) or environmental sensitivities, or to random effects, such as flicker noise or random walk. White process noise in bias does not cause changes in bias on average, but does cause angle random walk in gyroscope output or velocity random walk in accelerometer output, with a standard deviation that grows as the square root of time. The measurement and process noise in an inertial sensor's output can be determined by PSD and Allan variance analysis (see 19.5 through 19.9).

a) *Stability*. Calibration of bias, scale factor, input axis (IA) misalignment, and other inertial sensor model parameters over time determines

   1) *Short-term stability*, allowed variation over the duration time of a mission or over a specified segment of this duration time.

2) *Long-term stability*, allowed variation over the period from the last time a parameter is calibrated until it is used in a mission or over some defined time period if calibration occurs just prior to or during the first part of a mission.

b) *Repeatability*. Calibration of parameters before and after environmental excursions, such as vibration and shock, temperature cycle, radiation exposure, or turn-off and turn-on, determines

1) *Repeatability characteristics* of a parameter from before to after an environmental excursion, including the magnitude of any shift, the magnitude and time constant of any transient, and any change in trend from before to after the environmental excursion.

2) *Turn-on and warm-up characteristics* (magnitude and time constant) measured during a repeatability test across shutdown to ambient temperature and turn-on to operating temperature.

3) *Service life uncertainty* over the useful life of a sensor when periodically removed from storage conditions and measured at constant operating conditions (particularly important for those parameters that are calibrated only in the factory).

c) *Sensitivity*. Calibration of parameters at various temperature settings, magnetic fields, or other environmental states within the operating environment of the sensor determines sensitivity, which is the change in output or a parameter due to a change in an undesirable or secondary input. For example, a scale factor temperature sensitivity of a gyro or accelerometer is the change in scale factor due to a change in temperature.

The variation in a parameter over time and environmental variations after compensation with a calibrated model, such as for temperature, should be less than requirements. Normally, the variations are specified as 1-sigma in order to be able to root-sum-square their effects together. However, some other measure of allowed variation could be used, such as 2-sigma, 3-sigma, or maximum magnitude.

3.3 Test plan outline

Before performing a given class of tests on an inertial sensor, a test plan must be written. The overall table of contents for such a test plan could be as follows.

1) Overview (including description of sensor being tested and the types of tests)

2) References

3) Applicable documents (including contractual and performance and other specification documents)

4) Test conditions and equipment

5) Data acquisition equipment and software

6) Test procedures

7) Data analysis procedures

The IEEE standards listed in 2.1 describe the types of tests and the test procedures that are done on various types of gyroscopes and accelerometers. The remainder of this IEEE recommended practice describes the supporting facilities, equipment, and techniques for carrying out these tests and analyzing the results.

3.4 Test station log book

Each test station or series of tests should have a log book, where the test engineer or test technician notes the date, time, and information concerning events that occur during testing, such as

a) Calibration of test station equipment

b) Troubleshooting of problems

c) Test setup, test conditions (such as temperature or magnetic field), and test table orientation and/or angular rate

d) Start of a given test (namely, sensor serial number, type of test)

e) Name of the data acquisition file written by the data acquisition computer

f) Events that occur during a test, including changes in test conditions and test table orientation and/or angular rate

g) Termination of test

4. General equipment

4.1 Calibration of equipment

Test station equipment should be calibrated relative to primary standards periodically, such as once per year or at the start of a long test sequence (see Clause 21). This service could be provided by a calibration laboratory in a test organization as part of the total quality management effort of the organization.

4.2 Test station power supplies and grounds

There should be surge protection, regulation, and fuses or circuit breakers between the commercial ac electrical supply and the test station equipment. Fuses are a safety device to prevent a sensor under test from being damaged. In an expendable vehicle, such as a missile, fuses are usually not allowed because they provide an additional point of failure and because turning off a sensor is as bad as damaging it as far as completion of the mission is concerned.

An uninterruptable power supply (UPS) would keep a test running across momentary or long-duration power failures. An UPS could range from batteries charged by the commercial electrical supply to a large flywheel attached to a generator, where the flywheel is kept rotating by the commercial electrical supply or by, for example, a diesel engine if there is a commercial power failure.

Commercial equipment generally plugs into the commercial ac electrical supply outlets. Other devices and the inertial sensor under test could need special ac power supplies (such as for wheel motors) and dc power supplies (such as +5 V or ± 15 V; see Clause 5) that plug into ac outlets. These power supplies could be in an equipment rack adjacent to the test table if there are direct lines to the inertial sensor with acceptable cable wrap as the test table rotates. If there is continuous table rotation, then ac and dc power could go through slip rings. Alternatively, the ac and dc power supplies could be on the table top with the inertial sensor under test, with only the source power going through the slip rings.

Ground lines would go through slip rings. Power supply grounds should not share the same line as the grounds for the inertial sensor under test and other devices, such as thermistors. Ground lines should come to a common point, with ground loops avoided. There should be optical isolation between the data acquisition computer and the signals from the inertial sensor under test.

4.3 Time and frequency standard

When testing high-precision sensors, an inertial sensor test station should have an external frequency reference for timing interrupts and running counters because a data acquisition computer’s internal clock is inadequate.

The test station frequency reference could be a quartz crystal frequency standard, an embedded atomic clock, or a remotely located atomic clock whose output is piped into the test station. The quartz crystal

frequency standard, which could be on the table top with the inertial sensor under test, should be calibrated against an atomic standard before and/or after an experiment. The atomic clock could be kept close (within a few milliseconds) to the absolute time provided by a national time service radio broadcast (see 21.2).

For inertial sensor testing, the absolute value of time is not as important as is the precision and accuracy of the frequency reference. The absolute time of the start of a test should be noted within a few seconds accuracy, and the time of data points relative to the start of the test should be inferred from the count of data acquisition computer interrupts and the precise time between interrupts provided by the frequency standard.

An error in the frequency reference would directly affect the sensor scale factor measured in a test, namely, a ppm error in the frequency reference would, in general, cause a ppm error in a gyroscope or accelerometer scale factor measurement.

4.4 Precision voltage reference

The process of A/D or voltage-to-frequency conversion needs a precision voltage reference, which could be internal to a commercial device, such as a voltmeter, or could be a reference for the test station as a whole.

The accuracy of the precision voltage reference used in the readout of an inertial sensor, such as for an integrating voltmeter's reading of an analog-torque-loop voltage output or for controlling the height of a torque pulse in a digital torque loop, sets a limit on the measurement accuracy of an inertial sensor that needs such a reference in its readout.

The accuracy of a precision voltage source is typically no better than a ppm for nonsuper-conducting technology.

4.5 Voltmeters

A commercial integrating dc voltmeter can be used to measure the output of a torque-rebalance inertial sensor, where the dc voltage is integrated in the voltmeter for a given period of time, displayed on, for example, a seven-decimal-digit display, and output over a bus (such as IEEE 488™ [B6][7]) to the data acquisition computer (see 15.1). There is typically a dead zone between the end of one measurement and the start of the next, which could be undesirable for reading the primary output of an inertial sensor.

A simple rectifying ac voltmeter might be adequate for some applications. A true root-mean-square (rms) voltmeter may be called for when greater precision is required.

4.6 Ammeters and wattmeters

Commercial devices such as ammeters and wattmeters are less frequently used in inertial sensor performance testing, except for monitoring auxiliary signals, such as the power drawn by a mechanical gyro's wheel motor. The current through an inertial sensor's torquer is usually converted to a voltage by a precision resistor and read by an integrating voltmeter.

4.7 Resistance references

A reference resistor is used as a current-to-voltage conversion reference for the current output of an inertial sensor analog torque loop so the torque loop output can be read by a voltmeter. A solid-state temperature-to-current converter would also need a reference resistor to change its output to a voltage that can be read

[7]Numbers in brackets correspond to the numbers in the bibliography in Annex A.

by an A/D converter or voltmeter. Reference resistors are used in a bridge circuit for measuring the resistance of a thermistor or other such device whose resistance varies with temperature.

The performance of the bridge or current-to-voltage conversion circuit could be tested by replacing the thermistor or other such resistance by a decade resistance box, where desired resistances can be added together. The resistors in the decade box would need periodic calibration (see 4.1).

4.8 Magnetic field shielding

An inertial sensor under test could be covered with magnetic shielding for an experimental sensor that did not have such shielding. A production sensor would normally have magnetic shielding integrally designed into its case, if the sensor had magnetic sensitivities, so that the magnitude of the magnetic field seen in the application (such as from gimbal motors) multiplied by the magnetic sensitivity of the sensor after attenuation by the magnetic shielding is less than requirements.

Magnetic shielding is provided by an appropriate thickness of a material such as μ-metal, which will attenuate magnetic fields from penetrating into the interior it surrounds. Care must be taken to have shielding overlap areas where wires, etc., penetrate into the interior of the sensor.

4.9 Magnetic field generation and measurement

Magnetic sensitivity measurements of an inertial sensor involve placing a Helmholtz coil around the device. The Helmholtz coils have cylindrical symmetry to generate a uniform magnetic field within the cylinder. Structural support for the coils is provided by wooden or other such nonmagnetic framework.

With the sensor not in the coil, current is put through the coil, and the resulting magnetic induction strength within the coil is measured with a commercial Gauss meter (or with a magnetometer for low magnetic fields). Then the inertial sensor is placed within the coil, and the desired magnetic field is generated by putting appropriate current through the coils.

The magnetic induction levels would be of the order of the levels to be encountered in a mission, such as from nearby gimbal motors and from the 5 mT magnetic induction[8] from the earth's magnetic field; or they could be larger to amplify effects. An example magnetic induction sensitivity test schedule is

0, +50, +100, +50, 0, –50, –100, –50, 0 mT

If the inertial sensor were in a fixed orientation, such as IA vertical, while the magnetic field was varied, then a lumped bias and scale factor magnetic sensitivity would be measured by fitting a linear or higher order polynomial in magnetic induction strength to the inertial sensor output. Orienting an accelerometer IA up and down or rotating a gyroscope at various rates about IA at each magnetic induction level would allow the bias and scale factor magnetic sensitivities to be separated if the magnetic field were kept at a constant orientation relative to the inertial sensor axes during sensor reorientations.

4.10 Frequency synthesizers

Some readout systems read a frequency output from an inertial sensor (see 4.15). A commercial frequency synthesizer can be used to test such a readout scheme by generating a sinusoid or square wave at a specified frequency to determine whether the readout measures that frequency.

The frequency generated is more precise if an external frequency reference, such as a 10 MHz atomic standard, is input to the frequency synthesizer, rather than using the internal frequency reference within the frequency synthesizer.

[8] 0.5 Gauss.

4.11 Oscilloscopes

An oscilloscope is a useful tool for looking at inertial sensor test points for debugging purposes. An A/D converter reads the voltages in electrical waveforms and plots the waveforms on a screen versus time or versus each other. The plot can scroll off the screen as time progresses, or it can be repeated on the screen at a specified repetition frequency, which can be adjusted to match the repetition frequency of the signal so that slowly varying changes relative to the repetition frequency can become apparent on the screen.

4.12 Spectrum analyzer

There are commercial spectrum analyzers that will compute the frequency spectrum of a voltage waveform or a digital input. The same can be accomplished by acquiring the signal and passing it through the analysis software described in 19.5 if appropriate data acquisition and analysis hardware and software have been set up for inertial sensor testing.

4.13 Signal analyzer

A signal analyzer is a commercial piece of equipment that calculates the transfer function from one signal to another. The same can be accomplished by acquiring the signals and passing them through the cross PSD analysis mentioned in 19.10.2.

4.14 Voltage- or current-to-frequency converters

If a voltage or current is integrated and the accumulated value is converted to a square wave for which the time between rising edges represents a given increment of voltage or current integral, then the measurement of the frequency of the square wave gives a measure of the voltage or current, averaged over the acquisition interval. This can be a very elegant way of accurately measuring voltage or current, especially in inertial sensor testing that is interested in time integrals because frequency or period can be measured very accurately (see 4.15).

Commercial voltage- or current-to-frequency converters are available. However, the accuracy often required in inertial sensor testing is such that a specially built piece of equipment is likely required (see 15.3).

4.15 Frequency counters

There are commercial frequency counters that take a square or sinusoidal wave input and then output the frequency of the wave in its display or, for example, over the IEEE 488 bus. Such a device needs a timing reference, which can be either internally generated or from an external source. The latter option can provide greater accuracy than that obtained with an internally generated quartz crystal reference, especially when an atomic clock is used.

The frequency f_{in} of an input signal is typically determined by counting the number M of clock cycles for a given number N of rising edges of the input signal. The frequency of the input signal is

$$f_{in} = \frac{N}{M} \times f_{clk} \quad \text{Hz}, \tag{1}$$

where

f_{clk} is the clock frequency (Hz)
M is much greater than N

The quantization error in this measurement arises from the fractional timing pulse that is not counted at the rising edge interrupt. The quantization error decreases linearly with the number *N* of input rising edges that are measured. Some commercial frequency counters increase the resolution of a timing pulse by charging a capacitor at the moment of a rising edge interrupt until the next or second next rising clock edge. The fractional pulse missed in the counter is determined from the voltage on the capacitor.

A commercial frequency counter will often have a dead band between measurements made every few seconds. Coherency is thereby lost from one measurement to the next. In order to retain this coherency, which can be important for inertial sensor testing, continuous counter readouts are desirable, probably as a specially built piece of equipment (see Clause 14).

4.16 Temperature controllers

Temperature control of an inertial sensor itself would be provided by manufacturer-supplied electronics (see Clause 5).

If the inertial sensor were mounted on a thermally controlled mounting flange (see 6.2) or in a thermally controlled oven (see Clause 12), then commercial temperature control electronics would be required. The thermal controller would put current through heater strips or thermoelectric heater-coolers or command the flow of refrigerant to maintain temperature at a given set point, as monitored by a thermistor or other such device (see 4.17).

Care must be taken that the electric current that controls the temperature of an oven or mounting fixture does not interfere with the performance of the inertial sensor through self heating, electrical or magnetic interference, or other mechanisms. Such interference could more likely occur with a bang-bang rather than proportional controller.

4.17 Temperature-monitoring equipment

Temperature sensors can be placed on or within an inertial sensor, on a mounting fixture, or in electronics enclosures or exposed to the laboratory air. These temperature sensors should have good thermal contact with the parts whose temperatures are being monitored. One such solid-state temperature-sensing device has a current output that is proportional to the temperature. Another commercially available temperature-monitoring device is a quartz crystal oscillator whose frequency varies with temperature.

Another temperature sensor is a thermistor or platinum resistor, whose resistance varies with temperature. Hence, a small current has to flow through the device in order to measure the resistance with a bridge circuit. The bridge could be at a certain set point, with temperature variations around that set point creating a voltage output that can be read by a data acquisition computer's A/D converter. Because a thermistor's resistance is a nonlinear function of temperature, a look-up table or model is required to determine the temperature from the output voltage. For small temperature variations around the set point, a linear scale factor can be used.

Care must be taken that the current flowing through a temperature-monitoring device does not interfere with the performance of the inertial sensor. Some inertial sensors have an output signal that can measure temperature for compensation and/or control, independent of the primary output of the sensor that measures inertial input (angle change for a gyro or nongravitational acceleration for an accelerometer).

4.18 Bubble levels and tilt meters

A precision bubble level read by eye can be used in aligning a test fixture relative to the local vertical to within a few arcseconds (see 8.4).

A tilt meter measures the small deviation from horizontal as well as the horizontal acceleration. It has an electrical output that can be read by a data acquisition computer. Outputs below 0.1 Hz are normally considered to be due to tilt, whereas outputs above 0.1 Hz are normally considered to be due to horizontal acceleration. Examples of tilt meters are an electronically read bubble level or a pendulous device. A pendulous tilt meter that can measure large angular deviations is called an *inclinometer*.

Tilt angles are usually measured as rotations about east and rotations about north. The scale factor of the voltage output from a tilt meter can be calibrated by rotating the tilt meter a known angle from the horizontal (see 21.5). Measured tilt variations during an inertial sensor test can be used to compensate gyroscope output for motion of the gyro IA relative to the earth's rotation vector and to compensate accelerometer output for motion of the accelerometer IA relative to the local vertical.

An accelerometer with IA nearly horizontal can be used to measure tilt variations. Tilt variations during an accelerometer tumble test as well as angle setting errors can be compensated using dual orthogonal accelerometers (see Annex K of IEEE Std 1293-1998[9]).

4.19 Autocollimator

An autocollimator is an optical measurement system that measures the deviation angle of a fixture or a test assembly. A reflective mirror is attached to the item to be aligned, and the deviation between the primary and reflected image is measured using collimated light.

A plane mirror allows measurement of angular deviation in two directions. A porro prism with two orthogonal reflectors restricts measurement to deviation about one axis, but facilitates alignment about this axis because of insensitivity to misalignments in the orthogonal direction.

4.20 Displacement measurement systems

4.20.1 Capacitive

Capacitive displacement sensing can be accomplished with atomic-dimension precision for small gaps, for example, in inertial sensors themselves.

For micro- and macro-sized accelerometers, capacitive sensing is often used as the pickoff of proof mass motion, where the measure of acceleration is the proof mass displacement against an elastic restraint or it is the force or torque required to restore the proof mass to the null position relative to the case. See F.2.4 of IEEE Std 1293-1998 for a discussion of capacitive pickoffs in silicon chip accelerometers.

For spinning wheel gyroscopes, the movement of the spinning wheel relative to the case is often measured capacitively (electromagnetic and optical pickoffs are also used for gyroscopes and accelerometers). For a rate gyro, this movement against an elastic restraint is the measure of input angular rate. Other implementations restore the spinning wheel to a null position relative to the case by torquing the gyro (where the integral of the torque is the measure of angular displacement) or by torquing gimbals of the platform in which the gyro resides (to keep the platform inertially oriented).

Capacitive displacement sensing is also used in micro- and macro-sized Coriolis Vibratory Gyros for measuring vibration amplitudes and the out-of-vibration-direction motions that are the measure of input angular rate in these devices. These out-of-vibration-direction motions are just observed in an open-loop device, but suppressed in a closed-loop device.

For an example of capacitive displacement sensing in inertial sensor test equipment, see 11.5.2.2 on measuring centrifuge arm stretch.

[9]Information on references can be found in Clause 2.

4.20.2 Laser interferometer

Laser interferometry can be used to check the flatness of planar surfaces or the radius of curvature of spherical surfaces. Laser interferometry is also widely used to measure displacements of components in the direction of a collimated laser beam. The phase of the light reflected by a reflector attached to the component is compared in the interferometer to the phase of the light emitted by the laser, and relative displacement is deduced. Precision of the order of a fraction of the wavelength of light can be obtained in this manner.

A coordinate measurement machine (CMM) can be built by using three interferometers having mutually orthogonal beams. Another way of creating a precision CMM for measuring large components is to use a laser tracker. A laser tracker is composed of an electronic distance measurement (EDM) using a laser beam in the same optical head of a tracking theodolite. A corner cube retroreflector is moved over the surface of the component to be measured. The tracking theodolite measures angles, and the EDM provides the third dimension. Commercial distance measurement interferometers and laser trackers are available.

Environment affects interferometric measurements because the quantity measured is in fact the optical distance traveled by light, namely, $n \times d$, the product of the index of refraction n of the media in which light is traveling (air in general) and the actual distance d. The index n is a function of air composition (including humidity level), temperature, and pressure. For highly precise measurements, environment monitors have to be used to compensate for changes in environment factors. Shielding protection against transient air currents or averaging may also have to be used, although averaging reduces the measurement bandwidth.

4.20.3 Fiber-optic probe

Two classes of fiber-optics-based sensors can be used to monitor displacements.

The first class is based on deformation of somewhat straight fiber-optics embedded or rigidly attached to a large component. It is assumed that fiber deformation reproduces the component deformation of interest. The fiber-optics probe has to be judiciously located within or on the surface of the component, usually in conjunction with creating a structural model of the component. The model is also useful for interpreting the results. Deformation of the fiber is sensed by measuring the phase of coherent laser light traveling in the fiber probe. This sensing technique is somewhat akin to extensometry (namely, measurement of stress or differential elongation).

In the second class of fiber sensor, displacement is measured between the end of the probe and a reflective component closely located in front of the probe end. The sensing is based on the amount of light reflected back into the probe. This kind of sensor has a short distance range, but is very useful for vibration measurements.

4.21 Other general commercial equipment

It is often useful to measure the barometric pressure, relative humidity, and air temperature in the test laboratory. Commercial instrumentation for accomplishing these functions can have output on circular strip chart recorders or, more usefully, as voltage variations proportional to environmental changes that are input to the data acquisition computer.

Microscopes are used to examine silicon chip inertial sensors. A stroboscope can freeze the observed motion of vibrating elements.

4.22 Specially built equipment

Test equipment should be bought if possible as commercial-off-the-shelf (COTS) procurements. Readout of the primary output of an inertial sensor is one area where precise enough commercial equipment is often not available. For instance, equipment such as voltage-to-frequency converters (see 4.14 and 15.3), continuous frequency counters (see 4.15 and 14.1), and phase-locked loops (PLLs) (see 14.4) must often be specially built.

5. Sensor-specific equipment

Inertial sensors require various power supplies, such as

a) Low-voltage dc supplies as required by the sensor, single-sided or bipolar, such as +5 V for transistor-transistor logic or ± 15 V for crystal oscillators. Devices with small feature sizes, such as computer chip central processing units (CPUs) or field-programmable gate arrays (FPGAs), use 3 V or lower voltages.

b) Voltage for analog torquer or for the digital torque pulse height.

c) Higher voltage ac power supplies for wheel motors (such as 70 V), magnetic or electrostatic suspensions, resolver readouts, etc.

d) High-voltage (~1000 V) dc supply for laser gyro excitation.

These various power supplies should be regulated to keep the voltage level constant (both at dc and at frequency bands of interest) in the face of variations in the external voltage from which they are derived. Care should be taken in the design so that the power supplies do not interfere with the performance of the inertial sensor.

In laboratory testing, the power supplies are derived from the electric utility supply (see 4.2). During a mission, the power supplies are derived from the vehicle's power supply, which could be a turbine generator or a battery with or without an alternator or generator charging system. Examples of vehicle battery power supplies that drive dc-dc converters to other voltage levels are

Automobiles:	12 V open circuit (14 V under charge)
Trucks:	24 V open circuit (28 V under charge)
New automotive:	36 V open circuit (42 V under charge)

A missile power supply might be a 28 V battery, where the voltage under load is greater than 28 V at the start of the mission and less than 28 V at the end of the mission.

The cable with power, grounds, input commands, and output signal lines is attached to an inertial sensor with a manufacturer-specific connector.

Output signals can go through control loop electronics to apply torque, control an oscillator, control temperature, etc. Some electronics, including buffer amplifiers and perhaps some control loops, are within the inertial sensor case. Other electronics can be contained in a rack separate from the inertial sensor, including any special readout electronics.

Although sometimes not possible, it is desirable to have mission-level control and other electronics used in instrument-level tests of an inertial sensor.

6. Mounting fixture

6.1 Fixture mechanical design

An inertial sensor to be tested is attached to a mounting fixture or block with bolts torqued to a specified level. Fixture materials should be selected with due consideration of thermal coefficients of expansion and conductivity, magnetic permeability, durability, etc., relative to the requirements of the sensor being tested. Hard-coated aluminum fixtures with stainless steel thread inserts meet many of these desirable characteristics. Stainless steel mounting bolts are often used because of their nonmagnetic characteristics.

The mounting fixture is then bolted to other test equipment, such as a dividing head, rate table, vibration and shock machine, or centrifuge arm. The parallelism and perpendicularity of the mounting faces to the other equipment and to the sensor or sensors under test should be within specified tolerances. An adapter plate might be required between the mounting fixture and the other equipment, with due consideration for the effects on alignment, parallelism, and mechanical resonances.

The mounting fixture might contain one inertial sensor or contain two or more sensors with IAs parallel or antiparallel in order to increase test productivity by testing several sensors simultaneously. Simultaneous sensor testing can also help distinguish between noise inherent to the individual sensors and noise from common seismic and other input.

Care must be taken to avoid sensor-to-sensor crosstalk, such as mechanical coupling through the mounting fixture, electronic coupling through a common power supply system, or electromagnetic coupling between closely spaced sensors or signal lines.

Orienting sensors in the mounting fixture with IAs orthogonal is used in accelerometer testing to allow compensation for dividing head angle-setting errors in tumble testing (see 8.4 and 19.13.2.1).

6.2 Thermal control of fixture

The mounting fixture might be thermally controlled, in which case a thermal shim or spacer might be required between the mounting fixture and the other equipment to which it is attached. A fixture that is temperature controlled as a whole could surround the sensor under test. If only the mounting flange is temperature controlled, the sensor could be covered with insulation so that the heat flow path from the sensor is through the mounting flange.

If the control set point is sufficiently above room temperature, thermal control can be accomplished with electric strip heaters. Alternatively, the mounting flange could be attached to Peltier thermoelectric heater-coolers, which have the property that electric current flowing in one direction heats one side and cools the other, and vice versa if the current direction is reversed. Thus the temperature control point can be well above or below room temperature, which allows temperature sensitivity testing over a wide temperature range. Water condensation should be avoided at the lower temperatures.

Temperature control of the mounting fixture may not be required if the fixture and sensor under test are inside a heated and/or refrigerated chamber (see 12.1.2 and 12.2).

6.3 Vibration fixture

The vibration fixture should be designed to not have any structural resonances near the resonance frequencies of the sensor under test. This requirement implies that the fixture be fairly massive. The vibration fixture could be made of aluminum or magnesium. The latter is better because magnesium has high internal damping.

The fixture would be tested for resonance frequencies by mounting a dummy mass on it and conducting a frequency sweep (see 10.2.6). The accelerometers used to monitor the vibration amplitude should be mounted in close proximity to the instrument under test to minimize fixture resonance effects. Piezoelectric accelerometers are commonly used for this purpose.

A vibration fixture should allow different orientations of the inertial sensor IA and other axes relative to the vibration axis.

6.4 Centrifuge fixture

Analogously to the vibration fixture, a centrifuge fixture should allow different orientations of the inertial sensor IA and other axes relative to the centrifuge arm, if required. The centrifuge fixture may have to accommodate the mounting of a second accelerometer that is used to measure arm stretch (see 11.5.2.1).

6.5 Radiation test fixture

Besides providing required thermal and other environments, a radiation test fixture has to be able to orient an inertial sensor appropriately relative to the radiation source and the local vertical. To accomplish various orientations, the fixture could be cantilevered off a rotary table with the inertial sensor and its proximity electronics in the radiation beam and with the rotary table and the inertial sensor's nonproximity electronics out of the beam. The nonproximity electronics could, in addition, be shielded if the effects of radiation on the sensor and its proximity electronics were being determined separately from the effects of radiation on the nonproximity electronics.

The test fixture could have a second shielded inertial sensor out of the radiation beam to allow simultaneous testing of exposed and shielded sensors. The subtraction of the data from IA-parallel sensors (or addition for IA-antiparallel sensors) eliminates the effects from the exposed sensor's data of seismic, tilt, and other nonradiation common-mode effects during the experiment. Faraday shielding on both the exposed and shielded sensors and electronics might be required if an electromagnetic pulse (EMP) in addition to a seismic pulse is generated by the radiation source that is not in the natural environment being simulated, such as when using an X-ray machine.

The shift and transient in an inertial sensor's output during and after a radiation exposure in a single orientation contains the lumped effects on bias and scale factor.

If the effects of radiation on an accelerometer's bias and scale factor are to be separated, data can be taken before, during, and after a radiation exposure of a given magnitude with IA up and then with IA down. The average of the data at comparable time points in the two time series gives the time history of bias before, during, and after the radiation exposure, whereas half the difference of the data gives a similar result for the scale factor.

Similarly, the effects of radiation on a gyroscope's bias and scale factor can be separated by taking the sum and difference of data taken when rotating the gyroscope in one direction during a radiation exposure and then in the opposite direction during a second radiation exposure at the same level (see 19.13.3.1).

The variation of radiation levels from one test to another can obfuscate the above-described calibrations of gyroscope and accelerometer bias and scale factor. However, if radiation effects are linear with dose, appropriate dosimeter instrumentation allows the scaling of the effects from one radiation exposure to another, even if the radiation level in each exposure cannot be well controlled.

7. Test piers

7.1 Location of test piers

A test laboratory should be in a location as seismically quiet as possible. A remote location is preferable to an urban location, although this preference is not always possible.

The upper floors of a building have a more severe vibration environment than the ground floor. Therefore, inertial sensor test laboratories should be on the ground floor or in a basement. Moreover, test tables within the laboratory should be on piers or pads isolated from the floor, to minimize the effect of tilt and other motions when testing high-precision inertial sensors. Depending on local geologic conditions, a massive concrete test pier could be resting in soil or go down to bedrock.

The vibration and tilt environment of a test table should be evaluated so that environmental effects can be accounted for in test data.

7.2 Vibration environment of test pier

An inertial instrument test station receives vibration input from local cultural activity and from the general seismic background of the earth. Seismic amplitudes tend to die out within a few hundred wavelengths, where the speed of sound in soil is of the order of a kilometer per second. The frequency spectrum of the vibration input depends on the particular site and whether it is in an urban or isolated location. It is generally above 1 Hz, possibly with discrete spikes due to resonances in the local geology and test table. Earthquake frequencies can be below 0.1 Hz.

Local cultural activity (such as automobile and other traffic, rotary equipment in the building in which the test station is housed, fans in test equipment, and even people walking by the test station) causes horizontal and vertical vibration inputs and lower frequency tilts. Effects can be amplified or damped by local geologic conditions, such as land fill over bed rock, where surface vibrations are reflected from the bed rock to cause constructive interference at certain frequencies and destructive interference at others.

The general seismic background of the earth includes such phenomenon as the vibrations from ocean waves striking the sea shore. The surface and solid body seismic waves from an earthquake thousands of kilometers away can cause disturbances in inertial instrument test data. The different modes of vibration have different arrival times because of differing paths through the earth and differing speeds of travel. There can be considerable ringing in the earth for several hours after an earthquake, in addition to the initial and after-shock disturbances.

Seismic input averages zero over the averaging time of many types of measurements, either as a natural consequence of the measurement system itself (such as low-rate counter readings) or because high-rate sampling followed by digital filtering is employed. But such averaging cannot eliminate all seismic aliasing and other corruption, such as from earthquakes, parking lot speed bumps, or construction pile drivers. Some tests, such as noise measurements, might require use of a site remote from the usual facility.

7.3 Tilt and azimuth motion of test pier

A test table on a pier or laboratory floor will have diurnal, seasonal, and long-term tilt variations relative to the local vertical due to temperature, solar heating, ground water, and other local geophysical effects. There could be several microradians of tilt variation over a day and tens of microradians of tilt variation over weeks.

The data from an IA vertical accelerometer test are insensitive to such tilt variations, whereas the data from off-vertical positions in a tumble test are sensitive to them. Tilt meters could be monitored during a test in order to correct the tumble test angle readings for tilt errors relative to the local vertical. Alternatively, the

analysis technique of orthogonal accelerometer tumble testing described in Annex K of IEEE Std 1293-1998 can be used to correct for tilt errors, if accuracy warrants.

Tilt variations also affect the results of gyroscope testing, in that they change the orientation of the gyroscope IA or axes relative to the earth's rotation vector. Azimuth variations of the test station can be of the same order of size as tilt variations and similarly affect the results of gyroscope testing, but not those of accelerometer testing. Optical monitoring of test station azimuth variations by sighting on an external target can be corrupted by movements of the target due to the same geophysical causes (such as temperature) that cause the test station to rotate in azimuth and tilt.

Monitoring the azimuth variation of a tilt-stabilized platform or dual gyroscope testing may be required when testing high-accuracy (< 0.0005 º/h) gyroscopes.

7.4 Active control of test pad

A test pad could be on pneumatic isolators to attenuate vibration inputs. Tilt and azimuth monitoring equipment can be used to actively control a test pad if the pad is mounted on actuators. The monitoring equipment would have to be more accurate than the sensors under test in responding to the movements being controlled.

8. Accelerometer dividing heads (or turntables)

8.1 Use of accelerometer dividing heads

An accelerometer in its fixture is mounted on a dividing head (such as indexing head or turntable with rotation axis horizontal) to perform various gravity field laboratory tests. The accelerometer IA is usually perpendicular to the horizontal dividing head rotation axis (see Figure 1). Long-term drift and noise tests are done with the dividing head in a fixed position, usually with IA vertical, where the accelerometer output is insensitive to tilt variations.

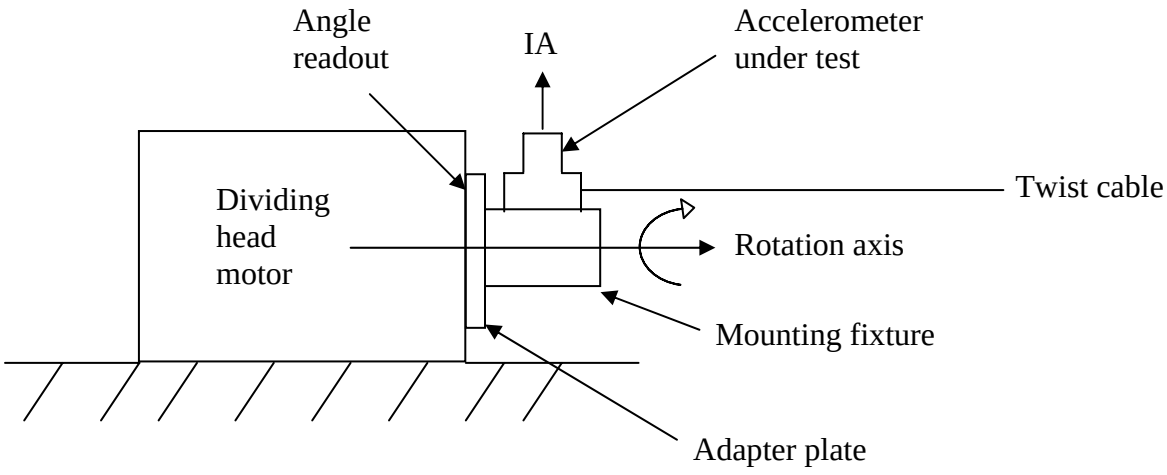

Figure 1— Dividing head for accelerometer tumble testing

In Figure 1, the accelerometer under test has IA perpendicular to the dividing head's horizontal rotation axis for calibrating bias and scale factor using the local gravity as a reference, IA misalignment using the local vertical as a reference, and some accelerometer nonlinearities. Sometimes tumble tests are done with the accelerometer IA parallel to the dividing head horizontal rotation axis for calibrating cross-IA effects.

Rotation of the dividing head between IA up and down is used to determine whether there is any shift or transient in an accelerometer's output across a change in input between plus and minus the local value of gravity. Up-down testing is also used to calibrate accelerometer scale factor and bias, with results that are insensitive to misalignments although the results could be aliased by other model parameters, such as nonlinearities, if they are not known from other tests.

Even if the scale factor and bias calculated in an up-down test are aliased by uncalibrated accelerometer nonlinearities, a sequence of such up-down calibrations over time at a given site gives valid measures of the stability of scale factor and bias. Similarly, a sequence of up-down calibrations across environmental variations (such as temperature, magnetic field, or vibration and shock) at a given site gives valid measures of the stability or repeatability of scale factor and bias. The stability and repeatability statistics of the bias and scale factor are also independent within required accuracy of the particular value of the acceleration due to gravity used as a calibration reference at the test site, even though the absolute value of the scale factor as a whole is very dependent on the value of this gravity reference.

For calibrating accelerometer bias, scale factor, IA misalignment, and other model parameters and for greater calibration accuracy, a dividing head or indexing table is required for placing the accelerometer IA at various discrete positions relative to the gravity vector besides just IA up and down (see 19.13.2.1; see also 12.3.4, 12.3.5, and Annex K in IEEE Std 1293-1998). Calibration tumble tests of a complete guidance system are sometimes done with continuous rather than discrete rotations.

The dividing head could be commanded to rotate continuously to calibrate accelerometer angular velocity and angular acceleration sensitivity model coefficients if the dividing head were equipped with slip rings. However, such calibration is probably best carried out on a rotary table (see Clause 9) and at the guidance system level rather than at the sensor level.

If great accuracy is not required for positioning accelerometer axes in the gravity field for calibrating scale factor and bias, a dividing head can be dispensed with. It is sufficient to attach the accelerometer to a block that is oriented by hand on a table surface to place the accelerometer IA in the up and down orientations.

8.2 Placement of dividing head

The dividing head table could be placed on a rigid table on a concrete seismic pier or slab isolated from the building floor to minimize tilt and azimuth movements, such as caused by diurnal and seasonal heating and ground water effects. The seismic and tilt environment of the pier and test table should be evaluated, including recording tilt data during tumble tests.

The horizontal dividing head rotation axis could be in any direction, unless a gyroscopic accelerometer was being tested. In that case, the horizontal dividing head rotation axis is usually oriented north, in order to simplify the correction to the gyroscopic accelerometer's output due to the effect of the earth's angular velocity.

8.3 Thermal control on dividing head

The accelerometer is mounted in a fixture (see Clause 6) that is attached to the dividing head faceplate with the use of an adapter plate if necessary. Insulation spacers or shims might be required between a temperature-controlled mounting fixture and the dividing head or adapter plate (see 12.1.1).

Alternatively, the dividing head mounting fixture could be inserted into a temperature-controlled chamber through a hole in the side of the chamber (see 12.1.2 and 12.2).

8.4 Alignment of dividing head and mounting fixture

The mounting fixture might have several accelerometer mounting surfaces to allow multiple accelerometer testing (such as IAs parallel, antiparallel, or orthogonal). The accelerometer IA is usually perpendicular to the horizontal dividing head rotation axis with either the output axis or pendulous axis (PA) parallel to the dividing head rotation axis, depending on which IA misalignment angle is to be estimated. Some tests are done with IA parallel to the horizontal dividing head rotation axis.

The dividing head angle at which a given mounting surface is perpendicular to the gravity vector can be determined by placing a horizontal precision bubble level approximately perpendicular to the dividing head rotation axis on the mounting surface in the up orientation. Precision bubble levels with a few arcsecond accuracy are commercially available. The calibration of the bubble level can be checked by the technique described in 21.5.

For a fine-resolution angle readout, the angle reading at bubble level null defines the up position of the dividing head for a tumble test. For discrete angle readout, such as every 1º, some dividing heads have a vernier adjustment to bring the nearest 1º angle position to the up position.

A bubble level positioned on the given mounting surface in the up orientation approximately parallel to the dividing head rotation axis can be adjusted to null by putting shims under the dividing head or using leveling jacks. In this manner, the dividing head rotation axis can be made horizontal within required tolerances.

Adjustment of the mounting surface so that it is vertical in the IA vertical position can be accomplished to within a few arcseconds with a precision bubble level. Electronic levelers and/or lasers can also be used. However, the internal misalignments of an accelerometer due to manufacturing tolerances could make the alignment of the accelerometer IA differ from the vertical in this orientation by several milliradians.

The IA misalignment about the dividing head rotation axis can be estimated by fitting to multi-position tumble test data and is generally ignorable if only IA up and down data are being used to estimate scale factor and bias. The misalignment of the IA from being perpendicular to the dividing head rotation axis and the coning of the dividing head about its rotation axis will alias the estimate of scale factor in an accelerometer-level tumble test. For measuring the stability of accelerometer model coefficients over time and their sensitivities to environmental variations at a given test station, this aliasing or biasing is ignorable.

For lesser accuracy accelerometers, the aliasing from milliradian misalignments is ignorable in determining absolute calibrations of model coefficients. For higher accuracy accelerometers, bias, scale factor, and IA misalignments are usually estimated in an inertial guidance system calibration before a mission, in which data from three nearly orthogonal accelerometers are used to eliminate the aliasing effect of misalignments and thus determine absolute calibrations (see K.2.6 in IEEE Std 1293-1998).

Dual orthogonal accelerometer testing can also be done on a dividing head to eliminate the aliasing from one misalignment angle (but not from the other IA misalignment angle or from dividing head coning) for testing accelerometers that are more accurate than the angle-setting precision of the dividing head (see Annex K of IEEE Std 1293-1998).

8.5 Wiring to dividing head

The electrical power, ground lines, and control signals to the accelerometer under test and for thermal control could go through slip rings on the dividing head, as can the output signals from the accelerometer and temperature monitors.

Because a dividing head does not rotate continuously, a more practical approach is to have these lines go through a cable that has sufficient slack to allowing twisting through a complete revolution. A discrete

position tumble test can be commanded for 360° in one direction and then 360° in the reverse direction to unwrap the cable.

8.6 Rotation of dividing head

Some dividing heads require manual rotation. A brake is released, the head is rotated manually to a new position and centered at the new angle by visual means (in some cases by looking through a microscope at a vernier scale), and then the brake is applied. Data are taken at the position, and then the process repeated for the angle sequence defined for the accelerometer tumble calibration test that is being performed.

Other dividing heads allow an angle to be commanded, and the table will automatically rotate to that angle. The table might have locking teeth (typically referred to as Hirth coupling) at certain discrete positions (such as every 1º), and/or there could be servo control at each commanded angle. In the latter case, a brake might have to be applied once the desired position is reached in order to obtain the quietest data. The time to go from one position to another should be noted. The rotation speed could be specified by the user, or it could be fixed in the equipment. Shocks involved in rotating the dividing head and engaging gear teeth or a brake could be measured by attaching piezoelectric accelerometers to the mounting fixture with epoxy or other means.

If the commanded angle has to be entered manually, there is a great deal of test technician involvement in carrying out an accelerometer tumble test. It is more desirable to command the dividing head angle under computer control, such as over the IEEE 488 bus (see 17.6).

The sequence of angle commands, the dwell time at each discrete position, and the amount of settling time before data are collected at a position could be specified in a test scenario file. Rotating the dividing head between IA up and down and determining the transient after reaching a new position can be used as a measure of the transient at any position. One cause of such a transient could be changes in thermal gradient when an accelerometer's orientation is changed. Whatever the cause, the inversion transient phenomenon should be characterized so that the settling time required before data are taken at each position in a tumble test can be rationally determined.

During a tumble test, the computer data acquisition system can read the test scenario file and issue dividing head rotation commands at the right times. The computer could also be controlling a thermal chamber in which the dividing head fixture is inserted so that a tumble test can be carried out at each temperature setting in the operating temperature range of the application for which the accelerometer is intended. Accelerometer model coefficients (including bias, scale factor, IA misalignment, and acceleration nonlinearities) are estimated at each temperature setting. Polynomial fits of the model coefficient estimates versus temperature yield calibrations of the model coefficients as functions of temperature.

Besides temperature, other environmental quantities (such as excitation voltage or magnetic field) can be varied, and tumble tests performed to determine the sensitivities of model coefficients to these environmental variations.

Automatic computer control of the dividing head rotation and environmental state increases productivity for production acceptance and characterization testing.

8.7 Readout of dividing head angles

If dividing head angles are commanded or manually set at given discrete values, it is not necessary to read out the dividing head angles, except for the human who is setting a manual angle or the servo or other equipment (provided by the manufacturer of the dividing head) that carries out the command to go to a certain angle. However, if the angle readout is available to the data acquisition computer, it could serve as a confirmation that the commanded angle has been obtained. The dividing head angle (either the commanded

or readout value) should be recorded along with the accelerometer output data by the data acquisition computer.

The dividing head manufacturer will specify the precision of the dividing head, such as an angle setting accuracy of 5 µrad and a repeatability of 1 µrad, with an accuracy of 1 µrad and a repeatability of 0.1 µrad being about the best possible. The tilt variation of the test pier or slab, which could be several microradians per day, has to be added to the angle setting error to obtain the total angle error because what matters in accelerometer testing is angle accuracy relative to the local vertical.

If tilt were constant during a tumble test, then tilt error and any overall bias in angle setting error would be absorbed in the estimate of IA misalignment. The measured stability of IA misalignment over days or weeks would have to be interpreted in light of possible variations in the tilt of the test table, which could be monitored with a tilt meter. The stability of bias and scale factor over days or weeks at a given test station would not be so affected if tilt were essentially constant during each tumble test lasting some number of minutes or hours.

If only IA up and down data are used to calibrate scale factor and bias, the calibration results are insensitive to small angle-setting and tilt errors because the cosine of a small angle is very close to 1. Similarly, if the dividing head is rotated 360°, any change in the IA vertical accelerometer output from before to after the rotation cannot be caused by the dividing head's not returning to the same angle value.

The technique of dual orthogonal accelerometer testing eliminates the effect of angle-setting errors and tilt variations during a test for testing of accurate accelerometers (see Annex K of IEEE Std 1293-1998).

9. Rate tables

9.1 Use of rate tables

A gyroscope in its fixture is mounted on a rate table to perform various laboratory tests. Long-term drift and noise tests are done with the rotary table in a fixed position, such as with IA vertical or with IA parallel or perpendicular to the earth's rotation vector.

Continuous rotations of the rate table at different rates and directions about the axis parallel to the gyro IA are used to calibrate gyroscope bias and scale factor (see 9.2.6 and 9.3.8), although gyro bias is more accurately calibrated in a drift test, after compensation for sensed earth rotation rate.

A gyroscope's dead zone is evaluated as follows: First, place the gyro IA perpendicular to the table rotation axis. Second, rotate the table slowly through the position where its IA is perpendicular to the earth's rotation vector. The dead zone, if any, typically occurs where the bias is cancelled by the input rate.

9.2 Single-axis rate table

9.2.1 Placement of rate table

The single-axis rate table depicted in Figure 2 has a vertically oriented ball- or gas-bearing rotation axis. For horizontally orientated single-axis rate tables, see Clause 8.

Precision bubble levels can be used to align the rate table axis along the vertical within specified tolerances by putting shims under the rate table base or using leveling jacks. The orientation of the vertical rate table relative to east-west and north-south is not particularly important if the single-axis rate table is used only for gyroscope scale factor measurements using complete table revolutions.

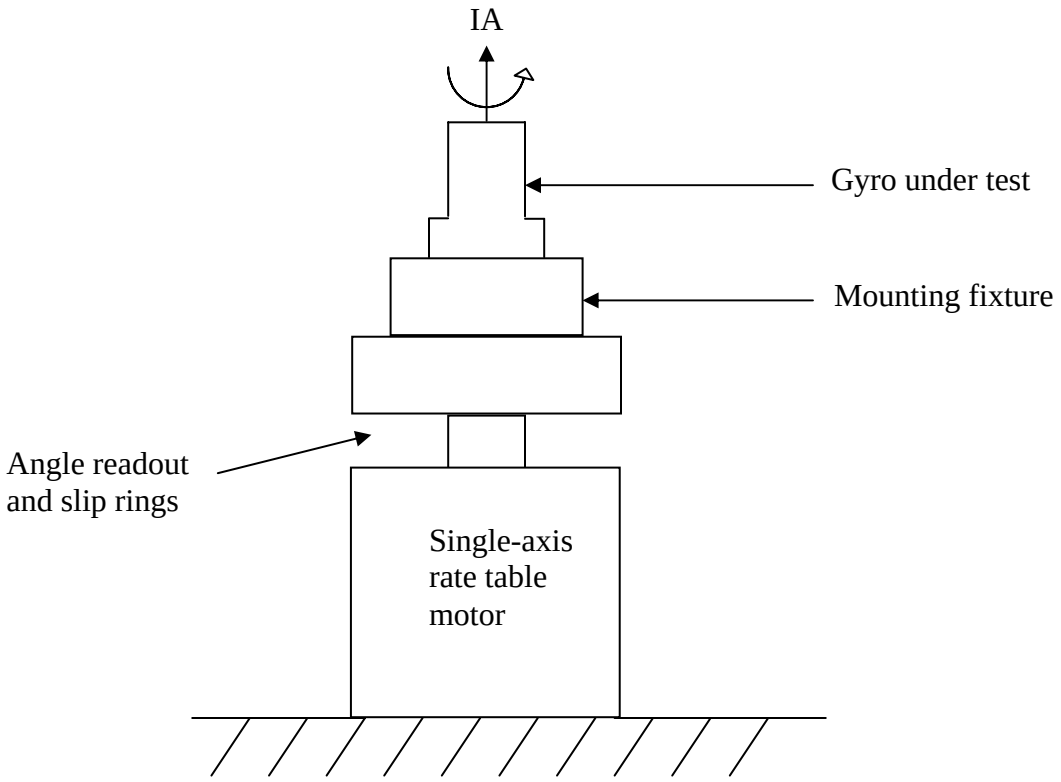

Figure 2— Single-axis rate table

9.2.2 Thermal control on rate table

The gyroscope is mounted in a fixture (see Clause 6) that is attached to the rate table faceplate with the use of an adapter plate if necessary. Insulation spacers or shims might be required between a temperature-controlled mounting fixture and the rate table or adapter plate (see 12.1.1).

Alternatively, the rate table mounting fixture could be inserted into a temperature-controlled chamber through a hole in the bottom of the chamber (see 12.1.2 and 12.2).

9.2.3 Control of rate table rotation

Manufacturer-supplied control electronics enable the rate table to be commanded to a desired position or at various rotation rates, such as between 0.1°/s to 1000°/s. Also, a sinusoidally or other varying rate with the rate table oscillating back and forth can be commanded.

9.2.4 Wiring to rate table

The electrical power, ground lines, and control signals to the gyroscope under test and for thermal control could go through slip rings on the rotary table, as could the output signals from the gyroscope temperature monitors (see 9.3.6).

The output signals could also go through a radio link (see 9.3.7).

9.2.5 Gyroscope oscillation on rate table

With the gyroscope IA along the rate table rotation axis, the rate table can be oscillated back and forth through an angle $\pm \theta$ at various frequencies, for example, using a periodic or linear chirp function, to measure the gyroscope transfer function.

If the rate table motor cannot input oscillations above a certain frequency, an eccentric mass can be rotated on the rim of the rate table plate at the high frequency. The oscillating mass unbalance causes the rate table to oscillate back and forth and thus input the desired high-frequency sinuoidal oscillation to the gyroscope.

9.2.6 Gyroscope scale factor calibration on rate table

Gyroscope scale factor is calibrated by continuously rotating the rate table at various rates with the gyroscope IA parallel to the rate table rotation axis and by analyzing the results as in 19.13.3. The scale factor calibration is only as good as the accuracy with which the rotary table rate can be controlled by the manufacturer-supplied inductosyn or other angle readout and the control electronics, except that the revolution trigger technique of 9.3.4 can be used to obtain more accurate results than allowed by the table rate control. If the rotary rate table is placed in a temperature-controlled oven (see 12.1.2 and 12.2), then the bias and scale factor calibrated at each temperature setting can be fit to polynomials in temperature to determine the gyroscope model coefficients as functions of temperature.

If scale factor asymmetry is known to be ignorable, then a possible test scenario is

+10°/s and then –10°/s
+100°/s and then –100°/s
+200°/s and then –200°/s
+400°/s and then –400°/s
etc.

Data from the + and – rotation rates are used to determine scale factor at that absolute value of rotation rate (see 19.13.3.1). Polynomial fits to the bias and scale factor as functions of absolute value of rotation rate determine whether there are any nonlinearities in these quantities (see 19.13.3.3).

To test for scale factor asymmetry, a test scenario as in Table 1 (in 9.3.8) can be used, and the scale factor and bias can be determined from data at adjacent rate table rates of the same sign or from a fit of a model to all the data (see 19.13.3.2 and 19.13.3.3).

9.2.7 Accelerometer testing on rate table

Pendulous and other accelerometers have angular velocity and angular acceleration sensitivities (see Annex C in IEEE Std 1293-1998). The angular-velocity-sensitive and angular-acceleration-sensitive coefficients in the accelerometer performance model can be calibrated using high-rate rotations on a rate table (see 12.3.21 in IEEE Std 1293-1998).

Accelerometer-level rotation rate tests would be done for characterization purposes. Rotation rate tests for strapdown guidance systems would be done in the normal calibration procedure to calibrate the radius vectors from the navigation center of the guidance system to the effective centers of mass of the accelerometer pendulums and to calibrate the angular-velocity-sensitive and angular-acceleration-sensitive model coefficients.

9.3 Two-axis rate table

9.3.1 Placement and alignment of rate table

A two-axis gyroscope rate table has a manually rotated horizontal trunnion axis and a rate- or position-controlled inner axis with ball or air bearings (see Figure 3). Alternatively, the trunnion axis could also be position or rate controlled.

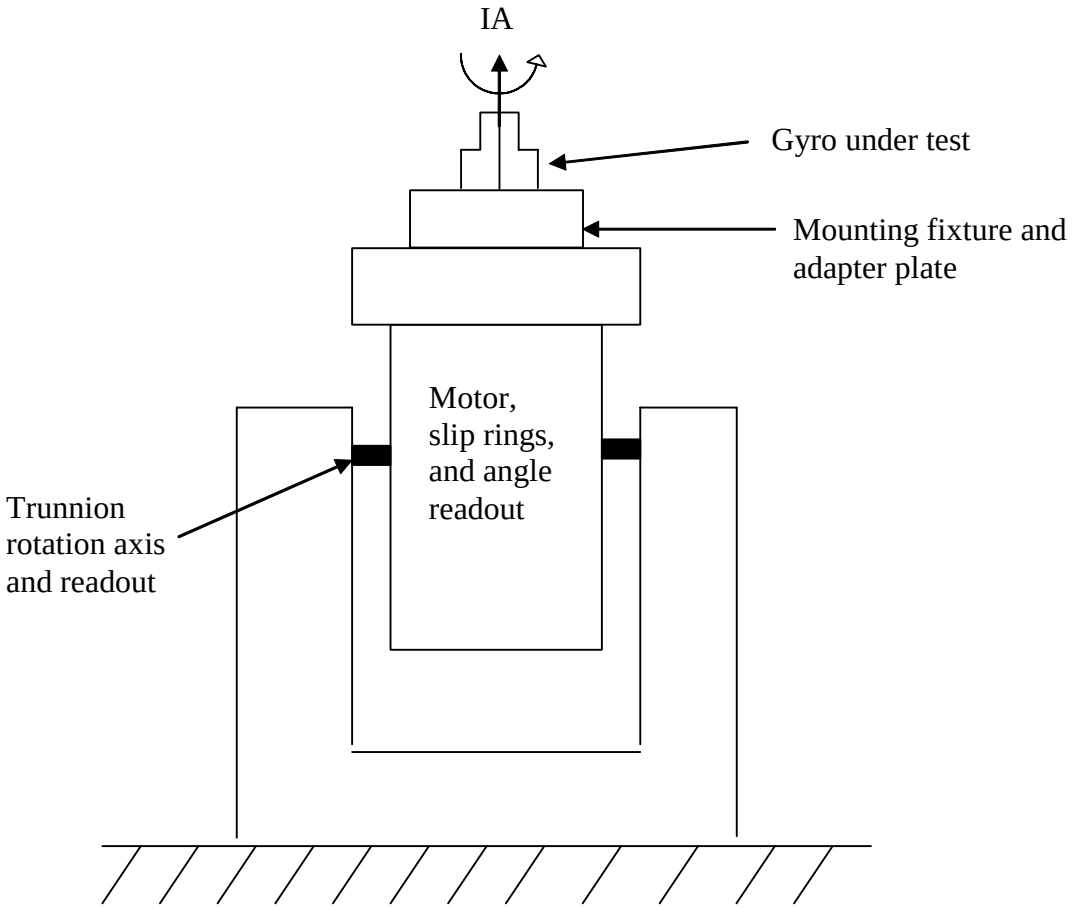

Figure 3— Two-axis rate table

The east-west and north-south lines can be determined by a theodolite survey and star sightings (see 20.6). Alternatively, the east-west direction can be determined by a gyrocompass, in which an accurate gyroscope's IA is alternately placed horizontally east and west (see 20.4).

A derrick, fork lift, or other piece of equipment is used to roughly align the trunnion axis east-west. Final alignment is performed using adjustment screws. The residual misalignment can be measured and used when processing test data.

The nonverticality of the inner gimbal axis is observed by rotating the inner gimbal to several positions with a level on the table top. This nonverticality is minimized by shimming the floor mounts or adjusting leveling jacks. The nonorthogonality of the plane of the adapter plate to the inner gimbal axis is observed by taking measurements at various orientations of the level on the adapter plate with the inner gimbal axis vertical. This nonorthogonality can be minimized by shimming between the adapter plate and the table top.

With the horizontal trunnion axis east-west, the inner gimbal axis can be rotated parallel to and perpendicular to the earth's rotation axis. The angle between the inner gimbal axis and the horizontal when the inner gimbal axis is parallel to the earth's rotation vector is the geodetic latitude of the test site (see 20.5).

9.3.2 Mounting fixture and thermal control on rate table

The gyroscope is mounted in a fixture (see Clause 6) that is attached to the rate table faceplate with the use of a steel- or hard-coated aluminum adapter plate if necessary. The adapter plate bolt holes also allow gyroscope electronics and other equipment to be mounted on the table top (see 9.3.5). If the diameter of the adapter plate is larger than the space between the trunnions, then the table could not be rotated all the way into the vertical down orientation. Insulation spacers or shims might be required between a temperature-controlled mounting fixture and the rate table or adapter plate (see 12.1.1).

Alternatively, the mounting fixture could be inside a temperature-controlled chamber on the table top (see 12.1.2 and 12.2). If low temperatures are required for the thermal chamber, then, for example, liquid nitrogen might have to be pumped into the inner gimbal through rotary joints.

9.3.3 Command and readout of rate table angles and angular rates

The desired trunnion axis angle for a test is manually set either with the perpendicular to the table top being vertical or at some other angle such as being parallel to the earth's rotation vector north or perpendicular to this vector. The angle between the perpendicular to the table top and the horizontal when the table-top perpendicular is parallel to the earth's rotation vector is the geodetic latitude of the test site (see 20.5).

Manufacturer-supplied electronics can be commanded to rotate the inner table angle to a desired value or to rotate the inner table angle at a desired rate. These commands can be manually entered, or the data acquisition computer can interface directly to the table controller to issue these commands in a defined testing schedule. The manufacturer will specify the accuracy of the inductosyn or other table angle readout and the commanded rate. For techniques to verify readout accuracy, see 21.5.

If the inner table angle is commanded to a specified value, a brake can be applied to rigidly hold that position. Alternatively, the control system can remain operative. In the latter case, there would be a certain amount of limit-cycling around the commanded position.

In commanded rate mode, the table rate is controlled at best to a few ppm, and possibly only to several tens of ppm, from one complete revolution to the next. The rate control is worse than this over shorter spans, such as 1°.

9.3.4 Revolution trigger for accurate gyroscope scale factor calibration

If scale factor has to be calibrated to, for example, the 0.1 ppm level, another technique has to be used to determine the gyro rate versus the table rate. Namely, there can be an optical trigger once per revolution of the table that is used to latch a 10 MHz continuous counter to measure the time to go that one revolution and hence the average table rate. The gyroscope accumulated angle output is also latched into the computer at the precise instant of the optical trigger crossing by interpolation from high-rate equal time samples of the gyroscope data.

There could be several optical triggers spread more or less uniformly around 360°. For each optical trigger, there is a gyroscope accumulated angle for each 360° revolution returning back to the same optical trigger.

The data from all the (perhaps overlapping) revolutions are averaged to get the average gyroscope accumulated angle per 360° revolution. The gyroscope scale factor and bias can be calculated from the data at two adjacent commanded table rates (see 19.13.3.2).

9.3.5 Equipment on table top

The gyroscope mounting fixture could be thermally controlled, or the gyroscopes could be contained in a thermally controlled chamber on the table top. Gyroscope proximity electronics and thermal control electronics would be on the table top. Electric power would be brought through slip rings in ac form if the dc power supplies for the table-top electronics were on the table top.

A data acquisition microprocessor could be on the table top. If precise timing signals are needed on the table top, they could be provided by a crystal oscillator if it were undesirable to bring timing signals through slip rings.

9.3.6 Slip rings

Slip rings are used to bring electric power and ground lines to the table top. Power grounds and data grounds should not share the same lines and slip rings.

Data from the table top could go through the slip rings to the data acquisition computer. This data could be the outputs from the gyroscopes under test and the data from other sources such as thermistors. Analog data, such as thermistor voltages, could suffer some degradation in going through slip rings.

A microprocessor on the table top could acquire data from the gyroscopes under test plus other data, such as thermistor voltages, through an A/D converter. The data are then converted to digital form and sent as a digital data stream through the slip rings to the data acquisition computer. A digital data stream (such as serial characters) does not suffer degradation in going through the slip rings as analog signals do. The digital data stream could be provided with error detection and correction bits.

9.3.7 Radio transmission of telemetry signals

Another technique is to avoid the slip rings altogether for signal transmission and send the data from the microprocessor on the table top to the data acquisition computer using a radio link (namely, wireless data acquisition). The slip rings are used only to bring electric power and grounding to the equipment on the table top.

As described in 11.5.5, there are commercially available modules to accomplish this radio transmission and the radio reception by the data acquisition computer. The data acquisition computer acquires the digital data stream from the radio link and also acquires other data, which are then filtered or averaged before being written to disk.

9.3.8 Test scenarios to measure gyroscope scale factor nonlinearities

Rotation rate tests are usually done with the gyroscope IA parallel to the table rotation axis oriented vertical or sometimes oriented parallel to the earth's rotation vector. A possible sequence of table angular rates for testing of scale factor asymmetry and nonlinearity over ± 90°/s is given in Table 1. It is desirable to analyze data from an integral number of table revolutions in order to average out error effects and to obtain more accurate data, especially if the table is provided with a revolution trigger.

The elapsed test time in Table 1 is 8.7 h for the positive and negative table rates combined. There has to be time allowed for accelerating from one table rate to another and for settling at the new table rate. The average gyro rate data for an integral number of table revolutions versus average table rate are analyzed for scale factor asymmetry and nonlinearity as described in 19.13.3.2 and 19.13.3.3.

Table 1—Example gyroscope rotation rate test scenario over ± 90°/s

Table rate† (°/s)	Number of revolutions	Duration (min)	Table rate† (°/s)	Number of revolutions	Duration (min)
+0.1	1+	>60	+30	19+	>3.8
−0.1	1+	>60	−30	19+	>3.8
+0.2	1+	>30	+35	23+	>3.9
−0.2	1+	>30	−35	23+	>3.9
+0.5	3+	>36	+40	19+	>2.8
−0.5	3+	>36	−40	19+	>2.8
+1	5+	>30	+45	22+	>2.9
−1	5+	>30	−45	22+	>2.9
+2	7+	>21	+50	24+	>2.9
−2	7+	>21	−50	24+	>2.9
+3	7+	>14	+55	18+	>2.0
−3	7+	>14	−55	18+	>2.0
+5	7+	>8.4	+60	19+	>1.9
−5	7+	>8.4	−60	19+	>1.9
+8	9+	>6.7	+65	21+	>1.9
−8	9+	>6.7	−65	21+	>1.9
+11	9+	>4.9	+70	23+	>2.0
−11	9+	>4.9	−70	23+	>2.0
+14	12+	>5.1	+75	24+	>1.9
−14	12+	>5.1	−75	24+	>1.9
+17	14+	>4.9	+80	26+	>2.0
−17	14+	>4.9	−80	26+	>2.0
+20	17+	>5.1	+85	28+	>2.0
−20	17+	>5.1	−85	28+	>2.0
+25	16+	>3.8	+90	29+	>1.9
−25	16+	>3.8	−90	29+	>1.9

† Start far enough before the integral revolution trigger (if there is one) so that the table rate reaches steady state before crossing the trigger; and go far enough beyond the trigger so that, when the trigger point is crossed after angular motion reversal, the table rate has reached steady state.

If it were known that there were no scale factor asymmetry or nonlinearities, then a rotation rate sequence as in 9.2.6, which has fewer positive rotations followed by negative rotations than shown in Table 1, could be used. The scale factor and bias at that absolute value of table rate are estimated with the positive and negative table rate data (see 19.13.3.1).

Additional input rates above and/or below the rates listed in Table 1 may be required to fully evaluate any scale factor nonlinearities. Below 15°/h, the earth's rotation vector can be used as an input rate, but special care would be required to determine the angle between the gyroscope IA and the earth's rotation vector. Having three gyroscopes and three accelerometers in a guidance system would help in this angle determination and calibration. Depending on the application, all gyroscope calibrations might be done using earth rate as a reference, or they could be done using the table rotation rate as a reference.

9.4 Three-axis rate tables for inertial sensor assembly (ISA) testing

An ISA has three or more gyro IAs, such as in an inertial reference unit (IRU), plus possibly three or more accelerometer IAs, such as in an inertial measurement unit (IMU). Testing an ISA can involve placing its axes at various angles relative to the earth's gravity and rotation vectors and rotating about its various axes.

Obtaining insight into the performance of all axes of an ISA can often be accomplished on a two-axis rate table (especially for discrete position testing), although some maneuvers may more easily be accomplished on or may require a three-axis rate table.

9.4.1 Setup of rate table

A three-axis rate table has three gimbal axes that can be commanded to go to specified angles or to rotate at specified rates (see Figure 4, where the outer gimbal is along the local vertical, which is not always the case). A possible initial orientation of the rate table on its test pier with gimbal angles 0º, 0º, 0º is with the middle gimbal oriented horizontally with its axis pointed east-west and the inner gimbal oriented horizontally with its axis pointed north-south, per the procedure in 9.3.1. The table angle readouts might have different readings in this orientation than the 0º, 0º, 0º values that are assumed in Equation (2). The offsets in the table angle readouts in indicating 0º, 0º, 0º in this orientation and any calibrations of table misalignments can be accounted for in analyzing data.

Thermal control requirements would be special to the ISA being tested (see 9.3.2). Electrical power and grounds go through slip rings (see 9.3.6). Data from the ISA could go through slip rings or a radio link (see 9.3.7).

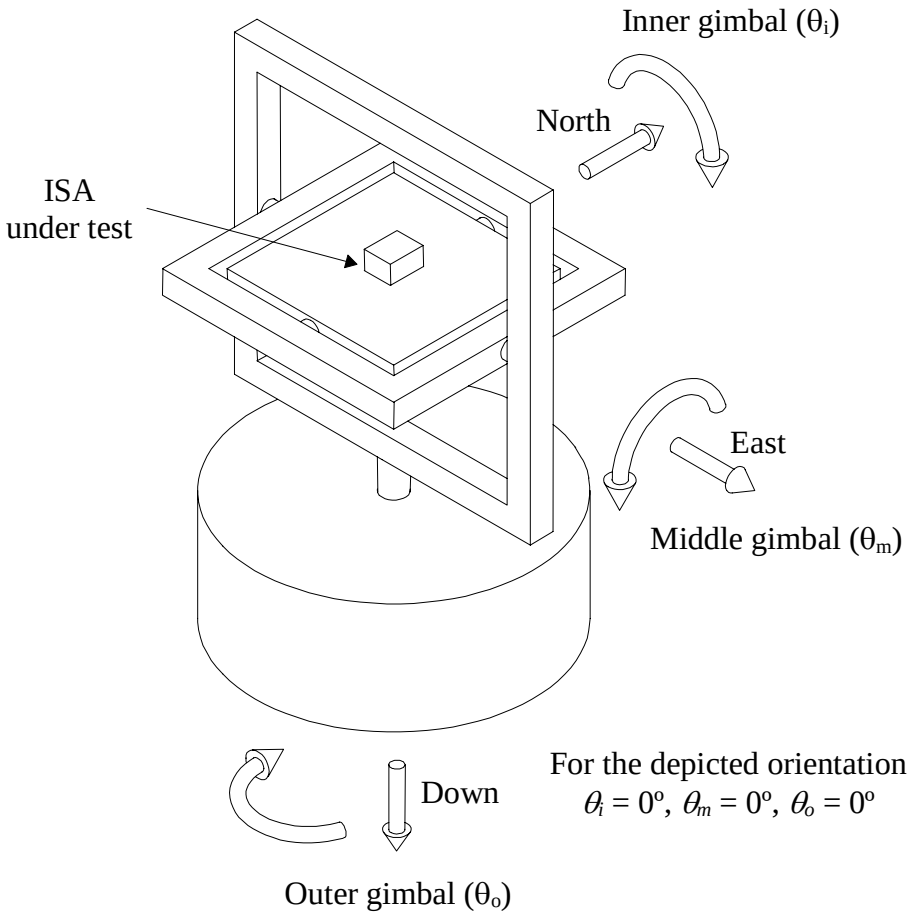

Figure 4— Three-axis rate table

9.4.2 Table orientations

The local vertical down frame has *X* axis north, *Y* axis east, and *Z* axis vertically down. Let θ_i, θ_m, θ_o be the inner, middle, and outer gimbal angles, respectively, of the rate table. The transformation matrix *A* from the local vertical down frame to the inner gimbal frame of the rate table is

$$A = \begin{bmatrix} 1 & 0 & 0 \\ 0 & \cos\theta_i & \sin\theta_i \\ 0 & -\sin\theta_i & \cos\theta_i \end{bmatrix} \begin{bmatrix} \cos\theta_m & 0 & -\sin\theta_m \\ 0 & 1 & 0 \\ \sin\theta_m & 0 & \cos\theta_m \end{bmatrix} \begin{bmatrix} \cos\theta_o & \sin\theta_o & 0 \\ -\sin\theta_o & \cos\theta_o & 0 \\ 0 & 0 & 1 \end{bmatrix} \quad (2)$$

for the configuration depicted in Figure 4. The transformation would be different for other rate table configurations. To put the table in the orientation depicted in Figure 4, the table angle readouts may be different.

Certain gimbal rotations for ISA calibration (see 9.4.3) might not be possible to do on a three-axis rate table because of the phenomenon known as *gimbal lock*. When the gimbals are lined up so that two of them are collinear, there is a loss of a degree of freedom so that rotations about some axes cannot be accomplished. This is not a concern for most calibrations because other calibration rotations could be just as adequate. If it were a concern, then a four-gimbaled rate table combined with a gimbal-lock-avoidance control algorithm would allow desired angular motions of the test article to be accomplished without the gimbals approaching a gimbal-lock configuration.

9.4.3 ISA calibration

An ISA is placed on a two- or three-axis rate table to orient the gyroscope and accelerometer IAs at various angles to the earth's gravity and rotation vectors and to rotate about various axes for calibration of the inertial sensor biases, scale factors, IA misalignments, and other model parameters. Note that an ISA is usually calibrated as part of an inertial system. Whereas a strapdown inertial system would have to be placed on the rate table, a gimbaled inertial system can use its gimbals like a three-axis rate table. Thus the gimbaled inertial system has an advantage in that a calibration can be performed just prior to the start of a mission. However, some inertial sensor model parameters, such as nonlinearities and sensitivities, often have to be calibrated in the factory and hence be adequately stable for the months or years that would elapse between calibrations.

Consider an ISA with three nearly orthogonal accelerometer IAs and three nearly orthogonal gyroscope IAs. A continuous or discrete multi-axis ISA tumble scenario is chosen to excite gyroscope as well as accelerometer model terms. With the sum-of-squares accelerometer observable at a fixed site on the earth (see Annex K of IEEE Std 1293-1998), tumbles are traversed without corruption of the accelerometer parameter estimates from angle-setting errors. For individual gyroscope observables, tumbles or rotations about each gyroscope IA parallel or antiparallel to the earth's rotation vector excite gyroscope model terms without corruption from angle-setting errors.

In general, two misalignments will be required to define each sensor's IA relative to a reference coordinate system. In many cases, one of the reference axes is defined along one sensor's IA, which eliminates two of the misalignments. A second reference axis is defined so that it is perpendicular to the first reference axis and is in the plane defined by the first reference axis and a second sensor's IA, which eliminates a third misalignment. The third reference axis is the vector cross product of the first two reference axes.

Various estimation techniques may be used to extract the inertial sensor model parameters from the tumble or rotation test data. Such techniques may include real-time sequential Kalman filter estimators, least-squares maximum-likelihood estimators (see 19.11.2), or other algebraic techniques. Some inertial sensor model coefficients, such as quadratic and higher order acceleration sensitivities, are held fixed at their sensor-level calibration values from vibration or centrifuge tests.

10. Vibration and shock equipment

10.1 Use of vibration and shock machines

A gyroscope or accelerometer in its fixture is mounted on a vibration or shock machine to perform various laboratory tests. A frequency sweep, such as from 20 Hz to 2000 Hz on an electrodynamic vibrator, can look for any structural resonances in the sensor that would be revealed by shifts in sensor output at vibration frequencies where there are resonances.

Shifts and transients are sought in the sensor output across exposure to vibration and shock levels encountered in applications. Performance through random vibration and shock can also be determined, such as whether the signal processing used for the sensor adequately compensates for any vibration rectification effects.

Tumble and rotation rate calibrations before and after exposure to vibration and shock can determine the repeatability of bias, scale factor, and other parameters across vibration and shock.

Sine vibrations at various levels and along various sensor axes are used to calibrate sensor model nonlinearities.

Sine vibrations along an accelerometer's IA are used to measure the accelerometer's transfer function, above about 15 Hz for an electrodynamic vibrator and above about 3 Hz for a hydraulic vibrator. For measuring an accelerometer's transfer function below 3 Hz, a double turntable centrifuge can be employed (see 11.4).

10.2 Vibrators

10.2.1 Electrodynamic vibrators

Most vibration exciters are electrodynamic, producing oscillatory forces by driving appropriate currents through a coil immersed in a magnetic field. The magnetic field is produced by a large permanent magnet assembly or by fixed conductive coils within a magnetic return structure. Electrodynamic exciters can produce useful acceleration waveforms within the frequency range from about 20 Hz to over 2000 Hz, although some vibrators have upper limits reaching 10 kHz to 100 kHz for small masses.

Low-frequency operation is limited by the available travel of the exciter armature within the constant part of the magnetic field. Peak-to-peak travel is typically limited to 1 cm to 1.5 cm on small shakers and rarely more than 2.5 cm on large ones, limiting acceleration to about 100 m/s^2 peak at 20 Hz. Low-frequency vibration may also be limited by the bandwidth of the power amplifier or by waveform distortion introduced by imperfections in the suspension, which constrains the armature motion to a single axis.

At high frequencies, acceleration amplitude is limited by the force rating or the voltage limits of the exciter. For example, with a suspended mass of 30 kg, including the tare weight of the armature and fixture, a 30 000 N exciter is limited to 1000 m/s^2 peak, or about 300 m/s^2 rms random. At very high frequencies, above 1000 Hz in the example of Figure 5, additional limits related to voltage capability and inductance may apply.

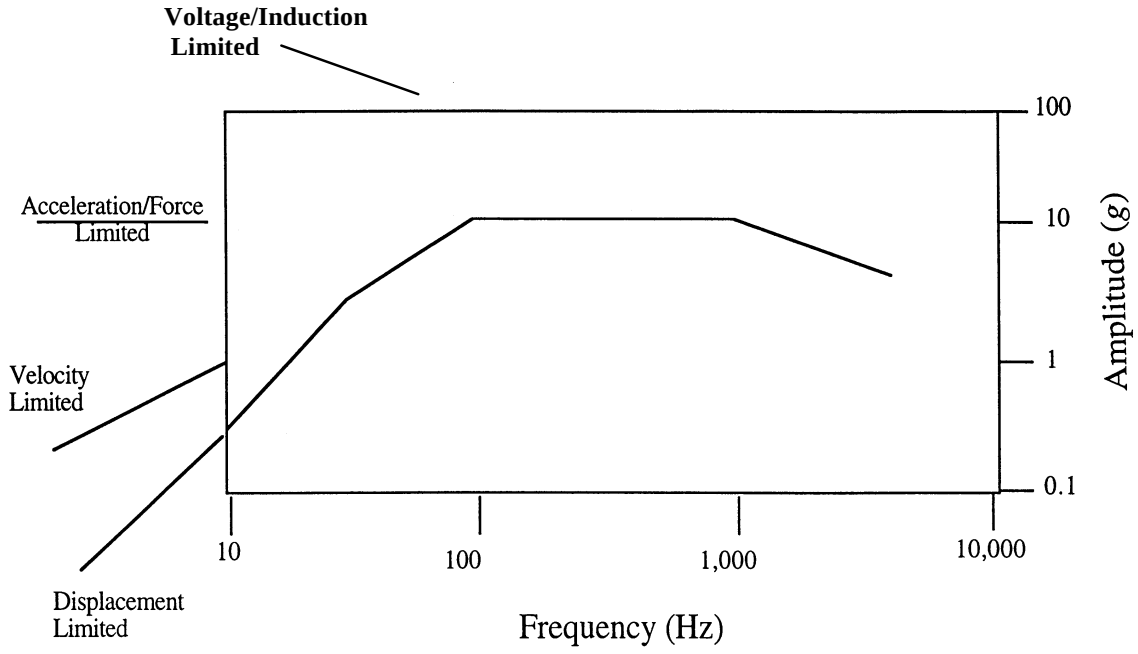

Figure 5— Example electrodynamic vibrator— maximum acceleration capability versus frequency

10.2.2 Hydraulic vibrators

For special applications that require larger acceleration at very low frequency, such as mimicking rigid body motions of a missile, hydraulic exciters are available that operate below 1 Hz at 50 cm peak to peak. These shakers are generally limited by valve operating speeds and fluid line compliances to operation at frequencies of at most a few hundred hertz.

The magnitude and stability of the hydraulic vibrator compliance under low-frequency vibration should be evaluated.

10.2.3 Vibrator orientation, slip tables, and attachment to floor

Electromagnetic vibration exciters are usually operated with the vibration axis vertical so that there is no side loading on the suspension and tilt effects are minimized (see Figure 6). They can be operated horizontally by coupling them to a slip plate supported by an oil film, as illustrated in Figure 7. The accelerometer under test in Figure 6 and Figure 7 has IA vertical, but other orientations are possible (see Annex L in IEEE Std 1293-1998).

In either case, vibrators are most commonly restrained by simply bolting them to a concrete floor at a location where they would not disturb other inertial sensors under test. In high-precision applications, where cross-axis and especially rocking motions must be minimized, the vibrator, and slip table if used, may be mounted to a large, pneumatically suspended, steel reaction mass (concrete is not rigid enough), with the vibration axis passed through the center of mass.

10.2.4 Mounting fixture and temperature control on vibrators

The requirements on a vibrator mounting fixture for an inertial sensor are described in 6.3.

If the inertial sensor under test has its own internal thermal control, then the test fixture mounting flange usually has to be controlled at some temperature, with the sensor control point being above the mounting flange control point. The fixture temperature control could also be used to control the temperature of a nontemperature-controlled sensor (see 6.2 and 12.1.1).

Alternatively, the vibration test fixture could protrude into a heated and/or refrigerated oven (see 12.1.2 and 12.2) to perform tests over a wide temperature range in a combined temperature-vibration environment.

10.2.5 Measurement and control of vibration

It is important to design the system for few or no resonances, to place the controlling accelerometer on the fixture as close to the test item as possible, and to run resonance searches slowly enough to allow high Q resonances to build up. These precautions guard against application of damaging vibration amplitudes during actual testing.

As depicted in Figure 6 and Figure 7, the motion applied to the test fixture is determined by a signal generator through a servo loop that uses a piezoelectric accelerometer for feedback. These accelerometers are typically accurate to about 3%, but can be calibrated to 0.5% by comparing to a specially calibrated piezoelectric or other accelerometer or by using laser interferometer techniques (see 10.5).

Because of the wide range of mechanical impedances represented by the test fixtures and test items that may be attached to a general-purpose shaker, it is impractical to provide a high-frequency, high-gain servo that attempts to servo directly to the applied wave form; instability would be a constant problem. Instead, a simple, robust servo is created by simply controlling the rms amplitude of the motion and allowing the drive to run otherwise open loop.

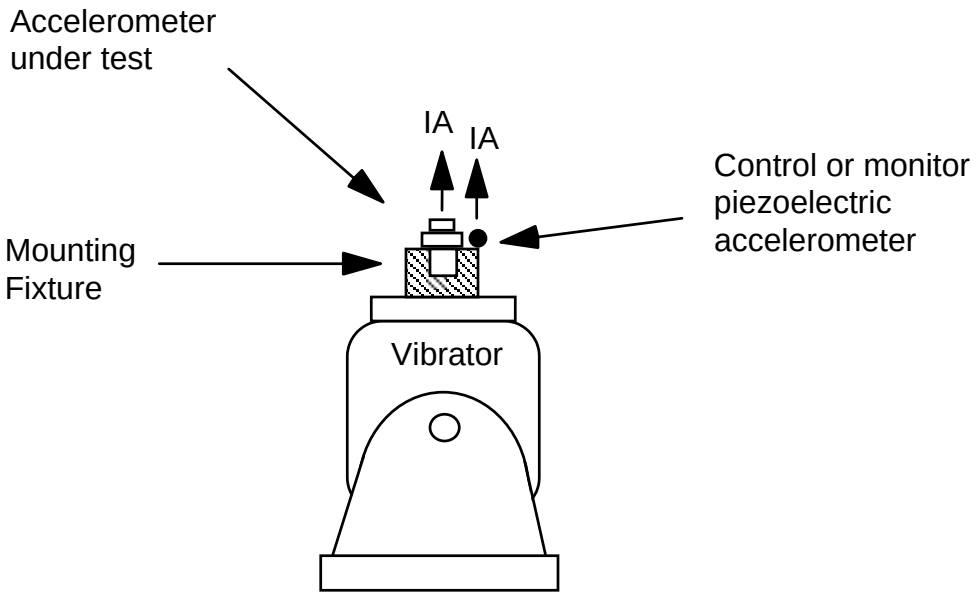

Figure 6— Vertically oriented vibrator

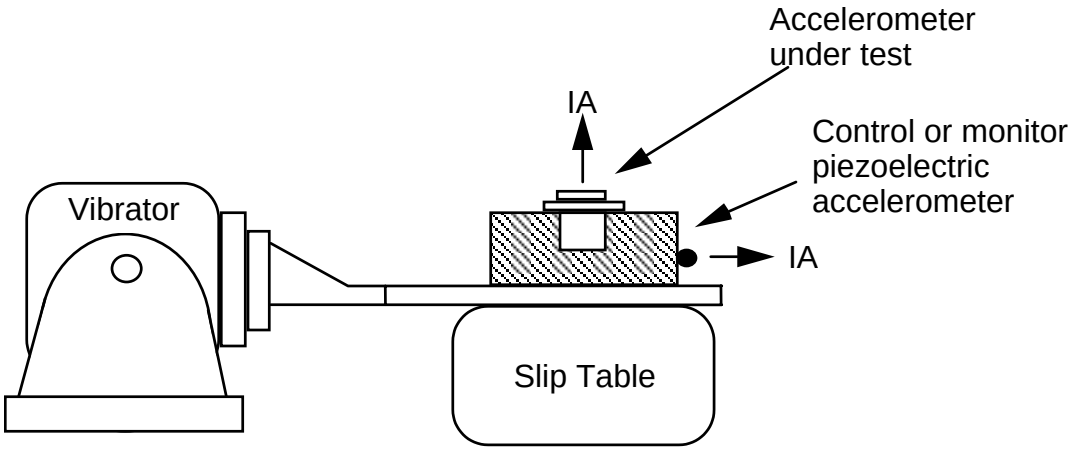

Figure 7— Horizontally oriented vibrator with slip table

Large amplitude vibrations are used to calibrate small nonlinearities (relative to performance requirements) with a few percent accuracy for accelerometers intended to measure near-dc input using the piezoelectric accelerometer or some other accelerometer or displacement monitor as a reference. Then the calibrated nonlinearities are used in compensating low-pass and dc acceleration measurements in a mission. Vibration and shock can also be used to calibrate accelerometer scale factor for some applications using a laser interferometer motion monitor (see 12.3.18 in IEEE Std 1293-1998).

Additional pre-mission tests are the application of random vibration and shock as controlled by a piezoelectric accelerometer. The tests determine whether there are any shifts in the tested accelerometer across mission-level or qualification-level environments. It is also determined whether the accelerometer performs through mission-level random vibration and shock, generally with the assumption that the nonlinear terms are small enough to ignore for mission-level vibration and shock, even though compensation might be used for dc and low-pass acceleration inputs. If nonlinearities are significant for mission-level random vibration, then vibration rectification compensation is required at higher as well as lower frequencies.

10.2.6 Types of vibration input

The vibration waveform can be a constant amplitude sinusoid at a constant frequency, or at a varying frequency, swept at some rate, such as 4 Hz/s linear variation or 1 octave/min logarithmic variation. A frequency sweep can be used to evaluate resonances in the accelerometer's structure or incipient instabilities in a servo loop. A constant frequency vibration with amplitude started and stopped, or varied in amplitude, such as between 10 m/s^2 and 200 m/s^2 every few minutes, can be used to calibrate nonlinear coefficients.

A white noise generator and a real or virtual filter bank can be used to apply random motion to a test item with any desired spectral shape. The controller for a desired input spectrum is first developed with a dummy mass in the fixture. Then with the real test article, the preprogrammed controller will typically apply a low level of vibration for several seconds to standardize the filter bank for resonances or notches in the test package frequency response before applying the full rms amplitude requested.

Many spectra are possible, depending on the application and the standards cited in 2.2, but a common spectrum for navigation grade accelerometers simulates the effect of a vibration isolator by rising to a peak in the range of 50 Hz to 100 Hz and then decreasing to a low level at higher frequencies.

10.2.7 Types of shock input

Processor-controlled electromagnetic shakers can also be programmed to apply a limited but useful range of shock inputs: full sine, sinusoidal with decaying exponential amplitude, and an approximation to half sine, among others. Their principal limitation in this area is their inability to produce shocks that entail a net change of velocity.

As with random vibration tests, the programming of the shock spectrum is developed with a dummy mass. Then with the real test article, the preprogrammed controller applies a low-level shock of the specified spectrum for calibrating the controller before applying the full amplitude requested.

10.3 Drop shock and hammer shock machines

Nonzero displacement shocks can be generated by dropping the test article from a specified height with controlled stopping elements (such as a rubber bumper or a steel, brass, or aluminum plate or ball) to set the shape, peak value, and duration of the shock.

A pendulum with a large mass at the end (such as a hammer head) can be allowed to fall from a certain height to swing back to the original height, where the test article is located. The contact shock with the test article can be varied by having the pendulum initial height vary from the same height as the test article to being above the height of the test article. Another device for imparting controlled shocks is a pneumatic hammer.

An inertial sensor's test fixture can be tapped with a hammer that has a plastic-coated head, where the plastic coat attenuates higher shock harmonics. The amount of shock imparted is not well controlled, although it can be monitored with a piezoelectric accelerometer. Use of a spring-loaded center punch to tap the fixture imparts a more reproducible shock. As long as there is no danger of damaging the inertial sensor, this hammer tap test is an easy way to see whether there is any shift in an inertial sensor's output across a shock event.

For a more complete description of shock tests and procedures, see ISO 8568 and ISO 16063.

10.4 Air guns

For applications where an inertial sensor is subject to a large shock, such as being fired in an artillery shell or in an automobile crash, the shock can be simulated by being fired from an air gun, and then being slowed by hitting an appropriate target. An air gun can be used in a laboratory setting, whereas use of artillery requires an outdoor proving range.

10.5 Shock and vibration monitors

Shock and vibration monitors are most commonly piezoelectric accelerometers, sometimes referred to as *crystal accelerometers*, although they may be any accelerometer that has sufficiently large range, sufficiently small mass, and sufficiently wide bandwidth.

A piezoelectric accelerometer is a small, electrically shielded inertial instrument in which a seismic mass is constrained relative to the case by a bonded or clamped-spring element of piezoelectric material. Such a structure produces an instrument with an equivalent circuit consisting of a voltage output proportional to the nongravitational acceleration, but with a capacitor in series, as shown in Figure 8. The significant characteristics of such a device are that it is an ideally linear device with the same output as any other accelerometer, but with no dc response, and with sensitivity that varies significantly with the magnitude of any capacitive elements (such as shielded cables) that are added to the output circuitry. They are typically very stiff, open-loop instruments with bandwidths of the order of several tens of kilohertz.

The sensitivity to capacity can be avoided by measuring the output through a device called a *charge amplifier*, but the lack of dc response is fundamental. A charge amplifier is essentially an op amp integrator whose input is a virtual ground. This circuit responds only to the charge output of the piezoelectric element, producing a scale factor whose units are $pC/(m/s^2)$. Either way, its characteristic output is that of a first-order high-pass circuit with no dc sensitivity. These ac instruments require a spectrum of unfamiliar calibration techniques with unfamiliar properties.

A simple example is their phase response at low frequencies. Because of their large bandwidths and small damping, piezoelectric accelerometers are often assumed to have near-zero phase shift at low frequencies, whereas in fact their first-order characteristic gives 45º phase lead at the corner frequency (typically about 10 Hz to 15 Hz), asymptotically approaching 90º at dc).

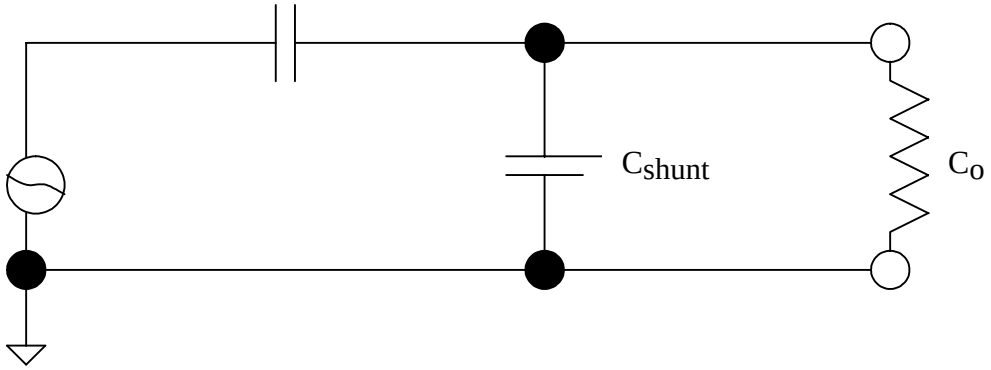

Figure 8— Low-frequency equivalent circuit

A piezoelectric accelerometer is calibrated by monitoring a test motion (often sinusoidal) to which it is subjected, either by measuring the distance amplitude of the motion or by comparing the piezoelectric accelerometer's output with that of a monitor piezoelectric accelerometer that has been calibrated by, for example, the National Institute of Standards and Technology (NIST) in the United States.

A hierarchy has developed in which a number of experiments have developed to the level of primary standards, and all remaining accelerometers are traced to these. At one time, the nature of the traceability was to try to compare a great many working accelerometers directly to the results of the primary experiments by running a select number of working accelerometers through the primary experiments and then using these as working standards. This proved inefficient, however. The early primary experiments were accurate, but tedious and time consuming to perform, while the next step, consisting of comparing working accelerometers to the comparison standards, was accurate and also quick. The actual comparison was done by exposing both accelerometers to a common motion and then comparing the outputs by means of a precision voltage divider. With this technique and with the development of dedicated comparison standards, the calibration community is able to work with special accelerometers that come with double-ended cases, which allow more accurate connections than was the case when two accelerometers were simply attached to a common test fixture. Relative motion is so small that it hardly matters what the common mode motion is at all.

As the calibration community has gained confidence in the new generation of comparison standards, calibration has evolved into a round robin technique in which a great many accelerometers are continuously compared to each other; and primary standards at NIST are introduced just often enough to maintain the overall integrity of the process. Most commercial laboratories deal in comparison standards only.

Over the years, several experiments have been run that have the potential to be considered as primary standards, and some of them have also been modified to supply motion sources that can be used in

conjunction with back-to-back comparison standards to cover special environmental areas. A few examples follow:

a) *Peak-to-peak amplitude sine wave*. This test is based on one of the ideal relationships for a sine wave:

$$G = A \times (2\pi)^2 \times f^2 \tag{3}$$

where

f is frequency (Hz)
A is peak-to-peak amplitude (m)
(less than about 10^{-2} m for electrodynamic vibrators)
G is peak-to-peak acceleration (m/s^2)

With peak-to-peak acceleration determined by means of an optical microscope measurement of amplitude (perhaps with a stroboscope) and almost any frequency standard, it is a simple test with accuracy on the order of a few percentage points. It is of questionable use as a primary standard, primarily because of the difficulty of characterizing the effects of wave-form distortion and because of the need to operate at fairly high amplitudes and/or fairly low frequencies. The same approximately sine wave motion can be used with a comparison standard, on the other hand, with better accuracy and more flexibility.

b) *Reciprocity*. Reciprocity is the name for a series of measurements run to capture the common sensitivities of a pair of reciprocal instruments based on measurements made with the force and velocity terminals interchanged. A reciprocal instrument is the special case of a bilateral electromechanical device in which the transfer function sensitivity for conversion of velocity to voltage is the same as that for current to force. The measurements typically involve very small signals; and in the normal situation where elastic compliance allows relative motion between two devices, a dozen or so measurements must be made with different size masses attached to one of the instruments in order to extrapolate to the zero compliance condition. It is a long and tedious procedure that is run occasionally by NIST and by a few other laboratories to maintain continuity with earlier measurements.

c) *Shock transient velocity change*. Another early experiment aimed at high-amplitude shock calibration used an impact between a dropped ball and an instrumented anvil to accelerate the anvil and a test instrument at up to 10^5 m/s^2. Numerical integration of the test accelerometer's output and comparison of the integral to a separate measure of the change of velocity during the shock allowed calibration of the test instrument at high accelerations. It was a primary standard, reasonably convenient although not terribly accurate. A newer version turns the ball drop axis on its side and propels the ball with compressed air rather than gravity. Addition of a comparison calibration standard to the anvil converts it to a comparison tester, no longer primary, but more adjustable, more repeatable, more convenient, and more accurate.

d) *Laser interferometer*. The latest device in the area takes advantage of technology that was not available a few years ago and may be the means to reversing a trend. As the name implies, the basic technology consists of attaching a fixture to a vibration exciter and attaching a mirror to the fixture so that the fixture's position as a function of time can be read out with the precision of an interferometer by counting fringes. In this case, the process is taken one step further by zero-beating the laser with the vibration exciter so that the fringes disappear. In this condition, the system is referred to as an *intrinsic standard*, taking advantage of both the phase and frequency stability of the helium-neon laser. The device is commercially available and reported to be at least as accurate as the NIST version. That is not likely to change the fundamental concept of traceability, however. That relationship seems to be needed. It could, however, change some aspects of the way the instruments are applied.

11. Centrifuge

11.1 Use of centrifuges

A gyroscope or accelerometer in its fixture is mounted on a centrifuge to determine the sensitivity of the sensor to high-level sustained acceleration. The centrifuge arm usually rotates in the horizontal plane about a vertical rotation axis so that the inertial sensor under test senses an acceleration of $r\omega^2$ along the centrifuge arm and the local value of gravity in the vertical up direction, where r is the arm radius and ω the centrifuge rotation rate (see 11.6.1 for other orientations).

If the centrifuge angular rate exceeds a gyroscope's angular rate capability, then either the gyroscope has to have its IA perpendicular to the centrifuge rotation axis, or the gyroscope must be mounted on a counter-rotating table at the end of the centrifuge arm.

A lesser accuracy centrifuge can be used to determine an accelerometer's overload capacity. Calibration rotation rate and tumble tests before and after the centrifuge exposure can determine whether there are any shifts in bias, scale factor, and other gyroscope or accelerometer model parameters across the centrifuge exposure.

One of the main uses of a precision centrifuge is to calibrate accelerometer nonlinear model coefficients (see IEEE Std 836).

11.2 Lesser accuracy and high-speed centrifuges

A lesser accuracy centrifuge with a short arm radius (less than a meter) can be used for determining accelerometer overload capacity and for doing other inertial sensor qualification testing. It can also be used for scale factor calibration for high-acceleration applications of lesser accuracy accelerometers.

As an example, consider an open-loop capacitive pickoff micromechanical accelerometer on a silicon chip that has to measure accelerations over 10^5 m/s^2. The silicon chip accelerometer and its readout electronics are mounted in a special fixture that is attached to the centrifuge arm with IA along the horizontal centrifuge arm.

A centrifuge that has been employed for calibrating accelerometer scale factor has an arm radius of 12 cm, for which a centrifuge rate of 8717 r/min provides 10^5 m/s^2 of acceleration. An attainable 17 435 r/min provides 4×10^5 m/s^2 of acceleration on the test article. Ultra centrifuges used to separate components from biological specimens attain over 10^6 m/s^2 of acceleration, although the structural stiffness of such a centrifuge's arm is not required to be as great as for measuring an accelerometer's scale factor. A high-speed centrifuge requires an armored containment vessel for safety.

The accuracy of the scale factor calibration is determined by how well the arm radius from the centrifuge rotation axis to the accelerometer's effective proof mass center is measured because the centrifuge rotation rate can be accurately measured. For the class of accelerometer considered, variations in arm length do not necessarily have to be accounted for if the micromechanical accelerometer fixture is well attached to the centrifuge arm. Alternatively, the variation in arm length at different rotation rates could be monitored and compensated for in estimating accelerometer parameters.

Data are collected at different centrifuge rotation rates to provide, for example, the following sequence of acceleration levels:

5×10^3 m/s^2
1×10^4 m/s^2
2×10^4 m/s^2
4×10^4 m/s^2
6×10^4 m/s^2
8×10^4 m/s^2
1×10^5 m/s^2

A quadratic polynomial is least-squares fit to the data to determine scale factor in V/(m/s^2), bias, and the K_2 nonlinearity term. The bias estimate can be compared with the zero-input bias measured with the accelerometer stationary with IA horizontal.

Results can be compared for the accelerometer IA toward and away from the center of rotation. The difference in scale factor measured in the two orientations can be taken only as a measure of the scale factor asymmetry to within the error in measuring the arm radii in the two orientations.

11.3 Precision centrifuge

11.3.1 Setup of centrifuge

The centrifuge arm rotates in the horizontal plane about a central hub that contains a drive motor, slip rings, and an encoder or other readout of centrifuge angle, from which can be derived centrifuge angular rate. The centrifuge angular rate is maintained at a desired value by a servo loop. The inertial sensor under test is mounted on a test fixture at the end of the centrifuge arm, where the fixture could allow the sensor IA to be oriented at various angles to the centrifuge arm, including toward the hub for positive acceleration inputs and away from the hub for negative acceleration inputs, depending on the type of test being conducted.

With the article under test at the end of the centrifuge arm along with the other required equipment and instrumentation (see 11.5.3), weights can be placed at other points on the centrifuge arm (including the antipodal point on the other side of the rotation hub) so that the arm is symmetrically balanced and the bearings evenly loaded when the arm rotates.

A tilt meter on the arm while the arm is put at various positions around its circumferential path can determine the verticality of the rotation axis, with appropriate adjustments being made. As the arm rotates, dynamic and aerodynamic forces cause arm stretch and droop, which can be monitored and corrected for by various means (see 11.5.2). In some centrifuges, the outer case rotates with the arm in order to eliminate the effect of aerodynamic forces on the arm.

11.3.2 Accelerometer nonlinearity calibration

For applications with moderate levels of acceleration (up to 200 m/s^2 or even over 1000 m/s^2), accelerometer scale factor and bias are calibrated in a gravity field tumble test. Nonlinear acceleration sensitive model coefficients are calibrated in centrifuge tests as explained in IEEE Std 836 or in a vibration test (see Clause 10 in this recommended practice and Annex L in IEEE Std 1293-1998).

A precision centrifuge for calibrating accelerometer nonlinear coefficients has a large arm radius (about 1 m to 10 m) and precision instrumentation for imparting known acceleration levels to the article. As described in IEEE Std 836, an accelerometer IA can be oriented at various angles to the horizontal centrifuge arm to calibrate along-IA and cross-IA nonlinearities.

Accurate calibration requires compensation for measured or estimated arm stretch and droop as described in 11.5.2.

11.3.3 Gyroscope acceleration sensitivity calibration

Centrifuge tests can also be used to calibrate gyroscope acceleration sensitivities, particularly for mechanical spinning wheel gyroscopes for which such sensitivities exist. If a single-degree-of-freedom gyroscope has its IA along the centrifuge arm, along-IA acceleration sensitivities can be calibrated after compensation for sensing varying horizontal earth rate as the centrifuge rotates and for sensing centrifuge angular rate due to misalignments and arm droop.

For two-degree-of-freedom gyroscopes and for a gyroscope IA not along the centrifuge arm, the gyroscope can be on a counter-rotating platform at the end of the centrifuge arm (see 11.5.3.2) to prevent the centrifuge angular rate from being input to the gyroscope. However, it is difficult to align and rotate the counter-rotating platform in the exact manner to cancel the centrifuge angular rate. Also, calibration of the gyroscope acceleration sensitivities has to take into account that the acceleration vector is rotating relative to the gyroscope frame.

If a gimbaled, inertially stabilized IMU is tested on the centrifuge, the outer gimbal of the IMU can be parallel to the centrifuge rotation axis and provide the function of a counter-rotating platform. However, the acceleration vector will rotate relative to the IMU inertially stabilized inner platform, even if it is constant in magnitude at a given centrifuge rotation rate. Even if the centrifuge input is not the type that would be seen in the mission for which the IMU is intended, it could be a useful test to see how well inertial navigation can be accomplished for an IMU that is spun up to high accelerations on a centrifuge and then spun down to stop at the original starting position.

11.4 Double turntable centrifuge

A turntable rotating at angular rate ω_2 can be at the end of a centrifuge arm rotating at angular rate ω_1, with an accelerometer's effective center of mass (ECM) being on the turntable rotation axis. The centrifuge and turntable rotation axes are vertical, and the accelerometer IA is horizontal. The centrifuge rate ω_1 serves to apply centripetal acceleration to the accelerometer under test, and the turntable rate ω_2 rotates the accelerometer IA into and away from the centripetal acceleration vector.

This test configuration allows a tumble test to be done at the end of the centrifuge arm and allows the measurement of the accelerometer transfer function at lower frequencies (such as 0.1 Hz) than can be accomplished using a vibrator (see D.3 in IEEE Std 836).

11.5 Centrifuge instrumentation

11.5.1 Measurement of centrifuge rate and angle

The centrifuge rotation angle must be read out to determine the centrifuge rotation rate relative to an accurate clock and frequency standard. There can be an optical disk or inductosyn encoder at the hub of the centrifuge arm with high-rate sampling and computation of the centrifuge rate for input to the arm rate control system that commands the centrifuge motor torque. The centrifuge rate can typically be controlled at the ppm level from revolution to revolution with somewhat less accuracy within a revolution.

The centrifuge rotation period can also be measured by an optical trigger on the outer wall of the centrifuge, which is pulsed when a reflector on the centrifuge arm goes by the laser transmitter on the wall (see 9.3.5). This optical trigger can be part of the capacitive sensing package discussed in 11.5.2.2.

11.5.2 Measurement of arm stretch and droop

The measurement of arm stretch and droop at different centrifuge rotation rates can be accomplished in a number of ways so that accelerometer data can be compensated to allow better estimation of accelerometer nonlinearity model coefficients.

11.5.2.1 Estimation from dual accelerometer data

Subclause 6.6.3 of IEEE Std 836 describes how dual accelerometer centrifuge testing can be used to simultaneously estimate the effect of arm stretch at different centrifuge rates along with the accelerometer nonlinearity model coefficients. Testing with the two accelerometer IAs parallel and antiparallel along the centrifuge arm is required.

11.5.2.2 Capacitive proximity measurements

The end of the centrifuge arm can be equipped with a vertical capacitor plate so that when the arm swings by a stationary second vertical capacitor plate on the wall, a measurement of the distance between the two capacitor plates can be made to measure arm stretch. The amount of arm droop can also be measured capacitively by variation in the distance of a horizontal capacitor plate at the end of the arm from a horizontal capacitor plate protruding from the wall. For a large centrifuge, increased stability results if the stationary horizontal and vertical capacitor plates are on a pier through the floor rather than on the wall.

One problem with this measurement technique is that the deformation of the centrifuge arm as measured at the end of the centrifuge arm does not necessarily define the variation in the radius and tilt at the location of the test article on the centrifuge arm.

11.5.2.3 Quartz rod

A nonload-bearing quartz rod can be inside the centrifuge arm cantilevered off the centrifuge hub so that arm stretch and droop can be measured by variation in the position of a fiducial mark on the centrifuge arm relative to a fiducial mark on the quartz rod.

11.5.2.4 Laser metrology

Laser metrology using the instruments described in 4.20.2 and 4.20.3 can be used to measure arm stretch and droop. If the laser beams are enclosed in tubes, the effect of air currents on laser propagation during centrifuge rotation can be reduced, although the effects of air pressure, temperature, and humidity variation remain.

A laser tracker can be used to first survey precisely the position of the various capacitor sensors placed on the wall surrounding the centrifuge (see 11.5.2.2). Static calibration of the capacitive sensors can also be performed with the laser tracker, as can measurements of the position and orientation of the inertial sensor or system under test.

Dynamic measurements can be obtained by using a wide-angle retroreflector mounted at the end of the centrifuge arm. If the centrifuge building is expected to move during the operation, multiple trackers can be used to provide a self-calibration network based on redundancy.

Centrifuge axis wobble may be measured by using a laser beam marker projecting toward the ceiling along the axis of the centrifuge. A beam displacement detector mounted on the ceiling can provide the angular displacement. The advantage of dynamic measurements is that the arm droop and stretch are continuously measured during the rotation as opposed to the discrete measurements provided by the capacitive sensors.

Photogrammetry is another technique that can be useful for the measurement of arm droop and stretch. Using multiple time-synchronized cameras, arm extremity and fiducial marks attached to the wall can be used to reconstruct the three-dimentional geometry. A redundant number of cameras can be used to self-calibrate the entire geometry of the facility.

11.5.3 Equipment on centrifuge arm

11.5.3.1 Proximity and data acquisition equipment

Equipment required to operate the test article (namely, accelerometer or gyroscope), such as power supplies, or frequency references, can be on the centrifuge arm with the test article, but at a smaller radius if necessary so that a less severe environment is experienced. Data acquisition equipment such as A/D converters can also be on the centrifuge arm.

11.5.3.2 Turntable

A turntable can be at the end of the centrifuge arm to counter-rotate to take out centrifuge rotation rate for gyroscope testing (see 11.3.3) or to rotate an accelerometer's IA into and away from the centrifuge centripetal acceleration vector for accelerometer transfer function and tumble testing (see 11.4).

11.5.3.3 Thermal control on centrifuge arm

To calibrate accelerometer model coefficients as functions of temperature or to demonstrate performance over the temperature range of an application, a thermal chamber would have to be placed on the centrifuge or double-centrifuge arm (see 12.2). For example, nontemperature-controlled operation over the range –65 °C to +85 °C might be required for automotive or military applications with or without thermal compensation.

To reach the lower temperatures, the thermal chamber might require liquid nitrogen (or carbon dioxide) cooling either from a liquid nitrogen dewar on the centrifuge arm or from liquid nitrogen piped onto the centrifuge arm through a rotary couple. The weight of the thermal chamber combined with the weight of the test article could reduce the acceleration that a centrifuge could impart to the test article due to the load on the centrifuge or double-centrifuge bearings.

Testing of a small test article, such as a silicon chip micromechanical accelerometer, allows thermal control with a small thermoelectric heater-cooler rather than a thermal chamber, with a resulting decrease in the load on the centrifuge or double-centrifuge bearings. Only electric power has to be brought through slip rings for the thermoelectric heater-cooler and article under test. The temperature of the test article could be monitored by a thermistor with a thermal controller maintaining the temperature at each desired set point within the operating temperature range.

Thermoelectric heater-coolers are commercially available so that current flowing in one direction cools a surface attached to the test article (perhaps covered with insulation) and discharges heat through another surface into a heat sink. Electric current flowing in the other direction heats the test article and cools the heat sink. In order to reach the lower temperatures on the test article, the heat sink might have to be provided with, for example, a pellet of solid carbon dioxide.

In order to test at lower temperatures without water condensation or frost buildup, the article under test, the thermoelectric heater-cooler, and the heat sink could be in a hermetically sealed chamber bathed in dry nitrogen on the centrifuge arm, or the whole centrifuge or double-centrifuge could be bathed in dry nitrogen.

11.5.4 Slip rings

Slip rings provide rubbing contact between the stationary and rotating parts of the centrifuge or double-centrifuge for the transmission of electric power and data signals. Ground lines would also go through the slip rings.

AC power could be transmitted through slip rings to regulated power supplies on the centrifuge arm to output the dc and ac voltage levels, frequencies, and phases required by the test article and other equipment.

Data from the test article could be A/D converted and otherwise signal-conditioned by a microprocessor and its associated electronics on the centrifuge arm before going through the slip rings as, for example, a digital serial data stream. The data acquisition computer off the centrifuge arm would acquire this data stream along with data from the centrifuge instrumentation, such as centrifuge rate and arm stretch and droop.

11.5.5 Radio transmission of signals

Data from the microprocessor on the centrifuge or double-centrifuge arm can be sent to the data acquisition computer using a radio link rather than slip rings (namely, wireless data acquisition). The slip rings then are used only to bring electric power and grounding to the equipment on the centrifuge or double-centrifuge arm.

There are commercially available modules to accomplish this radio transmission. The radio transmitter and its antenna on the centrifuge arm interface with the microprocessor. At a radio frequency of about 2 GHz, a 100 kb/s digital data stream is sent to the receiving antenna. The radio receiver interfaces with a board in the data acquisition computer.

The sending and receiving antennas are each single, omnidirectional rods. The receiving antenna could be right over the rotation axis of the centrifuge, and the sending antenna could be on the rotation axis so there is no Doppler shift between the sending and receiving antennas.

On a double-centrifuge, the receiving antenna would again be over the main centrifuge rotation axis. The sending antenna is on the turntable rotation axis at the end of the centrifuge arm. Again there is no Doppler shift between the sending and receiving antennas because the line-of-sight velocity between the sending and receiving antennas is zero.

The data acquisition computer acquires the digital data stream from the radio link and also acquires other data such as the centrifuge rotation rate. The data can be filtered or averaged before being saved to disk at a lower rate. It is generally good test philosophy to over-sample and acquire data at a high rate and then to filter and decimate to the lower rate required for analysis.

11.5.6 Vibrator on centrifuge arm

A vibrator can be put on a centrifuge arm to test the response of a device under vibration at high accelerations, specifically a gyroscope with a gas-bearing spinning wheel. The gyro can be oriented with spin axis vertical on the vibrator with vibration axis along the horizontal centrifuge arm. The results of the test may cause a redesign of the gas-bearing wheel.

The vibrator's electromagnets may not have enough force to vibrate the armature at high centrifuge rates. Therefore, a bungee cord can be attached to the vibrator, with its tension increasing as the centrifuge rotation rate increases, so that the vibrator electromagnets can vibrate the armature back and forth about its null position.

11.6 Other rotating inertial sensor test equipment

11.6.1 Turntable with tilted axis of rotation

Consider a single-axis turntable (see 9.2) whose rotation axis is tilted by a small angle ϕ to the vertical. Consider an accelerometer mounted on the turntable with its ECM over the turntable rotation axis and with its IA perpendicular to the turntable rotation axis.

Rotation of the turntable inputs a sinusoidal acceleration to the accelerometer with amplitude $g \sin \phi$ at the frequency of rotation of the turntable and allows the transfer function to be calculated for a low-level

accelerometer, such as for space or automotive applications (see D.4 in IEEE Std 836). However, this technique could not be used for a three-degree-of-freedom accelerometer (see 11.6.3).

11.6.2 Swinging pendulum

Let an accelerometer be at the end of a pendulum of length ρ that oscillates an angle $\pm \theta$ about the vertical. Let the accelerometer IA be along the pendulum axis toward or away from the center of rotation of the pendulum, and let the pendulum angular velocity at the low point of the swing be ω. At this low point, the acceleration sensed by the accelerometer is $\pm (\rho\omega^2 + g)$, where g is the local acceleration due to gravity and where the plus sign corresponds to IA pointing toward the pendulum center of rotation and the minus sign corresponds to IA pointing away from the center of rotation.

If $\theta < \pi$, then the sensed acceleration oscillates between $\pm (\rho\omega^2 + g)$ and $\pm g \cos\theta$, where the latter is zero if $\theta = \pi/2$. Hence the swinging pendulum can make sensed acceleration vary between zero and a positive or negative maximum, where the magnitude and frequency of the variation depends on the length of the pendulum.

If the arm is made to rotate continuously, then it acts as a vertically oriented centrifuge with $\pm g$ variations in the acceleration sensed along the centrifuge axis, plus the effect of any variation in arm speed from the bottom to the top of the swing.

11.6.3 Nonuniform mass cavity

An accelerometer within a nonuniform (lead or other dense material) mass cavity will sense different accelerations at the 10^{-8} m/s^2 level as the nonuniform mass cavity rotates at different angles relative to the accelerometer IA. Such a rotating mass cavity can be used to calibrate an IA-vertical seismometer that must sense 10^{-8} m/s^2 variations about 9.8 m/s^2 between perhaps 0.1 Hz to 100 Hz.

The same effect can be accomplished at low frequencies by moving a large lead ball near and away from the accelerometer. For example, a 50 kg lead ball moved to within a few centimeters of an accelerometer will cause of the order of 10^{-7} m/s^2 input to the accelerometer.

The lead ball or rotating mass cavity technique can be used to calibrate the scale factor of a single-degree-of-freedom low-level accelerometer intended for space applications, where the IA is oriented horizontally and the large mass brought near to and away from the accelerometer.

Unfortunately, this technique will not work for, for example, a three-degree-of-freedom low-level space accelerometer, such as the design that centers a proof mass in a cavity with electrostatic forces. The electrostatic support is not strong enough to counterbalance the vertical component of earth's gravity while the heavy mass is moved near to and away from the horizontally oriented IAs unless the suspension in the vertical direction can be greatly increased without uncompensably affecting the performance of the suspensions in the horizontal directions.

12. Environmental chambers

12.1 Thermal control on a test table, vibrator, or centrifuge

12.1.1 Flange temperature control

The mounting flange of an inertial sensor could be controlled at a certain set point with the internal temperature control of the inertial sensor provided by the manufacturer being at a set point somewhat above that of the flange. In this way, the inertial sensor control can be accomplished by heaters with heat flow out from the inertial sensor being through the mounting flange, especially if the inertial sensor were covered

with insulation. This approach would emulate the thermal control provided by a thermally controlled IMU in an inertial guidance and navigation system.

If there were no thermal control provided by the manufacturer for the inertial sensor under test, thermal control of the mounting flange would allow the inertial sensor to be operated at different temperature set points for temperature sensitivity tests (see 6.2).

12.1.2 Heated oven control

The whole inertial sensor could be inside a thermally controlled oven or enclosure on the table top, vibrator, or centrifuge, especially if the inertial sensor were not provided with manufacture-supplied thermal control and it were important to test the inertial sensor at a well-controlled temperature set point above ambient room temperature. The set point could be varied to test temperature sensitivity.

For the most precise control, a double oven could be provided. The outer oven would be controlled by heaters to perhaps 0.1 °C at a set point above room temperature, and the inner oven could be controlled with heaters to perhaps 0.01 °C or better at a still higher set point.

The oven or enclosure would be provided with a combination of electric strip heaters and insulation to obtain the required performance. There would be monitor and control thermistors or other temperature monitor devices (see Clause 16). Commercial temperature controllers could be employed, unless special control performance is required, in which case specially built controllers would be employed.

12.2 Refrigerated and heated chambers

To calibrate inertial sensor model coefficients as functions of temperature or to demonstrate performance over a wide temperature range (such as –65 °C to +85 °C for automotive or military applications), a refrigerated and heated thermal chamber would have to be employed. It could be placed on the table, vibrator, or centrifuge. Another option for a single-axis rotary table or a vibrator is to have the sensor mounting fixture protrude into the chamber, with the rotary table or vibrator not having to bear the load of the chamber.

Commercial refrigerators can reach these low temperatures, or liquid nitrogen (or carbon dioxide) cooling can be used. Which technique is employed could be decided on the basis of cost. For infrequent tests, liquid nitrogen cooling might be the optimal choice, whereas a refrigerator with recycled coolent has lower operating costs for frequent testing.

12.3 Barometric chambers

A temperature-controlled barometric chamber with a rapid drop in temperature and pressure to near vacuum conditions can be used to observe the effects of launching an inertial sensor or a whole inertial reference or guidance system into space and then to observe continued operation in the vacuum of space.

12.4 Equipment for electromagnetic susceptibility and emissions testing

An inertial sensor can be operated in a screen room to shield from external electric fields so that the electric field emanating from an operating sensor can be measured. A Gauss probe can detect if there is any magnetic field emanating from the operating sensor (see 4.9).

A dc electric field, an ac (such as radio frequency) electromagnetic field, or an EMP (such as caused by a nearby lightning strike) can be impinged on an inertial sensor to determine its performance through and across such an environment, if required. Performance through and across a dc magnetic field is discussed in 4.9.

An EMP can be generated by discharging a high-voltage capacitor bank across a spark air gap, where the pulse-generating equipment is sized to yield the environment to which the inertial sensor could be subjected in a mission.

12.5 Acoustic absorption and generation

If equipment in a test laboratory generates a great deal of acoustic noise, the walls of the laboratory, or of a smaller room built around the equipment, can be covered with acoustic absorbing tiles for the comfort and safety of persons involved in the testing. Acoustic absorbing tiles typically have cone-shaped protuberances to avoid the focusing of reflected sound and are made of a rubbery material that is highly absorbent of sound.

An inertial sensor can be placed in a chamber with a loud speaker to see whether the performance of the sensor is affected by the acoustic environment that might be encountered in a missile, helicopter, or other such mission. The shape of the chamber could be such that the sound from the loud speaker is focused onto the test article.

12.6 Other environmental chambers

The performance of an inertial sensor through and across exposures to sand and dust, salt spray, fungus, etc., can be tested, if required.

13. Nuclear radiation effects testing

13.1 Use of nuclear radiation testing

Testing is required at radiation test facilities to verify any requirements that are placed on inertial sensor performance during and after exposure to doses of radiation such as exposure associated with the natural space environment and/or from a hostile nuclear threat.

An inertial sensor to be tested is exposed to the radiation or beam from a nuclear radiation device. The sensor could be operating or nonoperating during the exposure and could have its input and other axes at various orientations relative to the radiation and the local vertical, depending on the type of test (see 6.5). Nonproximity sensor electronics can be exposed to the radiation along with the sensor and its proximity electronics, or one part can be exposed and the other shielded in order to separately determine the radiation sensitivities of the nonproximity electronics and of the sensor and its proximity electronics.

Shifts and transients in an operating inertial sensor’s output can be sought during and after exposure to the nuclear radiation as compared to the output before the exposure. Slew or tumble calibrations of bias, scale factor, and other model parameters can be compared from before to after the exposure for a sensor that was operating or nonoperating during the exposure and also can be compared during the exposure for operating sensors (see 6.5).

Physical mechanisms for predicting shifts and transients across the exposure should be derived, including the effects of temperature rise, physical damage, and charge accumulation; and the results of predictions should be compared with observed behavior. Theoretical predictions involve calculating energy deposition along the path of the radiation, including the effects of shadowing.

Physical mechanisms, including the effects of temperature rise, physical damage, and charge accumulation, should be modeled, and the results of predictions should be compared with observed behavior. Theoretical predictions involve calculating energy deposition along the path of the radiation. When performing this calculation, the effects of shadowing must be taken into account.

13.2 Basis of radiation testing requirements (radiation effects)

Specification of the radiation environment typically defines the various types (such as neutron, X-ray, gamma ray, and charged particles) and their relative concentration versus energy (namely, spectra). Radiation hardness specifications and effects testing typically fall into one the following categories:

a) Thermo-mechanical effects (TME) from rapid deposition of a high fluence of X-rays in the cold–warm end of the spectrum that cause a rapid temperature rise, temperature gradients, and stresses, with subsequent temperature transients

b) Ionizing dose rate effects from rapid deposition of high-energy X-rays, gamma rays, and/or electrons (such effects include survival, upset threshold, magnitude of transient effects, and recovery time)

c) Total ionizing dose (TID) effects (such as permanent degradation from mission cumulative TID)

d) Displacement damage from non-ionizing energy loss (typically due to cumulative fluence of high-energy neutrons and/or protons)

e) Single event effects (SEE) from low flux of energetic ionizing particles (typically protons and/or heavy ions (HIs) found in the natural space environments)

Given these combined environments, transient and permanent shifts may occur in sensor (and proximity electronics) performance due to heating, physical damage, and/or charge accumulation. Consequently, inertial instruments (namely, sensors plus proximity electronics) must be tested to determine whether they satisfy performance requirements, both during and following exposure to the combined specified radiation environments. The test facilities and test methods defined here are intended to collectively evaluate radiation effects on performance of the inertial sensing elements and on proximity electronics (required for proper instrument operation).

Particle fluence is expressed as the total number of particles per square centimeter that impinge on the device or sensor over the mission (or some specified segment of the mission time). The rate at which that fluence accumulates or is deposited is described as the particle flux in particles per square centimeter second. Because the various radiation effects are functions of the particle specie, the particle energy, and the target material, the radiation environment is specified as a set of spectra (namely, differential or integral particle flux or fluence versus particle energy) for each of the radiation (namely, particle) types. Also given that spectral characteristics of radiation simulators (namely, test facilities) will differ from spectral characteristics of the natural space and/or threat environment, selection of test flux and/or fluence for a given radiation type (namely, particle specie) is typically normalized to a single energy equivalence to allow more meaningful correlation of results and adjust for spectral differences between the specified environment and test facility.

The principal mechanism of energy deposition by gamma and high-energy X-rays as they interact with materials such as electronic semiconductor devices is in the form of ionization. The international system of units (SI) defines the gray (Gy) as the unit for absorbed ionization dose, where one Gy corresponds to the deposition of 1 J/kg.[10]

Ionizing total dose can lead to charge trapping in oxides and interface state formation at silicon/oxide interfaces (Ma and Dressendorfer [B15]). This development leads to shifts in device operating parameters. The rate at which the ionizing total dose accumulates within the sensor and/or proximity electronics (namely, dose rate, which is defined as the number of grays per second) may impact observed performance degradation due to the relative rate of recovery (or annealing) of trapped oxide charge and accumulation of interface states over time. Recent studies show some technologies are sensitive to low-dose rate enhancement of total dose effects in space so that degradation and failure occurs at a lower total dose than observed when exposed at higher dose rates (Johnston, et al. [B14]). Hence, tests for not only the effects of TID, but also the dose rate effects must be conducted (Messenger and Ash [B16] pp. 183 and 361).

[10]The centimeter-gram-second (cgs) unit for absorbed dose of ionizing radiation is the rad, which is defined as the absorption of 100 erg/g so that 1 rad = 0.01 Gy.

In modern integrated circuit (IC) technologies, single energetic particles can deposit energy in critical regions of the device to cause ionization and induce SEE (Shapiro, et al. [B17]). The amount of energy deposited is a function of the ion specie, its energy, and material properties of the device with which it is interacting (usually Si). The energy deposited by a particle per unit length of the device/material traversed is referred to as its *linear energy transfer* (LET) and is usually given in units of mega-electron-volt square-centimeter per milligram. Ions of high LET deposit more energy per distance traversed through the device than low-LET particles and, hence, induce greater ionization leading to greater risk of SEE. The probability of SEE is also a function of the technology and region of the device through which the ion passes.

HIs are of sufficient LET to directly induce single event transients and logic upset (SEU). Single event "latch-up" (SEL) occurs when a parasitic transmission path is turned on within the device active regions and held on due to regenerative feedback (Johnston and Hughlock [B13]). If latch-up continues uninterrupted, it can lead to permanent degradation and possible failure. Unlike HI, protons are not of adequate LET to directly cause SEE. However, protons with energies of roughly 30 MeV or greater can interact with the device to yield energetic secondary ions within the device that have adequate LET to cause SEE.

The facility types and standard test methods for radiation testing in each of the environments are described in 13.3 through 13.7.

13.3 TID effects testing

Radiation testing for the effects of TID is typically performed in a steady-state low-dose rate environment. Radiation sources available for total dose testing include X-rays, gamma rays (Co-60, Sr-90, and Cs-137), electrons, and protons (cyclotrons). As noted in 13.2, each source has different energies or spectral characteristics and, hence, will affect the inertial sensor and/or proximity electronics differently.

The most common source for total dose testing is the Co-60 source. The decay of Co-60 provides two characteristic gamma rays at 1.17 MeV and 1.33 MeV as it decays to Ni-60, with a half-life of 5.3 yr. The test article is placed in a chamber at a specified distance from the Co-60 source (for the desired dose rate). Testing should be performed in accordance with specific procedures as defined in MIL-STD-883E Method 1019 or MIL-STD-750E Method 1019.4.[11]

TID testing is typically performed with exposure occurring under active bias (namely, applied voltage) of active proximity electronics. All critical sensor/instrument performance parameters are evaluated at several TID intervals over some specified range of interest. A subset of critical sensor and/or proximity electronics performance parameters may be monitored in-situ during exposure. The exposure time(s) are selected to achieve a sequence of desired total dose intervals up through the specified TID requirement for the particular application. A specified total dose that may accumulate in time frames of 10^{-3} s to 10^{3} s in a strategic weapon launch or over years in space can be accomplished in hours using a Co-60 source. In many cases, TID testing is continued well past the specified TID requirement for a given program (possibly to parametric or functional failure of the sensor and/or critical proximity electronics) to determine range of design margin for that environment and mission/application.

13.4 Ionizing dose rate effects testing

The extremely rapid deposition of prompt ionizing radiation (gamma rays and X-rays) associated with a strategic weapon burst (on the order of 10^{-9} s to 10^{-3} s) can cause very large transients that may saturate and in some cases (if power is not interrupted) cause burnout of the sensor and/or critical proximity electronics to that inertial sensor. Testing for prompt dose rate effects typically are performed to

a) Verify survival of the sensor and proximity electronics up through maximum prompt dose rates as specified for a given mission, and

[11]Information on nuclear radiation test standards may be found in 2.3.

b) Determine the threshold for prompt-dose–rate-induced transient upset, magnitude of the transient response, and transient recovery time on the test article.

Dose rate testing is typically performed using either a linear accelerator (LINAC) or a flash X-ray machine (FXR). Dose rate testing is performed in accordance with MIL-STD-883E Method 1020 and Method 1021. Testing is typically performed over a series of pulsed ionizing dose rates starting at a level below expected (or required) upset threshold for the sensor and/or critical proximity electronics, and the testing is ideally carried through the facility maximum dose rate or sensor/electronics failure, whichever comes first.

Quite often survival testing is performed in a pinch-beam mode, with radiation pulse-widths on the order of 20 ns to 50 ns. Dose rate upset testing (with transient recovery time evaluation) is typically performed in wide-pulse mode (typically on the order of 1 μs to 10 μs). Like TID testing, dose rate testing is performed with sensor and active proximity electronics operating under active bias, possibly under dynamic operating mode (as required in the system application). Evaluation of critical sensor and/or proximity electronics operating parameters is often performed between the various dose rate intervals to determine whether the dose rate (or cumulative TID) has degraded performance.

Dose rate test facilities tend to create significant electrical noise during the radiation pulse within the test environment. In some cases, an EMP or system-generated EMP (SGEMP) as the pulse of gamma rays or electrons from the source interact with test system cabling and metallic enclosure. Therefore, care must be taken in shielding and grounding schemes in the test configuration to avoid or mitigate these effects along critical signal paths that could otherwise obfuscate measurement of the radiation-induced effects.

13.5 Displacement damage effects testing (neutron and protons)

A high fluence of energetic protons or neutrons can cause displacement damage that degrades crystal purity and structural regularity. Such degradation may, in turn, degrade critical electrical and mechanical properties (Messenger and Ash [B16]). Historically, displacement damage has been a concern due to the accumulation of neutrons from the hostile nuclear threat. However, displacement damage is also a concern for long-term space missions due to the gradual accumulation of significant proton fluence (such as protons trapped in the Van Allen Belt and solar protons). Neutron or proton irradiation is typically normalized to a 1 MeV equivalence into a given material to account for differences between the specified threat or mission environment and the test facility spectrum.

A burst of fast neutrons can be provided by a fast-burst nuclear reactor (FBR). A subcritical piece of plutonium with a hole in it has another piece of plutonium inserted into it and quickly withdrawn. While the other piece of plutonium is in the hole, the plutonium is at critical mass, which causes a burst of neutrons. An FBR can create a gamma radiation spectrum by having an appropriate target material between the test article and the source of neutrons.

In addition, there are water-cooled reactors that allow steady-state fast (rather than thermal) neutron irradiation.

Typically, neutron displacement testing requires reactor calibration to a 1 MeV equivalent spectrum, with neutron fluence measured in neutrons per square centimeter. Typically, neutron exposure is performed as a passive test (namely, no applied voltage or dynamic operating conditions). Samples of the test article are exposed to a sequence of neutron fluences (up through maximum required or specified fluence) with parametric testing and dynamic instrument operation evaluated on separate test samples exposed to different cumulative neutron fluences.

In some cases, the same sample may be exposed sequentially through the specified radiation levels with parametric measurement intervals applied. However, because neutron and proton irradiation leads to activation of the test articles, the delay cycle prior to safe handling levels often makes this approach more costly in time and, hence, less attractive than using multiple samples each exposed to a different neutron fluence.

Neutron testing for displacement damage should be performed in accordance with MIL-STD-883E Method 1017 or MIL-STD-750E Method 1017.2.

In addition, cyclotrons are available as proton sources that can be used to simulate the natural space environment to evaluate the effects of proton-induced displacement damage.

Testing for proton-induced displacement effects may be performed using a neutron test facility or a cyclotron, provided the displacement fluence for both the space mission environment and test facility (neutrons or protons) is normalized to a 1 MeV equivalent spectrum (either proton or neutron equivalence). Care must be taken in either case (cyclotron protons or FBR neutrons) to track cumulative TID to ensure that cumulative TID is kept sufficiently small (relative to the displacement fluence) or sufficiently characterized for its own effects, in order to isolate or identify the non-ionizing displacement-fluence-induced effects.

13.6 SEE testing

As described in 13.2, SEE are most likely to be an issue (if at all) for the proximity electronics that, in many cases, must be tightly coupled to the sensor during any and all in-situ radiation exposures. It is extremely unlikely that the inertial sensor itself will experience SEE. SEE may be induced directly by HIs associated with the natural space environment or through proton induced secondary ion emission due to trapped and solar protons in the natural space environment.

Testing to evaluate the risk and rate of HI-induced SEE in the proximity electronics associated with an inertial sensor should be performed in accordance with EIA JESD 57. HI testing is performed at a Van de Graaff generator. SEE testing must be performed with devices actively biased and typically operating in dynamic mode consistent with system application.

SEE testing to evaluate proton-induced SEE has not yet been standardized under MIL-STD-883E nor in ASTM methods. Testing for proton-induced SEE should be performed at a cyclotron facility. Because HI and proton beams may be collimated, it is reasonable to isolate the exposure of each potentially sensitive active device within the inertial instrument proximity electronics, while monitoring integrated instrument (namely, subsystem) performance for evidence of SEE. Testing should be performed at multiple proton energies and/or over a broad range of particle LETs in order to determine the SEE upset threshold and upset cross-section as a function of particle energy and/or LET.

13.7 TME testing

The rapid deposition of prompt X-rays from a nuclear weapon environment into the various materials associated with the structural (namely, packaging) and mechanical sensing elements of an inertial instrument can cause an abrupt temperature gradient across the material. The resulting mechanical responses of that material are called *thermo-mechanical effects* (TME).

The abrupt nonuniform temperature increases caused by the cold-warm portion of the prompt X-ray spectrum following a nuclear detonation creates internal pressure within the material. Before the material can expand, compressive and tensile waves (namely, shock) are propagated. In other words, the time for energy deposition and change in temperature distribution is short compared to the time required for the material to mechanically respond and reach equilibrium (namely, faster than the speed of sound in that material). As the shock wave traverses the structure or material, catastrophic failure can occur because the material cannot respond and expand to equilibrium quickly enough. This failure includes bond separation at material interfaces, change of phases within the material (such as vaporization and melting), spallation, blowoff, delamination, fracture, and cracking.

The nature and magnitude of TME depends on the X-ray flux and spectral properties and magnitude of the X-ray−induced temperature rise. TME is also a function of the material properties (such as atomic number,

specific heat, modulus of elasticity, Poisson ratio, expansion coefficient, and change of phase temperatures), material dimensions (such as thickness), and velocity of sound in the material. It also depends on structural geometry and physical properties at boundaries/interfaces.

Testing to simulate TME includes mechanical shock testing, magnetic flyer plate testing, gas-gun testing, and light-initiated high-explosive shock testing. This testing requires large facilities that provide high flux at the cold and warm end of the X-ray spectrum and over sufficient area for board and box level testing. These mechanical effects tests do not require active bias of proximity electronics or sensor excitation/bias. Sensor performance measurements can be performed before or after TME exposure or stress.

14. Counter and frequency readouts

14.1 Counters and continuous counters

Some inertial sensors have a square wave or sinusoidal output voltage. Examples are a pulse-torqued gyroscope or accelerometer, an analog torque signal that has gone through a current-to-frequency or voltage-to-frequency converter, and the vibrating beam accelerometer (VBA). The measure of the inertial sensor output (namely, nongravitational acceleration for an accelerometer, angular rate for a gyroscope) is the frequency of the output signal or is the number of rising zero crossings of the output signal that occur in a given period of time.

The rising zero crossings of the square wave or sinusoidal output voltage can be used to increment a counter. A Schmidt trigger can be employed to prevent noise jitter from causing multiple counts from a single zero crossing.

A pulse-torqued inertial sensor can have positive and negative pulses. Either an up-down counter can be used, or separate counters can be used for the positive and negative pulses.

The value of the counter is read by a data acquisition computer when there is an interrupt trigger from a clock counter (namely, event-per-time mode). Alternatively, the clock counter can be read when a certain number of rising edges have been output from the inertial sensor (namely, time-per-event mode). Time-per-event mode is likely to have greater resolution than event-per-time mode because the clock frequency (such as 10 MHz) is likely to be higher than the frequency output from the inertial sensor. Equal time samples (namely, event-per-time mode) are needed in guidance system applications, but time-per-event mode might be desirable in sensor-level testing because of the greater resolution.

The sensor counter reading at this interrupt time minus the sensor counter reading at the previous interrupt time divided by the time interval between interrupts is the frequency in the event-per-time mode if the counter is not reset between interrupts. The clock counter reading at this interrupt time minus the clock counter reading at the previous interrupt time divided by the number of sensor output rising edges is the period in the time-per-event mode. If the magnitude of the difference of counter readings is anomalously large, then the difference must be corrected, for the rollover of the binary counter length N bits that has occurred, by adding or subtracting 2^N.

Many commercial counters are reset when they are read and do not start counting zero crossings again until so commanded or after a certain period of time so that there is a dead zone between counter measurements (see 4.15).

However, when the reading of a continuous counter is triggered, the counter value is latched into a register, which is read by the computer; and the counter continues counting with no dead zone. Maintaining coherency between counter readings is of great value in inertial sensor testing. If a continuous counter is not commercially available, either as a separate device or on a board that plugs into the computer backplane, then a continuous counter might have to be specially built.

If there are two or more frequency outputs from a sensor, such as a dual-beam VBA, then the two or more counters should be latched simultaneously at an interrupt time. In this manner, the data have the same time tag despite whatever latency exists in the data acquisition computer's interrupt service routine.

14.2 Period readouts

Time-per-event mode counter output provides a period readout because the time divided by the number of rising edges output from the inertial sensor is the period of the sensor waveform output. If the fundamental output of the inertial sensor is supposed to be frequency, then one divided by the period is the frequency, albeit at a nonuniform output time interval. However, the output time interval is usually close enough to being constant that the resulting frequency measurement can be used in analyzing the results of sensor level testing, even though it cannot be used in an inertial navigation and guidance mission.

If a 10 MHz or other clock frequency does not have enough resolution for the period computation, then a larger number of events can be counted before the time counter is read. This is essentially applying rectangular filtering to the data.

If higher rate data are desired with higher resolution so that, for example, triangular filtering can be applied to the data to get greater quantization noise reduction, then the fractional pulse missed when the time counter is sampled can be determined. One way to determine the fractional pulse missed is to start charging a capacitor at the interrupt time until the second rising clock edge after the clock counter is read. The voltage on the capacitor is then a measure of the fractional pulse missed.

14.3 Frequency readouts

The event-per-time mode counter output divided by the time interval gives frequency at a uniform time interval, but typically with not enough resolution. The period readout at a nonuniform time interval can be interpolated in software to give phase information at a uniform time interval. The change in phase over a uniform time interval divided by the time interval gives the frequency, albeit with a certain latency.

Instead of interpolating to get phase, it could be extrapolated in software to obtain phase without latency, as is done in PLL hardware.

14.4 Phase-locked loops (PLLs)

An analog PLL slaves a high-frequency voltage-controlled crystal oscillator (VCO) to a lower frequency input signal, thereby getting greater resolution in reading out the phase of the input signal at uniform interrupt times. A VCO has a quartz crystal driven by an oscillator loop whose frequency varies with an applied voltage because of the piezoelectric effect in quartz.

The block diagram of a PLL is given in Figure 9. A square wave is input to the PLL, either as the direct output of an inertial sensor or as generated to have the same rising zero crossings as a sinusoidal wave output of the inertial sensor.

A VCO whose frequency is near some multiple N (namely, a power of 2) of the frequency of the input square wave runs a binary counter. The output of this counter divided by N is compared with a count of the input square wave rising edges. If the two counts differ, the voltage on the VCO is adjusted to bring the two compared values back into synchronism.

At an interrupt time, the VCO high-frequency counter is read by the data acquisition computer. The VCO count at this interrupt time minus the VCO count at the previous interrupt time gives a high-resolution measure of the change in phase of the original input signal between interrupt times. The interrupt rate must be high enough so that there is no ambiguity in the phase computation because of rollover of the VCO counter. The change in phase divided by the time interval is the frequency.

An analog PLL is likely to be a specially built device tuned to the frequency and phase resolution requirements of the particular inertial sensor whose output is being measured.

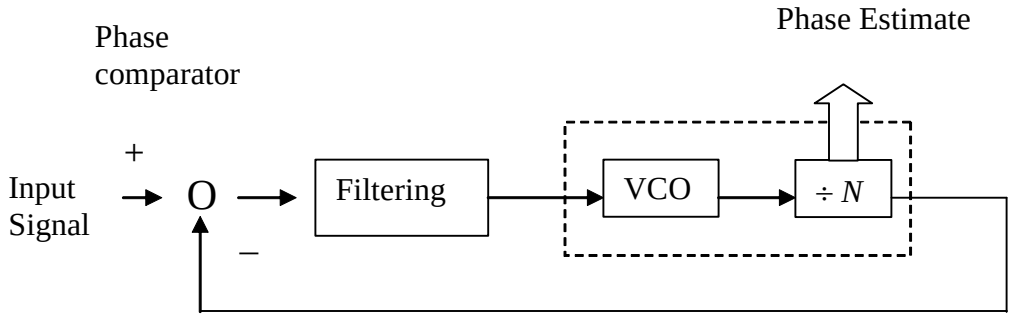

Figure 9— Analog phase-locked loop (PLL)

14.5 Other ways of reading out frequency

There are commercially available digital PLL chips.

A high-rate (namely, several megahertz) A/D converter could be used to read the voltage on a sinuosidal waveform. At an interrupt time, a least-squares fit of a sinusoid (namely, amplitude, frequency, and phase) is made to the A/D readings over one or a few cycles prior to the interrupt time. The fitted sinusoid's phase is output for the interrupt time.

15. A/D conversion readouts

15.1 Commercial voltmeters

A commercial integrating voltmeter provides a very accurate way to read out a primary voltage output from an inertial sensor, such as the output from an analog torque loop (see 4.5).

15.2 A/D converters

Other analog voltage signals from an inertial sensor test (such as auxiliary signals from the sensor and temperature readings) are most conveniently read by an A/D converter board that plugs into the data acquisition computer's backplane. Such an A/D converter would typically have 12 b of precision. The voltage range can be set to ± 1 V or ± 10 V, etc.

There could be sample-and-hold at an interrupt time, so that the A/D converter can cycle through reading the voltages with the assurance that they have the same time tag. True differential rather than single-ended readings can also be made, where the voltage difference between the input line and a ground line special to the channel is read.

15.3 Voltage- and current-to-frequency converters

The primary voltage or current output from an inertial sensor, such as the output from an analog torque loop, can be converted to a frequency by a voltage- or current-to-frequency converter (see 4.14), which can then be read by counters, etc.

One way to implement a voltage-to-frequency converter is to have a VCO (see 14.4) with a frequency that varies as a function of applied voltage, where the input voltage is amplified to a level that gives the desired frequency variation in the VCO over the possible range of input voltages.

16. Temperature monitoring

16.1 General comments

Temperature-monitoring equipment for inertial sensor testing should not disturb the performance of the inertial sensor. For example, large currents or switching frequencies should not be employed in the temperature monitoring.

Conversely, the temperature-monitoring electronics should not be disturbed by the operation of the inertial sensor. For example, ground lines for the temperature-monitoring electronics should not share the ground lines for power supplies.

The inertial sensor under test could have manufacturer-supplied internal temperature-monitoring devices with output signals that would have to be monitored during the test. Additional temperature sensors could be installed on the test station to monitor the temperature of the inertial sensor electronics of the case, of the flange, and of the air of the room in which the tests are conducted.

Signals from temperature-monitoring sensors would be acquired by the data acquisition system, whereas signals from temperature-controlling sensors would be used by temperature controllers to control the inertial sensor temperature or the temperature of a thermal chamber or oven in which the inertial sensor is tested.

16.2 Calibration of temperature readout

A manufacturer-supplied table gives the output of a temperature probe device (namely, resistance, voltage, or frequency) as a function of temperature. The determination of this calibration table by the manufacturer, or by the user if necessary, is described in 21.4.

The temperature probe output is usually a nonlinear function of temperature. Over a small temperature range, the function can be assumed to be linear, although with a scale factor that varies at different temperature reference points.

A bridge circuit to determine the resistance of a platinum resistor or thermistor can have a certain resistance set point with the voltage output of the bridge circuit varying as temperature varies about the temperature corresponding to the resistance set point. The voltage-to-temperature scale factor about the set point can be determined as follows:

a) Vary the temperature about the set point.

b) Determine the bridge output voltages at the temperatures off the set point.

c) Determine the bridge resistances (such as supplied by a decade resistance box, which would have to be periodically calibrated; see 21.3) that null the output voltages at these temperatures.

d) Compare the manufacturer-supplied resistance-versus-temperature table with the corresponding voltages.

A temperature probe device can be an integral part of an inertial sensor for temperature control and/or compensation. For temperature compensation, the inertial sensor scale factor, bias, and other model coefficients are calibrated at various temperature settings. The inertial sensor model coefficients are then determined as, for example, polynomials in the temperature probe output so that the relationship between the temperature probe output and temperature is not needed for temperature compensation purposes.

16.3 Types of temperature monitors

16.3.1 Platinum resistors, thermistors, and bridge circuits

The electrical resistance of a platinum wire varies with temperature so the current with a constant voltage into the wire is a measure of the temperature, in fact, one of the more accurate such measures.

Other devices called *thermistors* also have an electrical resistance that has large variations with temperature. If a thermistor inside an inertial sensor or on the test station equipment is made to be one leg of a bridge circuit with known resistances, then the voltage out of the bridge circuit is a measure of temperature. The bridge resistances are adjusted so at a nominal temperature the output voltage is zero. The variations in output voltage, as appropriately amplified and read by an A/D converter, are then a measure of temperature variations around the nominal temperature.

16.3.2 Thermocouple temperature reading

The contact between dissimilar metals generates a voltage that is a function of temperature. This phenomenon can be used to build a device to monitor temperature variations.

16.3.3 Semiconductor temperature reading

There are commercially available semiconductor chip devices whose output voltage varies with temperature.

16.3.4 Crystal frequency temperature reading

There are commercially available quartz resonator devices whose frequency varies with temperature. Because there are many ways to read frequency (see Clause 14), they provide an elegant way to monitor temperature.

17. Other monitoring and commanding

17.1 Analog input signals and signal conditioning

Analog signals could be near-dc voltages or contain near-dc information on a modulated carrier, which would have to be demodulated for input to the data acquisition computer. Perhaps the information is contained in the amplitude of an ac signal, which could be peak sampled, or the rms could be measured over some interval to generate a dc voltage. A bridge circuit can change temperature readings to voltages. Power and current can be changed to voltage with appropriate circuitry.

Before going to the data acquisition A/D converter, these various voltages must be signal conditioned. Signal conditioning involves amplifying and buffering the signals. For greatest accuracy, the signals should be read differentially. In other words, a ground reference for each signal is input along with the signal to the A/D converter. A signal and its ground reference should use a twisted shielded pair between the signal source and the A/D converter.

A number of signals can be multiplexed into a single A/D converter. The signals could be sampled and held at a common time and then sequentially A/D converted.

17.2 Analog output signals

Command signals from a computer can be in analog voltage form by using a D/A converter in the computer backplane. The output analog signals can be buffered and amplified before going to the commanded device.

17.3 Asynchronous interfaces

Input and output for the data acquisition computer can be over an asynchronous interface, such as RS-232 or RS-422, at various baud rates, such as 9600 baud or 19.2K baud. The asynchronous serial data stream contains a sequence of information bits, preceded by at least one start bit and followed by a stop bit. A parity bit may also be included depending on the application. Typically, the information bits make up an 8 b character.

17.4 Digital input and output signals

Digital input and output signals can be acquired through a parallel digital interface board in the computer backplane. The parallel lines carrying binary signals have appropriate signal conditioning with line drivers, line receivers, and buffering.

Ground loops can be avoided by having optical isolation for digital input/output (I/O) and other I/O boards in the computer backplane.

17.5 Microprocessor interfaces

Signals can be acquired from an inertial sensor under test by a microprocessor in proximity to the sensor with A/D and special readouts for the particular sensor (such as a PLL). The information can then be sent in a serial digital data stream to the data acquisition computer through slip rings, over a radio interface, etc.

This approach can be better than, for example, sending analog signals through slip rings to be read by an A/D converter in the data acquisition computer backplane.

17.6 IEEE 488 bus

Many commercially available pieces of test equipment, such as voltmeters and test tables, can be commanded and read over the IEEE 488 bus. Therefore, the data acquisition computer should have such an interface card in its backplane.

The IEEE 488 bus cable is daisy chained from the computer backplane to one device after another. A signal down the bus is recognized only by the device that is addressed.

The only problem with this type of interface is that it has been fairly slow (1 MB/s), although the speed of the revised standard is now faster (8 MB/s) and the throughput has been increased (see IEEE Std 488.1™ [B6]).

17.7 Other interface buses

Special applications can have special bus interfaces, such as the MIL-STD-1553 bus [B8].

I/O boards could be in a virtual machine environment (VME) or other such backplane, rather than in the data acquisition computer backplane, with registers on the boards having assigned VME addresses. A commercially available interface board in the data acquisition computer backplane or motherboard connected by cable to the VME backplane allows the computer to read and write data to the VME boards as if the board VME addresses were in the data acquisition computer address space.

17.8 Radio telemetry interfaces

There are commercially available modules to take data from a microprocessor interface to an inertial sensor under test, convert it to a 100 kb/s digital data stream, and send it from a transmitting antenna at a radio frequency of about 2 GHz to a receiving antenna, where a radio receiver interfaces to a board in the data acquisition computer (namely, PC) backplane (namely, wireless data acquisition).

See 9.3.7 and 11.5.5 for descriptions of this system for the rotary table and centrifuge applications, where avoidance of slip rings is advantageous.

18. Computer data acquisition, control, filtering, and storage

18.1 Real-time operation

The data acquisition computer can be of the PC variety or a computer workstation. Whatever the type, it has to be equipped with a real-time operating system with driver interfaces to the various boards and devices that acquire data from the test. Manufacturers of data acquisition systems and interface equipment often provide a complete environment in which to develop software with human-friendly interaction such as provided by a graphical users interface (GUI) and with display of graphical and other results as the test proceeds.

Data acquisition software is often interrupt driven, where the interrupt signal (such as at 100 Hz) is generated by an external timing source or possibly from the computer's internal clock. The interrupt handler in the operating system for the given type of interrupt would command and read the various data acquisition channels (namely, latched counters, A/D converters, and external devices such as voltmeters) into computer memory. Data can also be inserted into memory using direct memory access (DMA), where an external device contends for the computer bus simultaneously with the CPU and where the rate at which data are inserted into memory is governed by the timing hardware in the DMA device. External devices (such as test tables) can also be commanded over digital or other interfaces as part of the response to an interrupt.

Raw data could be acquired for a short period of time into a buffer in memory if the data acquisition rates are too high to keep up with writing data to disk for longer term storage. Computer memories can be quite sizable so large amounts of very high rate data can thus be accumulated to memory. When the short duration test with very high rate data is completed, the data can be written from memory to disk for later analysis.

The more common test is to write data to disk in real time while the test proceeds. Data can be acquired at high rates if necessary and then digitally filtered and decimated to a lower rate before being written to disk. Filtering before decimation prevents aliasing of high-frequency noise into the lower frequency saved data.

18.2 Initialization and running of test

With a GUI or dialog interface, the test engineer should be able to define the information about a test from which data are to be acquired, such as

a) The name of the output file or files, which could be automatically generated to include the date and time of the test as determined with sufficient accuracy from the computer clock.

b) The character string title for the test, which could be put in a header record of the output file along with the date and time read from the computer clock.

c) The type of test to be done (such as drift test, scale factor rotation rate test, or tumble test) in order to pick the version of the data acquisition program that should be used for the test.

d) If there is automatic control of test equipment, such as a dividing head or rate table, the name of a file containing a list of commands to be carried out, such as rotating the table at certain rates on a certain time schedule.

e) A list of data channels to be acquired and, for each channel,

   1) The name of the data channel (to go into the header record of the data file).

   2) The type of channel (such as digital, A/D, asynchonous interface, special bus interface) and its address.

   3) The data acquisition rate (hertz).

   4) Type of digital filtering to be applied (namely, none, rectangular, triangular, or some other type).

   5) Amount of decimation and output rate (hertz).

   6) Scale factor and offset of the data channel for conversion from measured units (such as volts) to engineering units (such as degrees Celsius for a temperature channel).

f) The duration of the test or whether to run continuously until stopped.

If scale factors for converting acquired data to engineering units are not provided at the start of the test, any real-time displays would be in raw units (such as volts). Such scale factors would have to be provided later when the data are analyzed after a test if they are not included in the header information in the file that is read by the analysis program.

After setting up the input and control parameters, the test is started. The test could run unattended without human intervention, except for monitoring display output to see whether the test is proceeding normally or whether manual operations could be required. Variation of temperature, magnetic field, test table orientation or rotation rate, etc., would have to be done by the test technician if these variations are not controlled by the test computer.

Every test station should be provided with a test station logbook, in which the test technician enters the date and time that operations are carried out in a test and all other activity such as setup and calibration of test equipment. The test station logbook is often hand written, but software could be created to allow entry into a computer file, although the computer would not necessarily be running when it is necessary to enter data in the logbook, such as when setting up an experiment. The entries in the logbook could be very important in analyzing data, such as the time and amount that a temperature or other such parameter is manually changed because the data acquisition computer is not recording this event in its output file if it is not controlling the temperature or other parameter change.

The real-time graphical or other display of selected data channels during a test can be very helpful in assessing whether the test is proceeding normally. A scrolling display could have the last few minutes, hours, or a day or more of data displayed. Different data displays could be called to the screen without disturbing the continued data acquisition during the test. If a disturbance is seen in the real-time display, it could perhaps be correlated with an event in or near the test laboratory.

Examples of events that have disturbed an inertial sensor test include a person walking by a test station, a truck or train passing outside a window, and earthquakes thousands of kilometers away. Data during a workday can be noisier than data taken overnight or on weekends because of cultural seismic and electrical activity. Inertial instrument test laboratories should be in remote locations, but this is not always feasible.

The possible formats for the test output file are discussed in 18.8.

18.3 Interfaces to computer backplane

The various devices discussed in Clause 14 through Clause 17 can be on boards in the computer backplane or in some other external backplane (such as a VMEbus backplane) that in turn is interfaced to the computer backplane. Alternatively, the device could be a stand-alone piece of equipment that has an interface board in the computer or external backplane. An A/D converter is likely to be on a backplane board, whereas an integrating voltmeter is likely to be a stand-alone piece of equipment.

18.4 Experiment control and automatic test equipment

The data acquisition computer could just acquire data and write them to disk with the test technician or engineer manually controlling the test station. For a single position drift test, no control operations are required. For an accelerometer tumble test or a gyroscope scale factor rotation rate test, the test table must be commanded to new positions or to rotate at different rates. For sensitivity tests, the temperature set point, magnetic field, excitation voltage, or other environmental conditions must be varied. The times when changes are manually made should be noted in the test station log so that later analysis of the data file can take into account when test conditions were changed.

Productivity is increased if the test table and environmental changes are under command of the test computer. The computer could then put flags in the output data file indicating when a test condition is changed, thereby simplifying the analysis task. Automatic control of the test equipment by the data acquisition computer is a necessity for production acceptance testing.

Flexibility in the control of testing is accomplished by having the computer read a test scenario file that can be edited to make changes.

a) For an accelerometer tumble test, the test scenario file could list the sequence of table angle settings, the amount of dwell time at each discrete table angle position, and the settling time before data are recorded.

b) For a gyroscope scale factor rotation rate test, the test scenario file could list the sequence of commanded rotary table rates, the amount of dwell time at each rate, and the acceleration in going from one rate to the next.

c) For a sensitivity test, the test scenario file could list the sequence of environmental condition values (such as temperature, magnetic field, or excitation voltage) and the dwell time for each condition. Not all environmental conditions could be under control of the test computer. For example, a magnetic sensitivity test might be done infrequently and, therefore, be done with manual changes to the magnetic field.

d) The sequence of vibration acceleration levels or centrifuge rotation rate levels would be under control of the test computer only if the tests are run frequently. It is more usual to have manual control of these machines with the test computer only acquiring data from the sensor under test and auxiliary signals.

18.5 Acquired signals

Examples of the data acquired in a test are as follows:

a) Primary inertial sensor output from one or multiple sensors under test

   1) Torque or force voltage or current from a rebalance device (from the integrating voltmeter or continuous counter reading of digital torque pulses or a voltage-to-frequency converter)

   2) Pickoff reading from an open loop device

   3) Optical gyro pulse output counter

4) Digital word from signal processor attached to sensor(s)

b) Auxiliary signals from sensor(s) under test
   1) Supply voltages, powers, or currents
      i) Laser, gas discharge, or wheel supplies
      ii) Magnetic suspension, resolver, pickoff, and torquer supplies
   2) Temperatures (from thermistors or other devices)
   3) Pickoff reading from a torque or force rebalance device
   4) Resolver and suspension readings
   5) Other monitor and test point signals

c) Dividing head or rate table data
   1) Table angle readout
   2) Time counter reading at revolution trigger

d) Environmental data
   1) Environmental chamber or oven temperature readings
   2) Electronics temperature reading
   3) Room temperature reading
   4) Tilt meter readings
   5) Magnetic field and other environmental readings
   6) Event flags (such as train detector or table revolution trigger)

The data could be acquired at different rates. The primary sensor output is typically acquired at a high rate and triangularly or better filtered and decimated to a lower rate (see 18.7). Auxiliary signals are typically acquired at a lower rate with rectangular filtering applied.

18.6 Event recording

In a long-term test, data acquired at a high rate could become too voluminous to record in raw form. Digital filtering and decimation is typically applied to save the data to disk at a lower rate (see 18.7 and 18.8). However, if an anomalous event occurred during the test, it could be useful to have recorded the raw high-rate data surrounding the event.

Therefore, the past 10 min or so of raw data could be saved in a circular or double buffer in computer memory, either in the main data acquisition computer or in a peripheral computer before the main data acquisition computer, while filtered lower rate data are saved to disk. If an anomalous event occurs (such as a shift in the sensor output or in an auxiliary signal), then the past 10 min of raw high-rate data are written to disk along with the subsequent 10 min of raw high-rate data.

18.7 Real-time digital filtering

18.7.1 Types of filtering and decimation

A good test philosophy is to acquire signals at a high rate and apply digital filtering before decimating and storing the data at the lower rate required for test analysis. Filtering before decimation (namely, discarding all but every m^{th} point) prevents aliasing of high-frequency noise into the low-frequency output.

If $x(n)$ is a digital word read by a computer at time $t(n)$, a causal finite-impulse-response (FIR) filter applied to the data stream has output $y(n)$ (see Rabiner and Gold [B10]) as follows:

$$y(n) = \sum_{i=0}^{N} a_i \, x(n-i) \tag{4}$$

where the a_i are the filter weighting coefficients. If the array of weighting coefficients is symmetric about its midpoint, the FIR filter has linear phase and the time tag associated with the output data point $y(n)$ is at time $t(n - N/2)$. If the sum of the weighting coefficients is not unity because of, for instance, using fixed-point computations, the output $y(n)$ could be divided by this sum in order to have unit gain through the filter.

A causal infinite-impulse-response (IIR) recursive filter applied to the data stream has the form (see Rabiner and Gold [B10])

$$y(n) = \sum_{i=0}^{N} a_i \, x(n-i) - \sum_{i=1}^{N} b_i \, y(n-i) \tag{5}$$

The behavior of an analog filter (such as using capacitors or inductors) can be emulated digitally with an IIR filter.

A data acquisition design could have a cascade of filters. For example, an analog filter could be applied to a voltage signal before it is converted and sampled by a digital processor, and then the digital processor could apply a cascade of digital filters (such as an IIR filter followed by an FIR filter) before the decimated output goes to disk storage.

An IIR filter can be less computationally intensive than a FIR filter for a desired noise attenuation performance so it is often used for high-rate applications. However, the linear-phase constant-time-delay characteristics of a symmetric FIR filter are desirable for navigation and guidance applications. Hence, only symmetric FIR filters for such applications will be discussed.

18.7.2 Rectangular filter

If a counter is sampled from the pulsed torque or other output of an inertial instrument, essentially rectangular averaging (namely, constant FIR filter weights $a_i = 1$ with output divided by $N + 1$) has been applied to the data. It is important that the counter be continuous (see 14.1) so that a pulse missed in one sampling interval will appear in the next interval. This continuity can be accomplished by latching the counter into a register to be read by the computer without affecting the counter or, if the counter is reset when it is read, without missing the next pulse during the reset.

The results obtained from a low-rate sampled continuous reset counter are the same as if the sampling were done at a high rate and the high-rate readings added or averaged to get the low–rate full-width decimated output. The relative quantization error associated with such rectangular counter averaging is proportional to T^{-1}, where T is the averaging or count interval (namely, width of the rectangular filter).

The pattern of slightly larger or smaller incremental counts in each high-rate sampling interval is lost by rectangular averaging. Faster attenuation of quantization noise can be accomplished if account is taken of this pattern, as happens with the triangular filter.

18.7.3 Triangular filter

Triangular filtering for an odd number of sample points $2m - 1$ utilizes the following FIR filter weights:

$$a_i = \begin{cases} \dfrac{i+1}{m^2} & i = 0, ..., m-1 \\ \dfrac{2m-i-1}{m^2} & i = m-1, ..., 2m-2 \end{cases} \tag{6}$$

The triangular filter can be implemented using fixed-point arithmetic double-running sum s_n and u_n as follows:

$$s_n = \sum_{j=0}^{m-1} x(n-j) \tag{7}$$

$$\begin{aligned} u_n &= \sum_{k=0}^{m-1} s_{n-k} = \sum_{k=0}^{m-1} \sum_{j=0}^{m-1} x(n-k-j) \\ &= \sum_{i=0}^{2m-2} a_i x(i) \end{aligned} \tag{8}$$

A circular buffer of length m is kept for the last m data points; and after an initial startup transient, a new running sum s_n of length m is expressed in terms of the old running sum s_{n-1} of length m by

$$s_n = s_{n-1} + x(n) - x(n-m) \tag{9}$$

The u_n running sums can be reset each decimation output time with two u_n running sums being accumulated at any time if half-width decimation is used, for example.

The computations can be done using fixed-point arithmetic additions with the double running sum filter output being divided by m^2 to obtain unit gain. If half-width decimation is employed, every raw data point is used with equal weight, partly in one output point and partly in another.

If Q is the quantization error in $x(n)$, then the quantization error in s_n/m is Q/m. The quantization error in s_n occurs in the last $\Delta t = t(n) - t(n-1)$ time interval, which is independent of the quantization error in the last Δt time interval in s_{n-1}. The quantization error in the normalized triangular filter output is, therefore, reduced by a further factor of $m^{-1/2}$ because this output is the average of m independent s_n/m. Thus the triangular filter reduces continuous counter or other quantization error by a total factor of $T^{-3/2}$, where T is the filter width.

To summarize, triangular filtering of high-rate continuous counter data obtains higher accuracy in shorter time than low-rate sampling (namely, rectangular filtering) of the continuous counter data.

18.7.4 Higher order filters

If there is curvature in the data, the triangular filter will misestimate the inertial instrument output at the midpoint time tag of the filter width interval. Because of this problem and to improve pass-band, transition-band, and stop-band performance, a higher order than triangular FIR filter can be used, although at the cost of having to do multiplications as well as additions rather than just additions in the signal processing computer.

Of particular interest for inertial instrument applications are polynomial-passing digital filters with decimation, which faithfully represent accelerometer output at the midpoint time tag of the filter width interval, even in the face of jerk or higher order changes in acceleration. The filter design technique

described in Wilkinson [B12] yields polynomial-passing FIR filters with high fidelity at low frequencies and good stop-band attenuation and can even contain a notch at a known corrupting frequency, such as due to dither.

18.8 Data storage

The data from a test is written in real time to a disk file. The file name should indicate the type of test and sensor being tested and the date and time of the start of the test. It would be desirable if the file had a header record containing information about the test, such as the date, time, title, and number and type of channels. Alternatively, the header record could be omitted. However, if there is a header record, it could save having to input such data to analysis software at a later time.

Typically, data from *N* channels is written at uniform time intervals to disk with all channels having the same output rate, such as once per second. The data acquisition rate could be higher with digital filtering and decimation down to the output rate. The time in seconds from the start of the file could be in the first channel in each data record, or it could be omitted. If a time tag were not included at this point, it would have to be added later because plotting software, for instance, usually needs a time channel against which other channels are plotted.

Sometimes the data channels are not output all at the same rate. For example, inertial sensor output could be at 100 Hz and various A/D converted analog signals (such as temperature readings) could be at 1 Hz. In this case, there could be a data record every 1 s with one hundred 100 Hz inertial sensor output points and *n* A/D converted analog signals in each data record.

Whatever data file format is chosen, the analysis software has to be coded to read the file and strip out the information that it needs.

If the data acquisition output file is recorded in binary form (such as double precision floating point for inertial sensor output and single precision floating point for A/D converted output signals), then disk storage requirements are minimized. However, if the data file is transmitted to another computer for analysis (see 18.9), then problems can arise if the other computer is of a different type from the data acquisition computer.

One way around this problem is to store the data as ASCII characters. The American Standard Code for Information Interchange (ASCII) assigns a certain 8 b pattern to each character and can be recognized by any computer. A binary floating point number can be converted to ASCII characters (such as –1.234567E–01), and vice versa, by the software facilities of the computer. Thus an ASCII data file can be transmitted to different types of computers with no problem.

Another solution is to have software on the other computer convert the data acquisition computer's floating point format into the given computer's floating point format. Because disk storage has become plentiful and inexpensive, the most straightforward solution is to store acquired data in ASCII character format.

An example data record format could be as follows:

a) Time in seconds from start (optional)

b) *M* channels in character floating point format with 15 digits after the decimal point

c) *N* channels in character floating point format with 6 digits after the decimal point

If there is a header record at the start of the file, it could include the number *M* of double precision channels and the number *N* of single precision channels, plus whatever other information is in the header (such as date and time of the start of the test, title or type of the test, serial numbers of inertial sensors being tested).

18.9 Data transmission

The data file from a test could be analyzed on the data acquisition computer, or it could be sent to another computer for analysis. The latter procedure could be preferable to enable the data acquisition computer to be fully devoted to testing.

The data file transmission to another computer could utilize a removable media, namely, removable disk, tape cartridge, optical disk (such as CD or DVD), or flash memory device. The data file transmission could also be done over a communications network using file sharing, using file transfer protocol (FTP), or attaching the file to an electronic mail message, either over a local network to a computer in the same facility or over the Internet to a computer as much as halfway around the world.

If a long-term drift test were being done, the data could be written to disk for several days or a week. Then the test could be stopped, the file transferred to another computer for analysis, and the test restarted. The duration of the gap in the data should be accurately noted.

Multiple files can be pieced together on the analysis computer using the gap durations to correctly increment the time tag across the gaps. In this manner, long-term drift data over weeks or months can be plotted as a whole with the ability to look at intermediate test results before the whole long-term drift test is completed.

It is possible to collect continuous data with no gaps if there is a multitasking operating system. The data acquisition computer can be commanded to close the data file and continue writing to a new data file with no loss of data. The closed data file is then sent to the analysis computer in the background of data continuing to be acquired from the test.

If data are being acquired at very high rates, lower priority operation in the background (such as transfer of data files) might not be possible unless the speed of the computer provides margin for time critical operations to be carried out without interference from background operations.

19. Data analysis

19.1 Data file format

The data file collected on the data acquisition computer could be analyzed on the same computer or sent to another computer for analysis. The latter option would allow the data acquisition computer to continue collecting data in parallel with analyzing data from past tests. Even if a data acquisition computer has a multitasking operating system, a time-critical real-time interrupt-driven data acquisition task could be incompatible with other activity occurring in the background, unless the computer were fast enough to provide adequate margin for carrying out real-time tasks without disturbance from the background.

As described in 18.8, the file could be in ASCII character form if it is sent to another computer with a different word architecture. The ASCII file could be converted to binary format on the analysis computer, or it could remain as an ASCII file. If there were a conversion from one file format to another, a time channel at equal time intervals could be added if it were not on the original data acquisition file.

As noted in 18.8, an example data record format is as follows:

a) Time in seconds from start (optional)

b) *M* channels in character floating point format with 15 digits after the decimal point

c) *N* channels in character floating point format with 6 digits after the decimal point

Typically, ASCII character data fields would be delimited by blanks or a special character (such as comma, semicolon, or tab), depending on the analysis software, where the read of the data record could use free format input if allowed by the computer language being used.

If there is a header record at the start of the file, it could say the number M of double precision channels and the number N of single precision channels, plus whatever other information is in the header (such as date and time of the start of the test and an experiment title). Some commercially available analysis software assumes every record is the same, containing $K = M + N + 1$ channels, so there could be no header record. The commercial software could plot one channel versus another, for example, each channel versus the first (time) channel. If the data records were at equal time intervals with no time channel, then the software would have to supply the time channel as the record number times the input time interval.

Depending on the experiment, other formats are possible, such as different channels being stored at different rates. One channel could be at, for example, 100 Hz, with 100 of these values being in a record with a number of other channels (such as A/D voltage readings) that are collected at 1 Hz. Specially written analysis software would then be required because commercial plot software, for example, usually assumes that all data channels are recorded at the same rate.

19.2 Plots versus time

A standard analysis applied to data, such as in a drift test (see 19.12), is to plot each data channel versus time, which could be the first data channel on the file. The time could be in seconds from the start of the test. Depending on the length of the test, the time channel could be converted from seconds to minutes, hours, or days for the plot x-axis display.

The data points versus time could be individual dots or other such plot symbol, or the dots could be connected by straight lines in the plot frame. The latter option is the most common.

If there were an error bar associated with each data point, such as provided by another data channel, then the error bar could be plotted with each data point at the center of its error bar.

19.2.1 Data filtering and averaging

If tens or hundreds of thousands of data points are collected during a test, there could be too many points to include in a plot frame. In this case, the plot software should have the option of applying several types of averaging or filtering to the data before decimating and plotting at a lower data rate. Besides reducing the number of plot points, averaging or filtering also reduces the noise in the data plots.

For voltage test points, rectangular averaging could be employed, where every m data points are averaged to generate one plot point (see 18.7.2). For the primary output signal of an inertial sensor, triangular filtering would be more desirable with, for example, half-width decimation (see 18.7.3).

19.2.2 Plot axes

Besides the time units to be used on the x-axis of a plot (such as seconds, hours, minutes, or days), the units of the y-axis should be specified. Input would be a scale factor A and offset B for each channel, with the conversion

$$\text{Plotted data in engineering units} = A \times (\text{raw data}) - B \tag{10}$$

where the offset B could be inside the parenthesis and it could be added instead of subtracted, depending on the convention chosen by the specially written software or the commercially available software. If the scale factor and offset for each data channel were not carried along in the header record, they would have to be input to the plot software. The latter option would be necessary in any case to override the information in the header record.

Also required are titles for each channel to appear on the plot axes. The title and date and time of the experiment (from the header record or special input) could also appear on the plot. The tic marks on the *x*-axis and *y*-axis of the plot could be automatically set from the minimum and maximum of the time and data, or these tic marks could be specified by inputting the plot minimum, maximum, and tic-mark spacing. Data points falling outside the input minimum and maximum would not be plotted.

19.2.3 Plot statistics

It would be desirable for the plot software to compute the mean of the data and the rms or standard deviation of the data about the mean and to print these statistics on the plot frame.

The formulas for the mean μ and rms σ of data $z_1, \ldots, z_m$ are

$$\mu = \frac{1}{m}\sum_{i=1}^{m} z_i \tag{11}$$

$$\sigma = \sqrt{\frac{1}{m}\sum_{i=1}^{m}(z_i - \mu)^2} = \sqrt{\frac{1}{m}\sum_{i=1}^{m} z_i^{\,2} - \mu^2} \tag{12}$$

The first formula for σ requires two passes through the data, the first pass to compute μ and the second pass to compute σ. The second formula for σ requires only one pass through the data, in which the sum of the data and the sum of the data squared are computed and then divided by *m*. Even though the second algorithm is useful for, for example, real-time operation, it requires many more decimal places of precision to be carried along in the computations than the first algorithm.

19.2.4 Removal of bad points

Bad points could be removed from the data before they are plotted so that automatically generated data scales or the computation of rms statistics would not be corrupted. A bad point could be replaced by the average of surrounding good points. However, the original raw data should still be saved in case further analysis is required.

One bad-point-detection algorithm is to compute the standard deviation or rms of the data about its mean and to mark a point as bad if it is more than *q* standard deviation from the mean, where *q* could be, for example, 5 or 11. (Too small a value of *q* runs the risk of rejecting good points along with the bad points.) After a pass through the data with points marked as bad, then a second or even a third pass can be made on the remaining points with recomputed standard deviation so that the standard deviation would not be corrupted by bad points.

This bad-point-detection scheme works only for stationary data. It could also be applied to data with a trend if the trend is removed from the data before applying the bad-point-detection algorithm and then the trend recomputed with the bad points fixed.

There should be a rationale for removing bad points from data plots, such as information that there was a seismic disturbance during a test, so that the bad points removed or replaced by the average of surrounding good points do not hide relevant information about the inertial sensor being tested, such as outlier points being due to a problem in the sensor itself or its readout scheme.

If two or more IA parallel or antiparallel inertial sensors are tested and all have outlier points at the same time, then it can usually be assumed that the bad points are due to an external disturbance rather than being inherent in the sensors.

19.2.5 Multiple plots per page or frame

Plots of a channel versus time can be generated with one plot frame per page. There could also be an option to have several plot frames per page or to have several channels plotted versus time on the same plot frame.

There could also be options to plot the log of data versus time or the log of time. However, log-log plots are usually done only for PSD or Allan variance plots rather than for raw data plots (see 19.5 and 19.6).

19.3 Plots of one channel versus another

It is sometimes useful to plot one data channel versus another, rather than versus time. Examples are as follows:

a) Plot of inertial sensor output versus temperature (or magnetic field, excitation voltage, etc.) in a test where the given environmental input is varying and other environmental inputs are constant.

b) Plot of accelerometer post-fit tumble residuals versus tumble test dividing head angle or versus along-IA acceleration level at that dividing head angle (see 19.13.2.1).

c) Plot of gyroscope estimated scale factor error in a rotation rate test versus rotation rate (see 19.13.3).

19.4 Polynomial and other linear least-squares-fit residual plots

19.4.1 Linear least-squares maximum-likelihood fit model

Let z_k be measurements modeled by the following equation:

$$z_k = \mathrm{g}(t_k, \alpha) + \varepsilon_k, \quad k = 1, ..., m \tag{13}$$

where

ε_k is zero-mean Gaussian measurement noise with standard deviation w_k

$\alpha = (\alpha_1, ..., \alpha_n)$ are parameters to be estimated

Assume that the model function g is linear in the parameters α:

$$\mathrm{g}(t_k, \alpha) = \sum_{i=1}^{n} \alpha_i \mathrm{g}_i(t_k), \quad k = 1, ..., m \tag{14}$$

$$\frac{\partial \mathrm{g}(t_k, \alpha)}{\partial \alpha_i} = \mathrm{g}_i(t_k) \tag{15}$$

The method of least squares seeks values for the parameters α_i for which

$$\sum_{k=1}^{m} \frac{\left(z_k - \mathrm{g}(t_k, \alpha)\right)^2}{w_k^2} = \text{minimum} \tag{16}$$

Because of the Gaussian measurement error assumption, least-squares estimates are also maximum-likelihood estimates.

19.4.2 Normal equations

The partial derivatives with respect to the α_i of the minimization expression in Equation (16) are

$$-2\sum_{k=1}^{m}\frac{\left(z_k-\sum_{i=1}^{n}\alpha_i \mathrm{g}_i(t_k)\right)}{w_k^2}\mathrm{g}_j(t_k,\alpha)=0\,,\quad j=1,...,n \tag{17}$$

which yields the following linear equations (called the *normal equations*) for the parameters α_i:

$$\sum_{i=1}^{n}A_{ji}\alpha_i=B_j\,,\quad j=1,...,n \tag{18}$$

$$A_{ji}=\sum_{k=1}^{m}\frac{1}{w_k^2}\mathrm{g}_j(t_k)\mathrm{g}_i(t_k)\,,\quad j,i=1,...,n \tag{19}$$

$$B_j=\sum_{k=1}^{m}\frac{z_k}{w_k^2}\mathrm{g}_j(t_k)\,,\quad j=1,...,n \tag{20}$$

The normal equations are solved with Gaussian elimination to determine values of the parameters α_1, ..., α_n that best fit the data in a least-squares sense. If the measurement noise standard deviations are the same at each time point, then the weights w_k can be taken as 1 because it is the relative size of the weights that matters in the least-squares fit.

19.4.3 Covariance of parameter estimates

The rms of the maximum-likelihood least-squares fit residuals is

$$\text{residual rms}=\sqrt{\frac{1}{m}\sum_{k=1}^{m}\left(z_k-\mathrm{g}(t_k,\alpha)\right)^2} \tag{21}$$

By maximum-likelihood theory, the covariance matrix σ_{ji} of the least-squares parameter estimates α_1, ..., α_n is bounded below by the inverse of A_{ji} multiplied by the mean square of the post-fit residuals if the $w_k = 1$ rather than measurement standard deviations:

$$\sigma_{ji} \geq (A^{-1})_{ji} \times (\text{residual rms})^2 \tag{22}$$

It can be shown that the Cramer-Rao lower bound in Equation (22) is more of an equality ($\approx$ instead of $\geq$) if division by m is replaced by division by $(m - n)$ in the equation for the post-fit residual rms. Note that if the number of measurements were the same as the number of parameters, the fit could be perfect with zero post-fit residual rms. Maximum-likelihood estimates are asymptotically normally distributed and unbiased, and the Cramer-Rao lower bound is asymptotically attained in the limit of a large number of measurements for zero mean additive Gaussian measurement errors and no unmodeled effects (Cramer [B3]).

The standard deviation σ_j of the estimate of α_j is

$$\sigma_j = \sqrt{\sigma_{jj}} \tag{23}$$

The correlation between parameter estimates is

$$\varepsilon_{ji} = \frac{\sigma_{ji}}{\sigma_j \sigma_i} \ , -1 \le \varepsilon_{ji} \le 1 \tag{24}$$

Nonzero correlation between two parameters means that the effect of a variation in one parameter can be partially masked by a variation in the other. If there were perfect correlation (+1 or –1) between two parameters, then the effect of one parameter on the data can be completely masked by the effect of the other parameter; and they both cannot be estimated simultaneously from the data.

Because the covariance matrix of the parameter estimates depends just on the partial derivatives of the model equation and the measurement standard deviations, but not on the data, the covariance matrix can be calculated for a given test scenario in advance of performing the test. Such timing can be helpful in test design.

19.4.4 Polynomial fit model

The formulas for fitting a polynomial to data are as given in 19.4.2 and 19.4.3 with the model in 19.4.1 being

$$\mathrm{g}(t_k, \alpha) = \sum_{i=1}^{n} \alpha_i (t_k - t_o)^{i-1} , \quad k = 1, ..., m \tag{25}$$

$$\mathrm{g}_i(t_k) = \frac{\partial \mathrm{g}(t_k, \alpha)}{\partial \alpha_i} = (t_k - t_o)^{i-1} \tag{26}$$

Better computational accuracy is obtained if the epoch time t_o is taken near the midpoint time of the data.

19.4.5 Trigonometric fit model

If the data were a function of an angle θ instead of time t, then it could be appropriate to replace the model in 19.4.1 by the trigonometric model

$$\mathrm{g}(\theta_k, \alpha) = \sum_{i=1}^{n+1} \alpha_i \cos(i-1)\theta_k + \sum_{i=n+2}^{2n+1} \alpha_i \sin(i-n-1)\theta_k , \quad k = 1, ..., m \tag{27}$$

Because the trigonometric coefficients (α_1, ..., α_{2n+1}) appear linearly in the model, the linear least-squares fit formulas in 19.4.2 and 19.4.3 apply and can be used to perform a trigonometric fit to the data.

19.4.6 Residual plots

The analysis software should have the option of least-squares-fitting a linear or higher order polynomial to data (or doing a trigonometric fit if appropriate) and plotting the post-fit residuals. The residual rms statistic should be displayed on the plot along with the estimated polynomial coefficients.

In a long-term drift test of an inertial sensor, its output could trend over time due to stress relaxation, magnetic decay, etc., in the materials used in constructing the sensor. A relevant requirement might then be to predict the trend some number of months ahead in time with specified accuracy from a least-squares fit of a trend (namely, first order polynomial) to a few days' data. If the variation in the output of an inertial sensor were due to random walk process noise, the trend would not always be in the same direction; therefore, future behavior would be unpredictable within the bounds provided by the random walk standard deviation.

19.5 Power spectral density (PSD)

The PSD of a time series of data is a characterization of the noise and other processes in the data as a function of frequency.

The PSD is defined to be the Fourier transform of the autocorrelation function of the data, where the autocorrelation is the expected value of the data multiplied by itself delayed. For a stationary ergodic time series, the autocorelation can be evaluated as the time average of the time integral of the data multiplied by itself delayed, and the PSD is equal to the expected value of the magnitude squared of the Fourier transform of the data. See IEEE Std 1293-1998, Annex I.

The PSD can be calculated in a number of different ways:

a) Measuring the rms value of the signal in successive frequency bands, where the signal in each band has been bandpass filtered because the PSD represents the energy in a signal as a function of frequency. See Equation (31).

b) Taking the Fourier transform of the autocorrelation function.

c) Computing the Fourier transform of the data over a finite time span and averaging either from successive time spans or, if over one long time span, in successive frequency bands. The Fourier transform of discrete data over a finite time span is calculated using the discrete Fourier transform, in particular using the fast Fourier transform (FFT) algorithm if there is a power of two number of points.

The Fourier transform $X(f)$ of a continuous function $x(t)$ and inverse Fourier transform $x(t)$ with frequency f in hertz are

$$X(f) = \int_{-\infty}^{\infty} x(t) \mathrm{e}^{-2\pi i f t} dt, \quad x(t) = \int_{-\infty}^{\infty} X(f) \mathrm{e}^{2\pi i f t} df \tag{28}$$

For a discrete time series of data, the continuous Fourier transform over an infinite range is approximated by the discrete FFT of a power of two number of points. The discrete Fourier transform has an exact discrete inverse Fourier transform.

The Fourier transform and the PSD are functions of positive and negative frequencies f:

$$\text{two-sided PSD}(x(t)) = |X(f)|^2 \quad -\infty < f < \infty, \text{ with averaging applied} \tag{29}$$

Because the PSD is defined as an expected value, it is necessary to average to accurately represent noise processes. For method c) in this subclause, either the PSD is calculated for successive time spans of (assumed ergodic) data, and the time span PSDs are averaged; or the PSD is calculated for the whole span of data, and the PSD values at adjacent frequencies are averaged with greater averaging at higher frequencies.

The one-sided PSD plots twice the two-sided PSD values for positive f because for a real-time series the PSD values for positive and negative frequencies are equal:

one-sided PSD(x(t)) = 2 $|X(f)|^2$ $0 < f < \infty$, with averaging applied (30)

The dc (namely, 0 frequency) value of the PSD is the square of the average of the time series and is not included in the typical log-log PSD plot. In fact, for numerical computation reasons, the data average is often removed from the data before computing the FFT and PSD.

By Plancherel's formula for the continuous Fourier transform or by Parseval's theorem for the discrete Fourier transform,

$$\text{total power in time series} = \int_{-\infty}^{\infty} |x(t)|^2 \, dt = \int_{-\infty}^{\infty} |X(f)|^2 \, df \tag{31}$$

Thus the PSD in square units per hertz represents the energy in a time series $x(t)$ in units split into frequency components. A spike in the PSD represents a sinusoid in the data either from environmental input or from an artifact of the readout.

White noise has by definition constant power at all frequencies and, therefore, is represented by a zero slope line parallel to the frequency axis in a PSD plot. Integration by parts in the Fourier transform shows that

PSD (derivative of data) = $(2\pi)^2 f^2$ PSD (data) (32)

$$\text{PSD (integral of data)} = \frac{1}{(2\pi)^2 f^2} \text{ PSD (data)} \tag{33}$$

Because random walk is the integral of white noise, the PSD of random walk is represented by a –2 slope straight line in a log-log plot.

The characteristic PSD log-log slopes of these and other noise processes are depicted in Figure 10 for gyroscope angular rate data and in Figure 11 for accelerometer linear acceleration data, where the actual PSD and frequency ranges are hypothetical. With real data, there would be gradual transitions between the different slopes, rather than the sharp transitions in Figure 10 and Figure 11; and the log-log slopes might be different than the –2, –1, 0, and +2 values depicted in the figures. There would be a certain amount of noise or hash in the plot curves due to the uncertainty of the measured PSDs.

Table 2 and Table 3 summarize the log-log slopes of the various noise processes in a gyroscope angular rate PSD or in an accelerometer linear acceleration PSD and also for the corresponding square root of Allan variance log-log slopes.

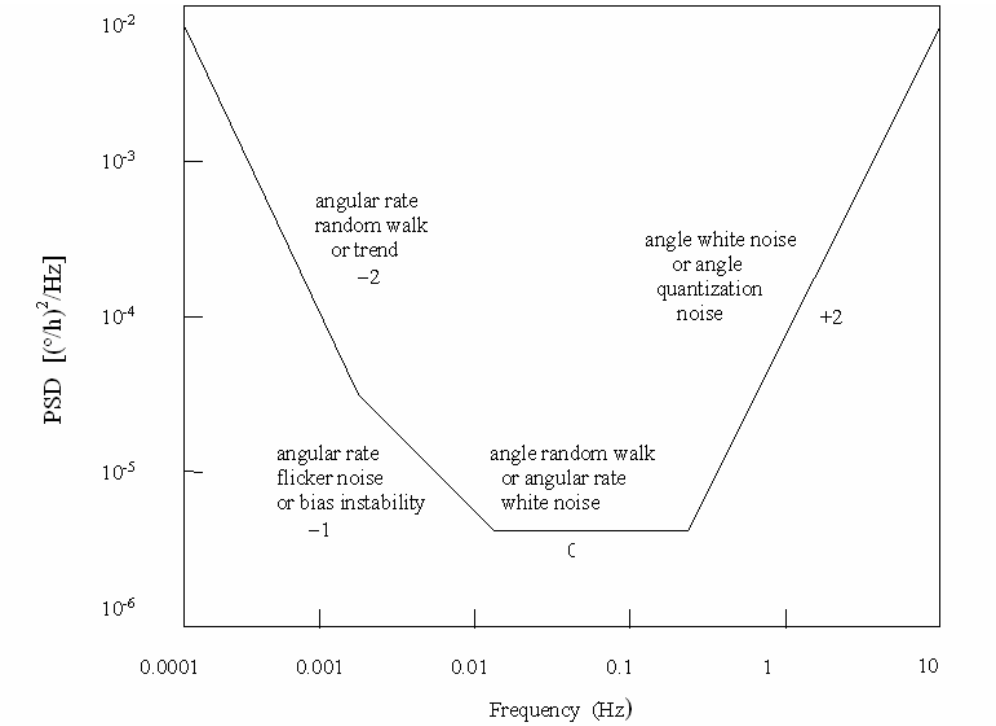

Figure 10— Typical slopes in $\log_{10}$-$\log_{10}$ plot of one-sided PSD versus frequency for gyroscope angular rate data

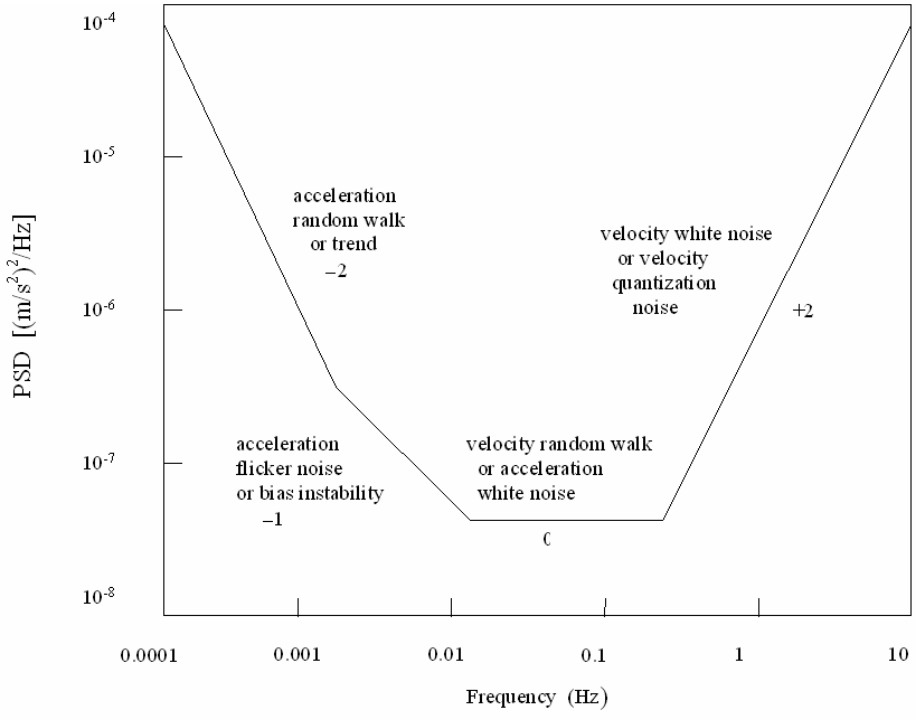

Figure 11— Typical slopes in $\log_{10}$-$\log_{10}$ plot of one-sided PSD versus frequency for accelerometer linear acceleration data

Table 2—Slopes in PSD and square root of Allan variance log-log plots for gyroscope angular rate data

Signal	PSD versus frequency	Square root of Allan variance versus averaging time	Clause
Angular rate trend	–2 †	+1	19.8.5
Angular rate random walk	–2	+1/2	19.8.3
Angular rate flicker noise or bias instability	–1	0	19.7.3
Angle random walk or angular rate white noise	0	–1/2	19.8.2
Angle white noise or angle quantization noise	+2	–1	19.8.4

† Artifact of finite Fourier transform.

Table 3—Slopes in PSD and square root of Allan variance log-log plots for accelerometer linear acceleration data

Signal	PSD versus frequency	Square root of Allan variance versus averaging time	Clause
Linear acceleration trend	–2 †	+1	19.8.5
Linear acceleration random walk	–2	+1/2	19.8.3
Linear acceleration flicker noise	–1	0	19.7.3
Velocity random walk or linear acceleration white noise	0	–1/2	19.8.2
Velocity white noise or velocity quantization noise	+2	–1	19.8.4

† Artifact of finite Fourier transform.

19.6 Allan variance

19.6.1 Allan variance definition

The Allan variance of a time series of data is a characterization of the noise and other processes in the data as a function of averaging time.

The unbiased variance of two data points x_{j-1}, x_j relative to their mean is

$$\frac{1}{2-1}\left\{\left[x_{j-1}-\frac{x_{j-1}+x_j}{2}\right]^2+\left[x_j-\frac{x_{j-1}+x_j}{2}\right]^2\right\}=\frac{\left(x_j-x_{j-1}\right)^2}{2} \tag{34}$$

This motivates the definition of the Allan variance of data x_0, x_1, ..., x_{N-1} taken at time interval Δt to be the average of the variances of adjacent pairs of data x_{j-1}, x_j:

$$\sigma_a^2(\Delta t)=\frac{1}{2(N-1)}\sum_{j=1}^{N-1}\left(x_j-x_{j-1}\right)^2 \tag{35}$$

For n = 1, 2, 3, 4, ..., $M \le N/2$, define a sequence

$$y_j(n) = \frac{x_{nj} + x_{nj+1} + ... + x_{nj+n-1}}{n}, \quad j = 0,\ 1,\ ...,\ \left[\frac{N}{n}\right] - 1 \tag{36}$$

and compute the Allan variance $\sigma_a^2(n\Delta t)$ for this sequence. The square root of the Allan variance is then plotted with log-log scales versus averaging time $\tau = n\Delta t$, n = 1, 2, 3, 4, ..., $M \le N/2$.

Other sequences of averaging time n may be used to facilitate analysis and computation, such as n = 1, 2, 4, 8, …, $M \le N/2$. The uncertainty of the Allan variance is dependent on the number [N/n] of clusters and increases as n approaches $N/2$. See Annex C of IEEE Std 952.

The characteristic root Allan variance log-log slopes of various noise processes are depicted in Figure 12 for gyroscope angular rate data and in Figure 13 for accelerometer linear acceleration data, where the actual root Allan variance and averaging time ranges are hypothetical. With real data, there would be gradual transitions between the different slopes rather than the sharp transitions in Figure 12 and Figure 13, and the log-log slopes might be different from the –1, –1/2, 0, and +1 values depicted in the figures. There would be a certain amount of noise or hash in the plot curves due to the uncertainty of the measured root Allan variance.

Table 2 and Table 3 summarize the log-log slopes of the various noise processes in a gyroscope angular rate root Allan variance, in an accelerometer linear acceleration root Allan variance and also for the corresponding PSD log-log slopes.

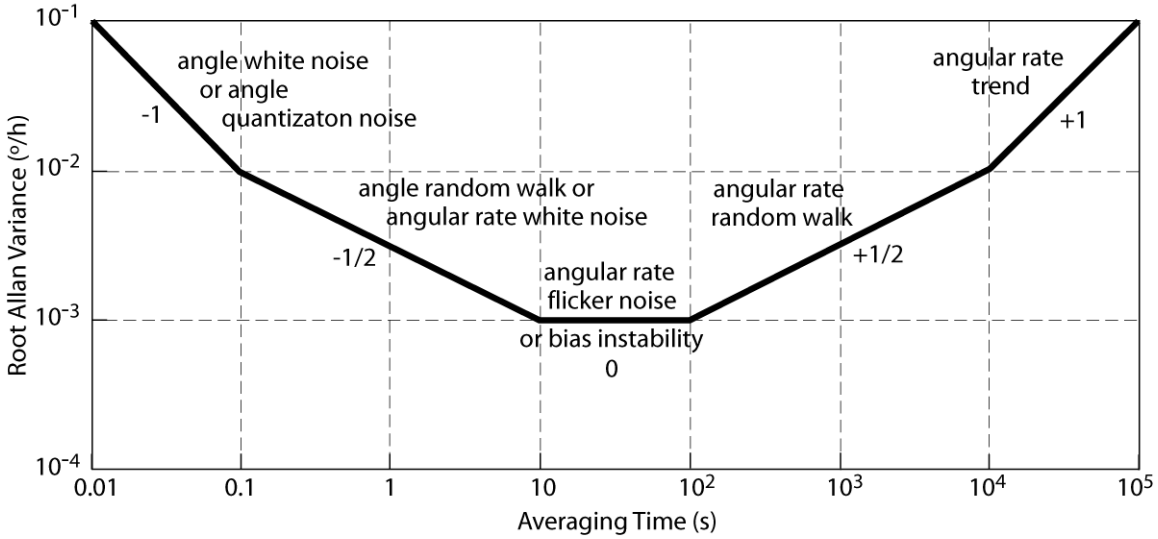

Figure 12— Typical slopes in $\log_{10}$-$\log_{10}$ plot of square root of Allan variance versus averaging time for gyroscope angular rate data

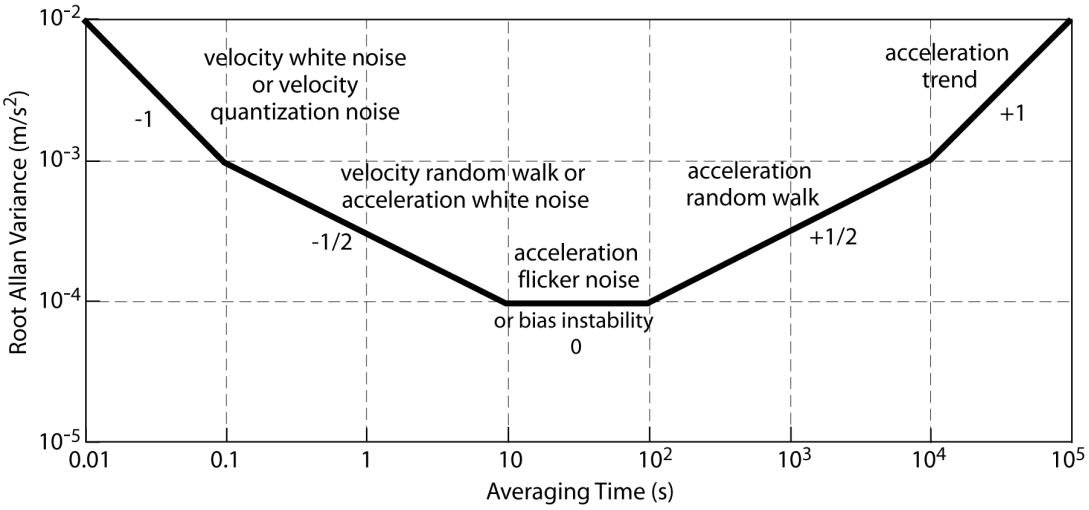

Figure 13— Typical slopes in $\log_{10}$-$\log_{10}$ plot of square root of Allan variance versus averaging time for accelerometer linear acceleration data

Note that, for angle or velocity quantization noise, the angular rate or linear acceleration standard deviation decreases as the first power of averaging time, whereas it decreases as the square root of averaging time for angular rate or linear acceleration white noise (namely, angle or velocity random walk). Flicker noise standard deviation is unchanged with averaging time. For angular rate or linear acceleration random walk, the angular rate or linear acceleration standard deviation grows as the square root of averaging time, whereas trend standard deviation grows as the first power of averaging time.

19.6.2 Example Allan variance noise analysis

Preprocessing the data or analyzing a subset of the data can be useful to determine some noise sources that are masked by other noise sources. However, the analyst should be cautioned that doing so may inhibit the ability of the analysis to resolve certain noise processes or may affect the value of the noise coefficient. The following are two example cases of Allan variance noise analysis:

a) Angular rate or linear acceleration data

   1) Plot the angular rate or linear acceleration versus time.

   2) If sudden bias changes are observed, process the Allan variance on a continuous part of the test file not affected by these events (to be able to determine the higher frequency noise terms such as quantization and angle random walk).

   3) Remove all deterministic behavior such as angular rate or linear acceleration ramp or periodic angular rate or linear acceleration. As this removing process can have an effect on the Allan variance results for “high” averaging times, the analysis should be limited to “low” averaging times.

   4) Compute the Allan variance, and plot the square root of the Allan variance versus time.

   5) Identify the noise coefficients.

   6) If the angle random walk or the velocity random walk cannot be determined due to the angle or velocity quantization noise, respectively, integrate the signal after removing the bias from the data, compute the Allan variance, plot the square root of the Allan variance versus time, and identify the noise coefficients.

b) Angle or linear velocity data

1) Plot the angle or linear velocity versus time.

2) If sudden angle or linear velocity changes are observed, process the Allan variance on a continuous part of the test file not affected by these events (to be able to determine the higher frequency noise terms such as angle white noise).

3) Remove all deterministic behavior such as the effect of earth rate or gravity, the effect of gyro angular rate bias and accelerometer bias, or periodic angle or linear velocity. As this removing process can have an effect on the Allan variance results for "high" averaging times, the analysis should be limited to "low" averaging times.

NOTE—As the angle random walk and the velocity random walk generate an angle and velocity ramp, removing the angle and velocity ramp by making a regression using the angle and velocity data will lead to underestimating the angle random walk and the velocity random walk.[12]

4) Compute the Allan variance, and plot the square root of the Allan variance versus time.

5) Identify the noise coefficients.

6) In case of long duration tests and when the intent of the test is to determine bias instabilities, for example, differentiate the angle and linear velocity data to obtain angular rate or linear acceleration data and proceed as in case a).

19.7 Noise processes

If the various types and levels of noise processes in an inertial sensor's output have been determined by PSD and/or Allan variance analysis, then this information can be used in the Kalman filter dynamic system model used for an inertial guidance and navigation system.

Including the correct noise processes in the Kalman filter dynamic system model allows error effects to be propagated for covariance analyses before a mission. It also allows better model coefficient calibration estimates to be obtained before a mission and better guidance and navigation to be carried out during a mission through the use of an optimal Kalman filter gain matrix.

19.7.1 Stochastic differential equation model

For guidance and navigation system applications, it is natural to use accelerometer-integrated velocity and gyroscope-integrated angle as observables $z(t_k)$ because the quantization noise in accelerometer acceleration and gyroscope angular rate measurements becomes white measurement noise $\theta(t_k)$ in the integrated observables $z(t_k)$. If there were random walk as well as white measurement noise in the integrated output signal $z(t_k)$ from an accelerometer (or gyroscope), add a state x_b to the dynamic system state vector with dynamic equation

$$dx_b(t) = [B + (1 + SFE)\, a_i + \ldots]\, dt + b\, d\beta_1 \tag{37}$$

$$z(t_k) = x_b(t_k) + \theta(t_k) \quad \text{(m/s or rad)} \tag{38}$$

where

a_i is nongravitational acceleration (specific force, m/s^2) for an accelerometer, or angular rate ω_i (rad/s) for a gyroscope, both along the IA

[12]Notes in text, tables, and figures are given for information only and do not contain requirements needed to implement this recommended practice.

B, SFE, ... is bias (m/s^2 or rad/s), scale factor error (dimensionless), and other model parameters for accelerometer or gyroscope (could be states in the guidance system calibration Kalman filter)

b is random walk standard deviation ($m/s/\sqrt{s}$ or $rad/\sqrt{s}$)

β_1 is unit Wiener random walk process (standard deviation grows as the square root of time)

θ is white measurement noise with standard deviation r (m/s or rad) for sampling interval $\Delta t = t_{k+1} - t_k$ s

The standard deviation of Δt increments of the Wiener Brownian motion process $\int b\, d\beta_1$ is $b\sqrt{\Delta t}$.

Let the accelerometer or gyroscope one-sided angular rate or linear acceleration PSD versus frequency f in hertz be of the form

$$\begin{matrix}\text{one - sided PSD} \\ \text{(angular rate or} \\ \text{linear acceleration)}\end{matrix} = \begin{cases} A & f < f_o \text{ angular rate or linear acceleration white noise} \\ \dfrac{Af^2}{f_o^2} & f > f_o \text{ angle or velocity quantization noise} \end{cases} \tag{39}$$

where A has units of $(m/s^2)^2/Hz$ for accelerometer linear acceleration data or $(rad/s)^2/Hz$ [converted from $(^o/h)^2/Hz$] for gyroscope angular rate data.

The two-sided PSD white noise levels versus frequency f in hertz (1/s) that generate the one-sided PSD in Equation (39) for an accelerometer or gyroscope are

$$\begin{matrix}\text{two - sided velocity or angle random walk} \\ \text{in acceleration or angle rate domain}\end{matrix} \quad \frac{A}{2} \qquad f < f_o$$

$$\begin{matrix}\text{two - sided velocity or angle white noise} \\ \text{in velocity or angle domain}\end{matrix} \quad \frac{A}{2(2\pi f_o)^2} \qquad f > f_o \tag{40}$$

The Fourier transform of white noise level σ^2 square units per hertz in a given domain is the autocorrelation function $\sigma^2\delta(t)$ units^2 in the time domain, where $\delta(t)$ is the delta impulse function. The dynamic system variable $x(t)$ whose unit time increments have this autocorrelation function satisfies the Ito stochastic differential equation $dx = \sigma\, d\beta(t)$, where $\beta(t)$ is a unit Wiener Brownian motion process. Therefore, the relation between the accelerometer or gyroscope dynamic noise model parameters b and r at the start of 19.7.1 and the PSD noise parameters A and f_o are

$$b = \sqrt{\frac{A}{2}} \qquad m/s/\sqrt{s} \text{ or } rad/\sqrt{s}$$

$$r = \frac{1}{2\pi f_o}\sqrt{\frac{A\Delta t}{2}} \qquad m/s \text{ or } rad \tag{41}$$

If a white noise process has one-sided PSD horizontal level A, so that the square-root Allan variance is $B/\tau^{1/2}$, then by 19.8.2

$$A = 2B^2 \tag{42}$$

19.7.2 Velocity and angle random walk per root hour

If A is the one-sided acceleration PSD white noise level in $(\mathrm{m/s^2})^2/\mathrm{Hz}$ of an accelerometer and B, in $(\mathrm{m/s^2})\sqrt{\mathrm{s}}$, is the corresponding square-root Allan variance $B/\tau^{1/2}$, then the accelerometer's velocity random walk coefficient in $\mathrm{m/s}/\sqrt{\mathrm{h}}$ is

$$b = 60\sqrt{\frac{A}{2}} = 60B \quad \mathrm{m/s}/\sqrt{\mathrm{h}} \tag{43}$$

It is traditional to express gyroscope angular rate in degrees per hour rather than radians per second [multiply by $\pi/(180 \times 3600)$ to convert from the former to the later]. If A is the one-sided angular rate white noise level in $(°/\mathrm{h})^2/\mathrm{Hz}$ of a gyroscope and B, in $(°/\mathrm{h})\sqrt{\mathrm{s}}$, the corresponding square-root Allan variance $B/\tau^{1/2}$, then the gyroscope's angle random walk coefficient in degrees per root hour is

$$b = \frac{1}{60}\sqrt{\frac{A}{2}} = \frac{B}{60} \quad °/\sqrt{\mathrm{h}} \tag{44}$$

Note that the gyroscope angle random walk coefficient in degrees per root hour can be determined from the square-root Allan variance plot of angular rate in degrees per hour from where the –1/2 slope straight line intercepts the 1 h time abscissa.

Expressing the angle or velocity random walk in units per root hour is useful for inertial navigation systems because it shows how much of an error accumulates after 1 h of inertial navigation due to white noise in a gyroscope's angular rate bias or in an accelerometer's acceleration bias. The standard deviation of the angle or velocity error after 4 h is twice as large and after 0.25 h it is half as large as it is after 1 h. It is important to include the conversion from one-sided to two-sided PSD as well as the conversion from seconds to hours in the random walk computation.

The angle or velocity error caused by an initial error in the inertial instrument angular rate or acceleration bias (due for instance to the bias calibration having been done some time in the past) will grow linearly with time, in contrast to the square root in time angle or velocity error growth due to white process noise in the angular rate or acceleration bias.

19.7.3 Flicker noise modeled as sum of exponentially correlated noises

Flicker noise can be modeled by a combination of Markov noise states. Consider the exponentially correlated noise state x_c satisfying

$$\mathrm{d}x_c(t) = -c_1 x_c(t)\,\mathrm{d}t + c_1 c_2\,\mathrm{d}\beta_2 \tag{45}$$

$$z(t_k) = x_b(t_k) + x_c(t_k) + \theta(t_k) \tag{46}$$

where the state x_b comes from 19.7.1 and

c_1 is inverse time constant of exponentially correlated noise

c_2 is scaling parameter of exponentially correlated noise

The effects of the accelerometer bias, scale factor, and other model coefficients and of the random walk, exponentially correlated, and white noise parameters are now combined into the observable.

The autocorrelation function of exponentially correlated or colored noise is (Jazwinski [B7] pp. 122 and 110)

$$\mathrm{E}\left[x_c\left(t_k\right)x_c\left(t_k+\tau\right)\right]=\frac{c_1c_2^2}{2}\exp\left(-c_1|\tau|\right) \tag{47}$$

and the two-sided PSD as a function of circular frequency $\omega = 2\pi f$ is

$$\mathrm{PSD}(\omega)=\frac{c_2^2}{1+\left(\frac{\omega}{c_1}\right)^2} \tag{48}$$

At low frequencies, this PSD has 0 log-log slope; and at high frequencies, it has −2 log-log slope. In between, there is a region where the slope approximates −1. Thus, flicker noise over a given bandwidth can be approximated as a sum of exponentially correlated noises.

The information in the PSD and/or Allan variance plots of gyroscope and accelerometer data indicates how an inertial guidance and navigation linear dynamic system model can be augmented with states to approximate the noise spectrum of the inertial instrument outputs. Having correct noise models in the guidance and navigation model leads to better performance for the calibration, alignment, and guidance Kalman filters.

19.8 Time series to verify PSD and Allan variance software

PSD and Allan variance software can be either commercially obtained or specially written. In either case, verification and validation of the software are desirable. Verification and validation can be accomplished by processing random-number-generated noise files and seeing whether the expected plots are obtained.

19.8.1 Random-number-generated noise

19.8.1.1 Random-number algorithm

A computer system could have a random-number generator in its software library, or one can be specially written, for instance, with the linear congruential algorithm

$$\begin{aligned} x &\equiv r\,s \bmod(p) \\ s &= x \end{aligned} \tag{49}$$

where

- p is a prime integer number
- r a primitive integer root of p (of the order of, but not too near, the square root of p as a heuristic criterion)
- s is a starting seed integer between 1 and $p - 1$
- x is an integer between 1 and $p - 1$ because the numbers between 0 and $p - 1$ form a number field modulo p if p is a prime integer, with the numbers between 1 and p –1 forming a multiplicative group modulo p

The starting seed s is updated to x after each pass through the random-number generator routine.

A primitive root r of a prime p is an integer between 1 and $p - 1$ so that the smallest positive power a with $r^a = 1 \bmod p$ is $a = p$ and the powers of r sweep out all values between 1 and $p - 1$ without repetitions. Thus with any starting seed, the numbers x sweep through the integers between 1 and $p - 1$ without repetitions until the p^{th} time that the subroutine is called. Different Monte Carlo simulations can be done with different values for the starting seed s.

Candidate values for p and r are

$$p = 2^{31} - 1 = 2147483647 \tag{50}$$

$$r = \begin{cases} 7^5 = 16807 < \sqrt{p} \\ 11^5 = 161051 > \sqrt{p} \end{cases} \tag{51}$$

A numerical check showed that both these candidate r are primitive roots of the given p. This and other random-number generators are discussed in Press, et al. [B9].

The least significant bits of s are less random than the most significant bits. The x/p simulating a sample from the uniform distribution (see 19.8.1.2) following an $x/p < 10^{-7}$ is less that 0.01, whereas, if it were truly random, it could be any number between 0 and 1. These and other features (such as "streaming" discussed in the reference) make the linear congruential random-number generator less than perfect, but on the whole it is not too bad.

19.8.1.2 Samples from uniform distribution

As the random-number subroutine is repeatedly called, the integer x varies in a pseudorandom fashion between 1 and $p - 1$. Thus the real number x/p varies between 0.0 and 1.0 as a sample from the uniform distribution, without ever equaling 0.0 or 1.0 and without repetitions for $p - 1$ calls to the random-number subroutine. It is important that enough digits be carried along in the modulo arithmetic computations (namely, at least 20 decimal places for the above example of p). Quadruple precision floating point arithmetic could be used with the final answer truncated with rounding to a 32 b integer.

19.8.1.3 Samples from Gaussian distribution

Once a sample from the uniform distribution is obtained, a sample from the unit Gaussian or normal distribution can be obtained as shown in Equation (52) and Equation (53). The cumulative distribution function of the unit Gaussian distribution is

$$\mathrm{F}(x) = \frac{1}{\sqrt{2\pi}} \int_{-\infty}^{x} \mathrm{e}^{-t^2/2}\, \mathrm{d}t \tag{52}$$

where $0 \le \mathrm{F}(x) \le 1$. If x is a random-number-generated sample from the uniform distribution between 0 and 1, then

$$y = \mathrm{F}^{-1}(x) \tag{53}$$

is a sample from the unit Gaussian distribution with $-\infty < y < \infty$. If a table is constructed of $\mathrm{F}(x)$ versus x, then inverse interpolation can be used to determine $\mathrm{F}^{-1}(x)$. The same technique can be used to simulate samples from any probability distribution with monotonically increasing cumulative distribution function.

19.8.2 White noise time series

19.8.2.1 White noise simulation

Let the time series x_n (n = 1, …, N) be σ multiplied by samples from the unit Gaussian distribution with some assumed time spacing, such as Δt = 0.1 s. Compute the PSD and Allan variance for N equal to a power of two (such as $N = 2^{16} = 65536$).

19.8.2.2 White noise PSD

The one-sided PSD plot should be a straight line (with some noise hash on it) parallel to the frequency axis at level $2\sigma^2\Delta t$ square units per hertz.

19.8.2.3 White noise Allan variance

The log-log scale square-root Allan variance plot should be a straight line with slope –1/2 that intersects the 1 s point at the value $\sigma\sqrt{\Delta t}$ units because the standard deviation of the average of samples from the Gaussian distribution goes down as the square root of the averaging time.

19.8.3 Random walk noise time series

19.8.3.1 Random walk noise simulation

Random walk samples x_n from a random walk stochastic process with standard deviation b can be generated at time interval Δt by

$$x_1 = 0$$
$$x_{n+1} = x_n + \sum_{i=1}^{m} b\, y_{ni}\sqrt{\Delta t / m} \tag{54}$$

where the Δt interval is broken into m subintervals for integration purposes (such as m = 10) and where the y_{ni} are samples from the unit normal distribution. The derivative process is white noise with standard deviation $b/\sqrt{\Delta t}$ at sampling interval Δt.

19.8.3.2 Random walk PSD

The log-log scale one-sided PSD plot should be a straight line (with some noise hash on it) with slope –2 that intersects the 1 Hz point at a value A, namely, the PSD curve in a linear-linear plot is A/f^2. The one-sided PSD of the derivative of the process is a horizontal line at level $(2\pi)^2 A$ so that

$$(2\pi)^2 A = 2\left(\frac{b}{\sqrt{\Delta t}}\right)^2 \Delta t \tag{55}$$

Thus the value of the one-sided random walk PSD A/f^2 at 1 Hz is

$$A = \frac{b^2}{2\pi^2} \ \text{units}^2 / \text{Hz} \tag{56}$$

19.8.3.3 Random walk Allan variance

Random walk x_j has stationary independent white noise increments ($x_j - x_{j-1}$) with standard deviation $b\sqrt{\Delta t}$. Then by the definition in 19.6, the square root of the Allan variance of random walk with averaging time Δt is $b\sqrt{\Delta t}/\sqrt{2}$.

Thus the log-log scale square-root Allan variance plot of random walk is a straight line with slope +1/2 that intersects the 1 s point at the value $b/\sqrt{2}$.

19.8.4 Quantization noise time series

19.8.4.1 Angular rate or linear acceleration quantization noise due to angular rate or acceleration A/D converter

If a rate gyroscope's angle-rate output or an accelerometer's linear acceleration output is measured by an A/D converter, the measurement is truncated to the quantization resolution of the A/D converter. Under the assumption that the value of the signal is changing rapidly with respect to the level of quantization, this is equivalent to subtracting a uniformly distributed random variable $n(t)$ from the true value of the signal. The probability distribution of n is given by

$$p[n(t)] = \begin{cases} \dfrac{1}{q} & 0 \le n \le q \\ \\ 0 & \text{otherwise} \end{cases} \tag{57}$$

where q is the resolution of the measurement device in angle-rate or acceleration units, respectively:

$$q = \begin{cases} q_\omega & \text{rad/s/bit} \quad \text{for a gyroscope} \\ \\ q_a & \text{m/s}^2\text{/bit} \quad \text{for an accelerometer} \end{cases} \tag{58}$$

The mean of quantization noise is $0.5\,q$, and its covariance is

$$\int_0^q \frac{(x - 0.5q)^2}{q} \mathrm{d}q = \frac{q^2}{12} \tag{59}$$

If the A/D quantization noise is uncorrelated in time, then it appears white with standard deviation $q/\sqrt{12}$. Thus by 19.8.2, gyroscope angular rate quantization noise or accelerometer linear acceleration quantization noise with sample time Δt in the angular rate or linear acceleration domain, respectively, has the following characteristics:

One-sided PSD: Horizontal straight line with level $\dfrac{q^2}{6}\Delta t$ square units per hertz

Square-root Allan variance: Straight line with slope –1/2 in log-log plot with 1 s

intercept point $\frac{q\sqrt{\Delta t}}{\sqrt{12}}$

NOTE—Angular rate and linear acceleration quantization noises have the same Allan variance asymptotic properties as angle and linear velocity random walk. Knowing the angular rate or linear acceleration quantization of the A/D converter will allow estimation of the angle or linear velocity random walk if the A/D converter quantization is larger than other sources of angular rate or linear acceleration white noise within the sensor, within its readout, or in the environment.

19.8.4.2 Angle or linear velocity quantization noise for integrating gyroscope or accelerometer

Suppose an integrating gyro's or integrating accelerometer's angle or linear velocity output, respectively, is measured by a continuous counter from the inherent frequency or pulse output of the sensor, such as for a laser gyroscope, VBA, or a pulse-torque-rebalanced damped accelerometer or damped spinning wheel gyroscope, or from the use of a voltage-to-frequency rather than A/D converter on the torquer output. Then the accumulated count value $count_j$ at time t_j is the integrated inertial sensor output (namely, angle for a gyroscope or velocity for an accelerometer) truncated to the quantization resolution q of the counter in angle or velocity units, respectively:

$$\text{quantization}(count_j) = q = \begin{cases} q_\theta & \text{rad/bit for a gyroscope} \\ q_v & \text{m/s/bit for an accelerometer} \end{cases} \tag{60}$$

which, by the argument in 19.8.4.1, causes white noise in angle or velocity with covariance

$$\text{covariance}(count_j) = Q^2 = \frac{q^2}{12} \tag{61}$$

Differentiating integrating gyroscope angle or integrating accelerometer velocity gives that gyroscope angle quantization noise or accelerometer linear velocity quantization noise with sample time Δt in the angular rate or linear acceleration domain, respectively, has the following characteristics:

One-sided PSD: Straight line in log-log plot with +2 slope and 1 Hz

intercept point $\frac{2\pi^2 q^2 \Delta t}{3}$ square units per hertz

Square-root Allan variance: Straight line in log-log plot with –1 slope and 1 s

intercept point $\frac{q}{2 \times (1\,\text{s})}$ units

where the quantization resolution q is in radians for the integrating gyroscope or meters per second for the integrating accelerometer so that "units" above is radians per second for a gyroscope, to be converted to degrees per hour, or meters per square second for the integrating accelerometer.

The PSD result follows from Equation (32) for the PSD of a derivative. For the Allan variance result, consider that the derivative computed from the count difference observable with sample spacing Δt is

$$x_j = \frac{count_j - count_{j-1}}{\Delta t} \tag{62}$$

Make the following reasonable assumptions:

a) The observable x_j is ergodic with time averages equal to ensemble averages so that the sum on j divided by $(N - 1)$ in Equation (35) is equal to integration over the probability distribution (expected value E).

b) The observable x_j has constant mean value μ from one time point to the next so that the mean value of $count_j$ satisfies $\overline{count}_j = \overline{count}_{j-1} + \mu / \Delta t$.

c) The noise in the count observables $count_j$ is uncorrelated from one time point to the next.

As a result, by Equation (34) and Equation (35)

$$\text{Allan variance of count difference observable } x_j = \frac{\mathrm{E}\left\{\left[x_j - x_{j-1}\right]^2\right\}}{2}$$

$$= \frac{1}{2\Delta t^2}\mathrm{E}\left\{\left[\left(count_j - (\overline{count}_{j-2} + 2\mu)\right) - 2\left(count_j - (\overline{count}_{j-2} + \mu)\right) + \left(count_j - \overline{count}_{j-2}\right)\right]^2\right\}$$

$$= \frac{\mathrm{cov}(count_j) + 4\,\mathrm{cov}(count_{j-1}) + \mathrm{cov}(count_{j-2})}{2\Delta t^2} = \frac{6}{2\Delta t^2}\frac{q^2}{12} = \frac{q^2}{4\Delta t^2} \tag{63}$$

so that the angular rate or linear acceleration root Allan variance with averaging time Δt is $q/(2\Delta t)$ in terms of angle or linear velocity quantization q. In terms of angle or linear velocity white noise standard deviation Q, the same argument gives that the angular rate or linear velocity root Allan variance with averaging time Δt is $\sqrt{3}\,Q/\Delta t$.

19.8.5 Trend time series

19.8.5.1 Trend simulation

Samples at time interval Δt from the trend $x = bt$ can be simulated by

$$x_1 = 0$$
$$x_{n+1} = x_n + b\,\Delta t \tag{64}$$

19.8.5.2 Trend PSD

The one-sided PSD computed over a finite interval with the discrete Fourier transform is A/f^2 with a –2 log-log slope like random walk (namely, an artifact of using the discrete Fourier transform; see I.7.1 in IEEE Std 1293-1998), where the intercept at 1 Hz is

$$A = \frac{(2\pi)^2 b^2}{\Delta t} \tag{65}$$

19.8.5.3 Trend Allan variance

By 19.6, the Allan variance of the trend *bt* with averaging time τ is

$$\sigma_a^2(\tau) = \frac{1}{2(N-1)} \sum_{j=1}^{N-1} (b\tau)^2 = \frac{(b\tau)^2}{2} \tag{66}$$

Thus the log-log square-root Allan variance plot of a trend should be a straight line with slope +1 that intersects the 1 s point at the value $b/\sqrt{2}$.

19.9 Allan variance autofit procedure

The types and levels of various noise processes in a time series of data can be determined by drawing straight lines with a ruler through segments of the PSD or square-root Allan variance log-log plots and determining the slopes and 1 Hz or 1 s intercepts of the lines. There is a certain amount of judgment required in picking appropriate segments and drawing straight lines through the centers of the segments with noise variations on either side of the lines.

In the case of the Allan variance, a technique called *autofit* has been devised to let the judgment be done by a least-squares fit to the Allan variance as described in Sargent and Wyman [B11].

19.10 Regression analysis and cross PSD

19.10.1 Regression of one data channel versus others

Let an inertial sensor's output be $z_k = z(t_k)$ at times t_k, and let there be other signals $y_\ell(t_k)$ (ℓ = 1, …, p) measured in the test. Suppose it is hypothesized that the $z(t_k)$ is a function of the $y_\ell(t_k)$:

$$z(t_k) = \alpha_1 + \sum_{\ell=1}^{p} \alpha_{\ell+1} y_\ell(t_k) \tag{67}$$

The linear regression of z on y_1, …, y_p consists of estimating the α_1, …, α_{p+1} using the linear least-squares estimation technique described in 19.4.1 to 19.4.3. The post-fit residual plot shows the inertial sensor's output freed of the effects of the other signals, such as temperatures.

One problem with the linear regression approach is that there can be phase lags between variations in $y_1(t_k)$, …, $y_p(t_k)$ and the response $z(t_k)$.

19.10.2 Cross PSD

Under the assumption that the dynamic dependency between the inertial sensor output $z(t_k)$ and another data channel $y(t_k)$ involves a linear transfer function, the cross PSD between the two channels can account for any frequency-dependent phase lags. The normalized magnitude of the transfer function, the phase lag, and the coherency between the two signals are plotted versus frequency to determine whether there is any relationship between the two time series. See Bendat and Piersol [B2].

19.11 Parameter estimation

19.11.1 Model coefficient calibration

Calibration of inertial sensor model coefficients at the inertial guidance system level typically utilizes a Kalman filter to estimate the bias *B*, scale factor error *SFE*, and other inertial sensor parameters in the dynamic system model given in 19.7.1, where the state vector (which is estimated by the Kalman filter) is augmented by the model parameters with state equations

$$\frac{\mathrm{d}B}{\mathrm{d}t} = 0 + \text{noise}, \ \frac{\mathrm{d}SFE}{\mathrm{d}t} = 0 + \text{noise}, \ \text{etc.} \tag{68}$$

The Kalman filter is a sequential estimator and is often run in real time. It is not discussed further here because it usually is not employed in sensor-level tests, which are the subject of this recommended practice.

Calibration of inertial sensor model coefficients from sensor-level test data typically employs a least-squares maximum-likelihood estimator using an I/O performance model:

$z(t_k)$ = (sensor output) / (nominal scale factor)
= B + (1 + SFE) × (acceleration or angular velocity input)
+ (IA misalignment angles) × (cross-axis acceleration or angular velocity)
+ … (69)

The least-squares maximum-likelihood and Kalman filter estimators generally give the same estimation results. Batch least-squares estimation is more straightforward to implement than the Kalman filter, although it does not run in real time.

An inertial sensor performance model is often linear so the linear least-squares maximum-likelihood estimation technique described in 19.4.1 to 19.4.3 applies.

19.11.2 Nonlinear least-squares maximum-likelihood estimation

If the performance model were nonlinear or if estimated misalignment angles or angle-setting errors were not small and so appeared within sines and cosines, then nonlinear least-squares maximum-likelihood estimation would have to be used. Another example where nonlinear estimation is required is fitting an exponential or other nonlinear model function to data, such as for the warm-up transient in an inertial sensor after it is turned on. When fitting such nonlinear model functions to data, good first guesses for the model parameters are generally required to obtain convergence to the maximum-likelihood parameter estimates in the iterative estimation process.

Nonlinear estimation requires that a first guess $\alpha_o = (\alpha_{o1}, \ldots, \alpha_{on})$ be made to the true values of the parameters $\hat{\alpha} = (\hat{\alpha}_1, \ldots, \hat{\alpha}_n)$ in the nonlinear model function g:

$$z_k = \mathrm{g}(t_k, \alpha) + \varepsilon_k, \ k = 1, \ldots, m \tag{70}$$

where the measurement error ε_k is zero mean Gaussian with standard deviation w_k. Values $\hat{\alpha}_i$ are sought for the parameters α_i for which

$$\sum_{k=1}^{m} \frac{\left(z_k - \mathrm{g}(t_k, \hat{\alpha}) \right)^2}{w_k^2} = \text{minimum} \tag{71}$$

Let

$$\Delta\alpha_i = \hat{\alpha}_i - \alpha_{oi} \ , \ i = 1, ..., n \tag{72}$$

Assume that

$$\mathrm{g}(t_k, \hat{\alpha}) = \mathrm{g}(t_k, \alpha_o) \ + \ \sum_{i=1}^{n} \frac{\partial \mathrm{g}(t_k, \alpha_o)}{\partial \alpha_i} \Delta\alpha_i \tag{73}$$

$$\frac{\partial \mathrm{g}(t_k, \hat{\alpha})}{\partial \alpha_i} = \frac{\partial \mathrm{g}(t_k, \alpha_o)}{\partial \alpha_i} \tag{74}$$

With these assumptions, the partial derivatives with respect to the α_j of Equation (71) are

$$-2 \sum_{k=1}^{m} \frac{\left(z_k - \mathrm{g}(t_k, \alpha_o) - \sum_{i=1}^{n} \frac{\partial \mathrm{g}(t_k, \alpha_o)}{\partial \alpha_i} \Delta\alpha_i \right)}{w_k^2} \frac{\partial \mathrm{g}(t_k, \alpha_o)}{\partial \alpha_j} = 0 \ , \ \ j = 1, ..., \ n \tag{75}$$

which yields the following linear equations (called the *normal equations*) for the adjustments $\Delta\alpha_i$:

$$\sum_{i=1}^{n} A_{ji} \Delta\alpha_i = B_j \ , \ \ j = 1, ..., n \tag{76}$$

$$A_{ji} = \sum_{k=1}^{m} \frac{1}{w_k^2} \frac{\partial \mathrm{g}(t_k, \alpha_o)}{\partial \alpha_j} \frac{\partial \mathrm{g}(t_k, \alpha_o)}{\partial \alpha_i} , \ \ j, i = 1, ..., n \tag{77}$$

$$B_j = \sum_{k=1}^{m} \frac{\left(z_k - \mathrm{g}(t_k, \alpha) \right)}{w_k^2} \frac{\partial \mathrm{g}(t_k, \alpha)}{\partial \alpha_j} , \ \ j = 1, ..., n \tag{78}$$

where the matrices A_{ji} and B_j have the same expressions as in 19.4.2 (where the g_i are the partial derivatives with respect to α_i), except that the data residuals appear in the formula for B_i rather than the data.

The first guess for the parameters α_o is adjusted by the solution to the normal equations, and the normal equations are reformed with the new values of the parameters. The normal equations are again solved to obtain further adjustments to the parameters, and the iteration continues until convergence is obtained to the parameter values $\hat{\alpha}$ that best fit the data in a least-squares sense. The only difference between linear and nonlinear least-squares estimation is the necessity of iterating in the latter.

Because of the additive Gaussian measurement error assumption, least-squares estimates are also maximum-likelihood estimates, and the formulas for the covariance of the parameter estimates in 19.4.3 apply to nonlinear least-squares estimation as well as to linear least-squares estimation.

19.12 Analysis of gyroscope and accelerometer drift data

Accelerometer drift data are often collected for the IA vertical orientation, where accelerometer output is insensitive to tilt and azimuth variations. Gyroscope drift data are often also collected for the IA vertical orientation, but other orientations can be used, such as IA parallel to the earth's rotation vector, where gyroscope output is insensitive to tilt and azimuth variations.

One purpose of a drift test is noise analysis via PSD and Allan variance plots. For low-noise sensors, special techniques could be required to separate the noise in the sensor from that in the environment, such as testing at a remote site or using dual sensor IA parallel or antiparallel test techniques.

The most accurate estimate of gyroscope bias is often from a drift test, where the output is averaged for a sufficiently long time to minimize the effect of noise and the gyroscope bias is this output minus the sensed component of earth rate calculated using a previously calibrated value of gyroscope scale factor from a rotation rate test (see 19.13.3). However, in some gyroscopes with acceleration sensitivities, bias and other parameters are best simultaneously estimated in a multiposition tumble test (see 19.13.2.2); or at least the values of these other parameters from such a tumble test can be used in compensating drift data to better estimate the gyroscope bias from drift data.

Accelerometer bias is best estimated simultaneously with scale factor, misalignment, and other parameters in a multiposition tumble test (see 19.13.2.1), or at least in an IA up-down test, rather than just from drift data.

Another purpose of drift tests is to measure the long-term stability of the sensor. A drift test can be run for days, weeks, or even months. The data can be acquired at a high rate, digitally filtered, and stored to disk at a lower rate. The data acquisition can be interrupted every week or so to save and plot the data file, and the data acquisition can be quickly restarted. Multiple data files can be merged together, and the measured time across the gap can be used to increment the time tag from one segment to the next.

The plot of the data over weeks or months indicates the lumped stability of the scale factor and bias. Periodic accelerometer tumble or gyroscope rotation rate tests can separately measure the stability of scale factor, bias, and other parameters. It has to be determined whether there is any disturbance in the drift test by such periodic calibration tests. For instance, the behavior across rotating the sensor to different orientations should be determined (such as is there any shift, transient, or change in trend).

A drift test can also reveal the sensitivity of an inertial sensor to environmental inputs. If a part in 10^{-7} accuracy accelerometer were being tested, the lunar-solar earth tide could be sought in drift data (see Annex M in IEEE Std 1293-1998). The disturbance from an earthquake thousands of kilometers away could also be seen in gyroscope and accelerometer drift data.

19.13 Analysis of data with varying test conditions

19.13.1 Detection of the times of changes in test conditions

If test conditions are controlled by the data acquisition computer, the data file from a test can have flags indicating when a test condition is changed (see 18.4). If the test conditions are changed manually, then the time of the change in a test condition can be detected in a number of ways.

If the quantity that is changed is acquired by the data acquisition computer (such as a test table angle or a thermistor reading of temperature), then the time of the change is apparent.

If the primary output of the inertial sensor is affected by the change, then when a change in settled output is detected, the time of change of the quantity can be flagged.

If all else fails, the time of change of a quantity relative to the start of the test can be determined from the test station logbook, which supports the importance of maintaining a good logbook.

Because a quantity might not change instantaneously when it is commanded to change, the end of the data span with the old value of the quantity should be somewhat earlier than the time when the quantity is observed to change. The start of the data span with the new value of the quantity should be somewhat after the time when the quantity has reached its commanded value to let transients subside.

19.13.2 Analysis of tumble test data

19.13.2.1 Analysis of accelerometer tumble test data

Once the accelerometer data have been collected into settled segments at each tumble test position, the average of the settled data and the dividing head angle at each position are stored into an array or file. Least-squares estimation of the accelerometer model coefficients can then be done.

The tumble test calibration of accelerometer scale factor, bias, and other parameters uses the local value of plumb bob gravity g as a reference. Dual orthogonal accelerometer testing can be employed to allow estimation of angle-setting errors along with sensor parameters for accelerometers that are more accurate that the dividing head on which the tumble test is done (see Annex K of IEEE Std 1293-1998).

Repeated calibrations over time or over environmental variations such as temperature determines the long-term stability or sensitivity of the parameters, respectively. Calibrations across environmental variations, such as temperature cycle, vibration and shock, or shutdown, determine the repeatability of parameters.

Post-fit tumble residuals should be plotted versus tumble angle or along-IA acceleration level to determine whether there are any systematic errors in the tumble residuals.

19.13.2.2 Analysis of gyroscope tumble test data

If a gyroscope has acceleration sensitivities, then a tumble test can be done to calibrate its model coefficients, as for the dynamically tuned gyro (DTG), as explained in IEEE Std 813.

19.13.3 Analysis of gyroscope rotation rate test data

Once the gyroscope data have been collected into settled segments at each table rotation angular rate with the gyroscope IA parallel to the table rotation axis, as in 9.2.6 or 9.3.8, the average gyroscope angular rate and the average table angular rate at each rotation test rate are stored into an array or file.

If the actual table angular rate varies about the commanded angular rate by less than the accuracy being sought for the gyroscope scale factor, then the average gyroscope indicated rate is adequate. However, if the table angular rate cannot be controlled to the accuracy required for the scale factor measurement, then the gyroscope accumulated angle at each revolution trigger has to be determined from the data (see 9.3.4). The change in gyroscope accumulated angle from one revolution trigger to the next divided by the time to rotate through that revolution is the average gyroscope angular rate at a table angular rate of 360° divided by the time to go one revolution. The average gyroscope angular rate and table angular rate are calculated over the number of revolutions accumulated at the given commanded table angular rate.

Let

ω_j is average table angular rate for data segment j [°/h, rad/s]

ω_{ex} is sensed component of the earth's rotation rate ω_e (usually the vertical component ω_{ev} because gyroscope scale factor tests are often done with the gyroscope IA parallel to the rotary table rotation axis oriented vertically) [°/h, rad/s]

E_j is raw average gyro angular rate output at table rate ω_j [units such as volts or counts]

S_0 is nominal gyro scale factor [(°/h)/unit, (rad/s)/unit]

$\omega_{g\,j}$ is S_0E_j, which is the nominal gyro indicated angular rate at table angular rate ω_j [°/h, rad/s]

ε_K is gyro scale factor error (ppm)

S is $S_0(1 + 10^{-6}\varepsilon_K)$, which is the gyro scale factor [(°/h)/unit, (rad/s)/unit]

D_F is gyro bias [°/h, rad/s]

Assume the model equation

$$\omega_{g\,j} = S_0E_j = [\omega_j + \omega_{ex} + D_F][1 - 10^{-6}\varepsilon_K] \tag{79}$$

Then calibrate the scale factor error ε_K from the table rotation rate test data according to 19.13.3.1, 19.13.3.2, or 19.13.3.3.

19.13.3.1 Scale factor error calibration assuming scale factor linearity

If gyro scale factor is known to be linear (as determined from previous tests) and if bias can be assumed constant at a value D_F as calibrated in an earlier drift test (after compensation for sensed earth rate in the drift test), then the scale factor error ε_K can be determined from data at a single rotation rate via

$$\varepsilon_K = 10^6\left[1 - \frac{\omega_{g1}}{\omega_1 + \omega_{ex} + D_F}\right] \tag{80}$$

If bias D_F cannot be assumed constant from the time the drift test was done to the time that the rotation rate test is done, then the data at two rotation rates can be used to estimate scale factor error with the effect of bias removed:

$$\varepsilon_K = 10^6\left[1 - \frac{\omega_{g1} - \omega_{g2}}{\omega_1 - \omega_2}\right] \tag{81}$$

If complete revolution rotations are done with the table axis in any orientation (including vertical), then the scale factor results are insensitive to

— Small misalignment angles between the gyroscope IA and the table rotation axis because the cosine of a small angle is very close to 1 and

— The angle between the earth's rotation vector and the table rotation axis because the component of earth rate along the table rotation axis drops out of the formula for scale factor error in terms of the data.

The most accurate calibration results are obtained if ω_1 and ω_2 are widely separated, even of opposite signs (see 9.2.6). However, use of oppositely signed ω_1 and ω_2 presupposes that there are no bias or scale factor asymmetries, and widely separated ω_1 and ω_2 presupposes there are no nonlinearities. If such do not exist, as determined on a sample of gyros as in 19.13.3.2 and 19.13.3.3, then production scale factor error calibrations could use a few widely separated and oppositely signed table rates.

Bias can also be estimated from the data at two rotation rates via

$$K_F = \frac{\omega_{g1} + \omega_{g2}}{2\left(1 - 10^{-6}\varepsilon_K\right)} - \frac{\omega_1 + \omega_2 + 2\omega_{ex}}{2} \tag{82}$$

However, the rotation rate test estimate of bias does not have as low an uncertainty as the drift rate test estimate of bias.

If complete revolution rotations are done with the table axis parallel to the earth's rotation vector (so that $\omega_{ex} = \omega_e$), then the bias results are insensitive to small misalignment angles between the gyroscope IA, the table rotation axis, and the earth's rotation vector.

19.13.3.2 Scale factor error calibration using adjacent table rates to determine scale factor nonlinearities

Given a rotation rate test scenario as in Table 1 (in 9.3.8), the scale factor error ε_K can be determined for adjacent pairs of rotation rates ω_j and ω_{j+1} via Equation (81) and plotted versus $(\omega_j + \omega_{j+1})/2$. If the scale factor error varies with table rate, then the gyro scale factor has nonlinearities. If the scale factor error is different for positive and negative rotation rates, then the gyro scale factor has asymmetries.

19.13.3.3 Estimating scale factor nonlinearities from plurality of table rates

Alternatively, for positive and negative table angular rates ω_j, assume that the observable at each table angular rate is

$$\omega_{gj} = D_F + \frac{1}{2} D'_F \operatorname{sign}(\omega_j + \omega_{ex}) + (1 - 10^{-6}\varepsilon_K)(\omega_j + \omega_{ex}) - \frac{1}{2} 10^{-6}\varepsilon'_K |\omega_j + \omega_{ex}| + SF_{oq}(\omega_j + \omega_{ex})|\omega_j + \omega_{ex}| + SF_2(\omega_j + \omega_{ex})^2, \; j = 1, \ldots, N \tag{83}$$

where the small scale factor error $10^{-6}\varepsilon_K$ does not multiply the small bias D_F in order to have a linear estimation problem, and where

$$\text{bias for positive input angular rates} = D_F + \frac{1}{2} D'_F \tag{84}$$

$$\text{bias for negative input angular rates} = D_F - \frac{1}{2} D'_F \tag{85}$$

$$\text{scale factor error for positive input angular rates} = \varepsilon_K + \frac{1}{2}\varepsilon'_K \tag{86}$$

$$\text{scale factor error for negative input angular rates} = \varepsilon_K - \frac{1}{2}\varepsilon'_K \tag{87}$$

$$\text{quadratic for positive input angular rates} = SF_2 + SF_{oq} \tag{88}$$

$$\text{quadratic for negative input angular rates} = SF_2 - SF_{oq} \tag{89}$$

Do a least-squares fit of bias D_F, bias asymmetry D'_F, scale factor error ε_K, scale factor asymmetry ε'_K, odd quadratic SF_{oq}, and quadratic SF_2 to the observables ω_{gj} ($j = 1, \ldots, N$).

The plot of bias and scale factor error calibration results (namely, the former from a drift test, the latter from a rotation rate test) over time indicate the stability of bias and scale factor error, and such results across environments (such as vibration and shock, temperature cycle, shutdown) indicate the repeatability of bias and scale factor error. The sensitivities of bias and scale factor error are determined from the calibration results at different set points based on temperature, magnetic field, excitation voltage, etc.

19.13.4 Analysis of sensitivity data from changing environmental conditions

Once inertial sensor data have been collected into settled segments for each environmental set point, the sensitivity to variations in the environmental quantity (such as temperature, magnetic field, excitation voltage) can be determined. If the data are collected in a single position for all environmental settings, then a lumped scale factor and bias sensitivity (or the sensitivity of some other combination of model terms including misalignment, depending on the orientation) is determined by dividing the change in the sensor output by the change in the environmental quantity.

If a tumble or rotation rate test is done at each environmental set point, the sensitivities of scale factor, bias, and other parameters can be individually determined by estimating the parameters at each environmental setting and dividing the changes in the estimated parameters by the change in the environmental setting.

A higher order polynomial model can be fit to the model coefficient values at each environmental setting for modeling the sensitivities over wide environmental changes, especially for temperature changes over, for example, –55 °C to +85 °C.

19.13.5 Analysis of accelerometer vibration rectification data

Subclause 12.3.17 and Annex L of IEEE Std 1293-1998 describe the calibration of accelerometer model nonlinearities from the average accelerometer output during sinusoidal vibrations along various axes and cross axes, where the average accelerometer output is equal to model coefficients to be estimated times the rectified average of powers of the acceleration input. From a 1% piezoelectric accelerometer monitor of the vibration acceleration input, the rectified average of powers of the acceleration input can be calculated with sufficient accuracy to allow estimation of small nonlinearity coefficients, such as cross-IA sensitivities.

However, the K_2 along-IA nonlinearity in a quartz or silicon VBA is large and must be calibrated to more decimal places than the precision of a piezoelectric monitor accelerometer. One solution is to monitor the motion with a laser interferometer or a well-calibrated force rebalance accelerometer with small nonlinearities (if the latter has a high enough bandwidth).

Another solution, as described in the following paragraphs in this subclause, is to monitor the motion with the accelerometer under test itself. Namely, the bias K_0, scale factor K_1, and quadratic nonlinearity K_2 can be calibrated to some accuracy in a gravity field tumble test (see 19.13.2.1). The goal is to improve the calibration accuracy of K_2 and to calibrate other coefficients such as K_3 and K_4 in a vibration test.

Suppose the VBA model equation for the frequency f of an individual resonator or for the difference frequency f from a dual resonator VBA (see Annex D of IEEE Std 1293-1998) is

$$f = K_0 + K_1 a + K_2 a^2 + K_3 a^3 + K_4 a^4 \tag{90}$$

where a is the acceleration along IA.

Vibrate along IA up or down, where the analysis is insensitive to small mounting misalignments, so that

$$a = \begin{cases} \text{vibration acceleration} + g & \text{if IA up} \\ \text{vibration acceleration} - g & \text{if IA down} \end{cases} \tag{91}$$

where g is the local acceleration due to gravity (see 20.1 and 21.1). For 20 Hz vibrations at up to, typically, 80 m/s^2 rms amplitude, let the VBA frequency output be sampled at, for example, 1 kHz. Convert the 1 kHz frequency samples to acceleration using the tumble test calibrated values of K_0, K_1, and K_2, and zero values for K_3 and K_4.

Let the data be collected for an integral number N of vibration cycles, where the vibration amplitude varies slightly from one cycle to the next. Form the sum (or integral) of all the measured data with theoretical value given on the right side of the equation

$$\Sigma f = \begin{cases} NK_0 + K_1(0 + Ng) + K_2\Sigma a^2 + K_3\Sigma a^3 + K_4\Sigma a^4 & \text{if IA up} \\ NK_0 + K_1(0 - Ng) + K_2\Sigma a^2 + K_3\Sigma a^3 + K_4\Sigma a^4 & \text{if IA down} \end{cases} \quad (92)$$

where the sum of the vibration acceleration over an integral number of cycles is theoretically zero, even if a is not known to enough decimal places to have this occur numerically. However, a is known to enough decimal places to adequately calculate the rectified Σa^2, Σa^3, and Σa^4. Note that if the IA were horizontal, Σa^3 would be zero.

Using the Σf data from three of more vibration levels with IA up and from three or more vibration levels with IA down, do a least-squares estimate of K_0, K_1, K_2, K_3, and K_4. The K_2, K_3, and K_4 estimates are of interest, whereas the K_0 and K_1 estimates absorb systematic errors in the experiment and hence are not valid estimates of these parameters.

Repeat the above analysis by using the estimated values of K_2, K_3, and K_4 and the tumble values of K_0 and K_1 to calculate the acceleration a at each sample time. Iterate the analysis until stable estimates of K_2, K_3, and K_4 are obtained.

Note that calibrating accelerometer nonlinear coefficients in a vibration test is possible only if the accelerometer output does not shift across vibration and shock. Also, harmonic distortion in the vibrator producing pure sinusoidal motion could alias into the estimation of the accelerometer nonlinear coefficients.

19.13.6 Analysis of accelerometer centrifuge data

IEEE Std 836 describes the estimation of accelerometer nonlinear model coefficients from precision centrifuge testing at several centrifuge rotation speeds and with IA at various angles to the centrifuge arm. Compensation for such effects as arm stretch and droop is also discussed.

19.14 Database of test results

A computer database of test results for serialized inertial sensors from a given manufacturer can be created. Data should be retrievable by serial number, date, operating hours, data type, etc. Included would be calibration results for scale factor, bias, and other parameters; temperature, magnetic, and other sensitivities; noise parameters and statistics; performance across turn-on, temperature cycle, vibration and shock, and other environments; operating hours, on-off cycles, and failure and repair data; and results from qualification and engineering evaluation tests as well as acceptance and normal operating tests.

Data could even be included from subcomponent tests during manufacture and from calibration tests of sensors in guidance systems.

Queries to the database should allow plots of parameters versus time or operating hours for given sensors or classes of sensors or for when certain conditions are satisfied.

The database could reveal if the sensor requirements for short- and long-term stability over time and for repeatability across environments are being met. The database could also be used for problem solving, such as investigating causes of failures.

20. Geophysics instrumentation

20.1 Gravimeters

An IA vertical accelerometer measures the plumb bob gravity at a site because, when fixed to the earth, it measures the upward reaction of the support to gravity pulling down. (Note that in free-fall, the output of an accelerometer is zero because gravitation accelerates the case and the proof mass equally, and it is the relative motion between the proof mass and the case that creates an accelerometer's output).

The plumb bob gravity includes the gravitational attraction of the earth, the effect of the earth's rotation centripetal acceleration, and lunar-solar earth tide effects. The tidal acceleration is due to the difference between the lunar and solar attractions at a site and at the center of the earth, the variation in the earth's attraction caused by the variation in the distance of the site from the center of the earth due to tidal deformation and ocean tide loading, and the gravitational attraction of the solid earth and ocean tide deformations. The tidal variations in the magnitude and direction of the instantaneous plumb bob gravity acceleration about their averages are approximately $\pm 1.5\times10^{-6}$ m/s^2 and $\pm$ 0.15 µrad, respectively, with a 12.4 h period.

The dynamic range of a conventional accelerometer is often not great enough to measure the plumb bob gravity with sub-ppm accuracy. Also, an accurate measurement of gravity requires accurate values for the accelerometer's scale factor and bias, which are calibrated using plumb bob gravity as a reference in a tumble test or IA up-down test at a site with a known value of gravity (with correction for tidal effects if accuracy warrants).

Therefore, the calibration of the magnitude of the plumb bob gravity at a test site in SI units (namely, meters per square second) requires a special device called a *gravimeter*. The gravity measurement at a site is best accomplished by an organization that specializes in performing such surveys.

One type of gravimeter is an IA-vertically oriented accelerometer with a close-to-local-value-of-gravity bias subtracted in its mechanization so that it very accurately measures variations in gravity with part-per-billion accuracy. If this device is brought from a reference site with a known gravity value in SI units and if its bias does not change significantly in the time that it takes to travel from the reference site, then an absolute measure of the average plumb bob gravity is accomplished after correction for the known lunar-solar earth tide effect. Surveyed referenced sites are usually no more than a few hours by automobile from any given site in the United States.

Another technique for measuring the absolute value of gravity in SI units is to measure the period of a pendulum, which as Galileo discovered depends on the acceleration due to gravity at the site and the length of the pendulum. Special construction of the pendulum allows automatic compensation for the effect of temperature variations on the length of the pendulum, and also the device could be temperature controlled. Special double-ended pendulums allow period measurements in inverted orientations with averaging of the two measurements common mode rejecting a number of error effects. Because the period of the pendulum can be very accurately measured with an atomic clock, accuracy approaching a part per billion is obtained. Again, it is helpful if the pendulum gravimeter is brought from a site with a known value of gravity.

The most accurate absolute measure of gravity in SI units is accomplished with a falling corner cube laser gravimeter. In an evacuated tube about a meter high, a corner cube reflector is allowed to fall, and its trajectory is observed with a laser interferometer. A transparent shield falls ahead of the corner cube to eliminate any residual air friction. Absolute plumb bob gravity measurement accuracy approaching a part per billion is obtained.

In the earth's rotating frame, the forces acting on the falling corner cube are the gravitational attraction of the earth and the tidal attractions of the moon and sun, the centrifugal force due to the earth's rotation centripetal acceleration, and the Coriolis force due to the velocity of the corner cube in the earth's rotating frame. If the site coordinates are accurately known, the rotating frame forces can be accurately compensated. The gravitational and tidal acceleration and corner cube initial conditions are then estimated from fitting the numerically integrated corner cube trajectory to the laser interferometer data. Correction has to be made for the variation in gravitational acceleration along the trajectory due to the earth's gravity gradient of 3.07×10^{-6} m/s^2 per meter. The gravitational acceleration vector estimate thus obtained for a given height at the test site, after correction for the lunar-solar earth tide, has to have subtracted from it the earth's rotation centripetal acceleration vector pointed toward the earth's rotation axis to obtain the average plumb bob gravity acceleration magnitude, which is used as a reference in calibrating accelerometer scale factor (see 19.13.2.1).

The most accurate measure of the variation in gravity acceleration is provided by the superconducting gravimeter, where a liquid-helium-cooled proof mass is levitated by a superconductingly generated magnetic field with a superconducting magnetometer readout. The accuracy of gravity variation measurements approaches the part-per-trillion level.

20.2 Tilt and azimuth motion

A test pier can vary in tilt relative to the local vertical due to temperature variations, ground water effects, etc. This variation can be measured by a tilt meter (see 4.18). The lunar-solar earth tide varies the direction of the local vertical relative to the earth's rotation axis by about ± 0.15 μrad with a 12.4 h period (see 20.1). In the unlikely event that a 10^{-6} °/h gyroscope were being tested, the tidal tilt variation and also the 10^{-7} earth rate precession-nutation of the earth's axis of rotation would have to be compensated for using known models.

The test pier can rotate about the vertical in azimuth due to the same causes involved in tilt variations. Optical techniques can monitor the azimuth motion of a test pad relative to an external target some distance away; but if the external target rotates with the test pad, no information about the absolute rotation of the test pad can thereby be obtained.

Transfer of alignment from star sightings to a test pad is often used to determine the horizontal north direction at the test pad. Continuous monitoring of the star direction can determine the azimuth variation of the horizontal north direction, but is not usually done for reasons of practicality and necessity.

Continuous monitoring of the horizontal north direction can be accomplished by a gyrocompass (see 20.4).

20.3 Seismometers

A seismometer is a vertically oriented open-loop accelerometer with a proof mass on a spring with a low natural frequency. The velocity coil or other pickoff of the motion of the proof mass is the measure of the ground motion acceleration input from about 1 Hz to several hundred hertz. A seismometer can measure the effect of earthquakes thousands of kilometers away.

A nearby earthquake can make the seismometer hit its stops. A force rebalance accelerometer would be required to measure large low-frequency accelerations, and accelerations below 1 Hz, although it could not perform as well as a seismometer for the higher frequency inputs. Soil greatly attenuates high-frequency seismic motions within a few hundred wavelengths, where the speed of seismic waves is of the order of a kilometer per second.

The seismic effects of local cultural activity (such as from automobiles, trucks, trains, or construction activity) depend on the local geologic conditions. Surface vibrations can travel through soil down to bedrock and be reflected back to cause constructive interference at certain frequencies. What frequencies

come through to an inertial sensor on a test table depends on the pier on which the test table rests and the structural resonances in the test table.

20.4 Gyrocompass

A gyrocompass determines the horizontal north direction by detecting the earth's rotation angular velocity vector with a spinning wheel or optical gyroscope with IA horizontal. If the IA of the gyroscope were oriented nearly east or west on a tilt-stabilized platform and if its bias were accurately calibrated and stable, then the gyroscope output would directly measure the offset of IA from the horizontal east-west direction. The horizontal north direction can be inferred from this measurement. When IA is oriented horizontally east-west, the gyroscope output is proportional to the sine of the offset from east-west, whereas when IA is oriented horizontally north-south, the gyroscope output is proportional to the cosine of the offset from north-south.

Gyroscope bias instability prevents absolute measurement of the horizontal north direction with measurements at a single position. However, if every few minutes the IA is alternately put east and west in the horizontal plane by a 180° rotation, then the gyroscope bias can be estimated simultaneously with the offset angle from east-west. All that is required is that the bias be stable for the few minutes of dwell in the east and west orientations. The dwell at each orientation has to be long enough to get adequate quantization resolution from the gyroscope output. The accuracy of the determination of the horizontal north direction depends on the precision of the gyroscope, the accuracy of the level determining system, and the accuracy of the 180° rotation. Arcsecond-level accuracy is obtainable.

The resolution of a torque-rebalance spinning wheel gyroscope is enhanced for the gyrocompass application by having a pulse-torquing scale factor so that full scale is a fraction of an earth rate. When oriented east or west, the loop is captured; and when rotating between east and west, the IA is only momentarily north or south with perhaps the stop being hit.

If necessary, the horizontal north direction of the earth's rotation vector determined by a gyrocompass can be corrected for the 0.3 arcsecond wobble offset of the earth's axis of rotation from the earth's axis of figure published by the national time services and the International Earth Rotation Service (see 20.6).

The horizontal north direction can vary as seen from a test pier because of the azimuth motion of the test pier due to the same causes involved in the tilt motion of the pier, namely, seasonal and daily temperature variations, ground water effects, etc. (See 7.3.)

20.5 Surveying and global positioning system (GPS) positioning

20.5.1 Theodolite triangulation

A theodolite is a telescope on a tripod with the telescope being able to rotate horizontally in azimuth and vertically in elevation. There are readout scales in azimuth and elevation, accurate to about an arcsecond. A plumb bob suspended beneath the tripod and bubble levels in the azimuth rotation plane allow the tripod legs to be adjusted so that the azimuth rotation plane is horizontal.

For almost two centuries, the theodolite has been used to triangulate most of the populated land areas of the world. A tape measure is used to measure the distance between nearby points, and the theodolite is used to measure the relative azimuth and elevation angles between the nearby and distant points. Then trigonometric formulas are used to calculate the distances between the nearby and distant points. Star sightings are also used to determine the geodetic latitude and longitude of fiduciary triangulation points (see 20.6).

The modern theodolite has a laser range finder to measure the distances between distant as well as nearby points and a GPS receiver to measure the GPS coordinates of a point. A surveyor's theodolite for use in

underground tunnels is equipped with a gyrocompass, which uses a gyroscope to sense the direction of the earth's rotation angular velocity vector in the horizontal plane with accuracy approaching an arcsecond.

With such measurement techniques, the coordinates of an inertial sensor test station can be determined relative to an ellipsoid of reference, which coincides closely to the geoid (namely, the mean sea level surface of the earth). Prior to the advent of GPS, an outside agency would have to be hired to survey the test site. The World Geodetic System WGS-84 ellipsoid has the following parameter values for the equatorial radius ρ and the degree of flattening *f*:

$$\rho = 6378.137 \text{ km} \tag{93}$$

$$f = 1/298.257223563 \tag{94}$$

The site coordinates determined relative to this ellipsoid are

- ϕ is geodetic latitude (namely, the angle between normal to the reference ellipsoid at the site and the equatorial plane, positive to the north)
- λ is longitude east of the Greenwich meridian
- h is height above the reference ellipsoid (m)

20.5.2 Relationship between geodetic and geocentric coordinates

Given geodetic coordinates ϕ, h, the geocentric latitude ϕ' and radius R from the center of the earth are determined for $h << \rho$ by (*Astronomical Almanac* [B1])

$$R \sin \phi' = (\rho S + h) \sin \phi \tag{95}$$

$$R \cos \phi' = (\rho C + h) \cos \phi \tag{96}$$

where

$$S \text{ is } (1 - f)^2 C \tag{97}$$

$$C \text{ is } [\cos^2 \phi + (1 - f)^2 \sin^2 \phi]^{-1/2} \tag{98}$$

Given earth-centered, earth-fixed (ECEF) Cartesian coordinates x, y, z with z along the earth's axis of figure toward the north, x in the equatorial plane through the Greenwich meridian, and y completing the right-hand system, the relations between R, λ, ϕ', and ECEF Cartesian coordinates are

$$x = R \cos \lambda \cos \phi' \tag{99}$$

$$y = R \sin \lambda \cos \phi' \tag{100}$$

$$z = R \sin \phi' \tag{101}$$

or conversely

$$R = \sqrt{x^2 + y^2 + z^2} \tag{102}$$

$$\phi' = \arcsin\left(\frac{z}{R}\right) - \frac{\pi}{2} \le \phi' \le \frac{\pi}{2} \tag{103}$$

$$\lambda = \arctan\left(\frac{y}{x}\right) - \pi \le \lambda \le \pi \tag{104}$$

where the quadrant of λ is determined by the signs of x and y.

Given the ECEF Cartesian coordinates, the first guess for the geodetic latitude is

$$\phi_O = \arctan \frac{z}{\sqrt{x^2 + y^2}} \tag{105}$$

Then there is an iteration to determine the geodetic latitude ϕ (*Astronomical Almanac* [B1]):

$$\phi = \arctan \left(\frac{z + \dfrac{(2f - f^2)}{\sqrt{1-(2f - f^2)}} \rho \sin\phi_o}{\sqrt{x^2 + y^2}} \right) \tag{106}$$

If $(\phi - \phi_O)$ is not small enough, then ϕ_O is set equal to ϕ, and the iteration continues.

The height above the reference ellipsoid is (*Astronomical Almanac* [B1])

$$h = \frac{\sqrt{x^2 + y^2}}{\cos\phi} - \frac{\rho}{\sqrt{1 - (2f - f^2)}} \tag{107}$$

20.5.3 GPS positioning

The GPS has 24 operational 11-h-58-min period satellites plus spare satellites in orbit around the earth. The satellites are equipped with cesium and rubidium atomic clocks. The satellites emit radio signals at two frequencies (namely, L1 = 1575.42 MHz and L2 = 1227.6 MHz, more being added) with timing pulses phase encoded (with 180° phase changes) in the carriers. Also phase encoded in the carriers is ephemeris information, from which the motions of the satellites can be derived. The L1 C/A code is for public use and the L1 P(Y) code is encrypted, as is the L2 P(Y) code. Each satellite has a different phase-encoding scheme so that all satellites are able to share the same frequency bands.

The GPS control stations determine the orbits of the GPS satellites and uplink the orbit parameters to the satellites, which broadcast the orbit parameters along with the timing signals.

A GPS receiver at a stationary site or on a moving vehicle measures the time of arrival of the timing signals (which are emitted by all satellites at the same time) relative to its clock. From the time-of-arrival measurements from four or more satellites (or three satellites at the surface of the earth), the GPS receiver clock error and the distances to the satellites are calculated about once a second. Corrections for ionospheric effects are made based on data received on two different frequencies if the receiver has the P(Y) encryption key. Corrections for neutral atmosphere effects are made using a model. From the distances to the satellites and the broadcast satellite ephemeris data, the site or vehicle coordinates are calculated.

The resulting position coordinates have about 15 m accuracy now that selective availability is turned off or if the user has an encryption key. Selective availability is the deliberate degradation of the GPS positioning and timing information and degrades accuracy to about the 100 m level if the encryption key is not available to obtain information from the satellite signal to correct for the deliberate degradation.

Differential GPS positioning has an earth-fixed site broadcast the difference between its measured GPS coordinates and its true site coordinates. A GPS receiver that can receive that information along with the GPS satellite data can apply that correction to its measured coordinates to obtain about 1 m accuracy in positioning, provided the separation between the two sites is no more than a few hundred kilometers.

Commercially available geophysics dual-frequency phase-tracking receivers (independent of encryption) are used to track the phase of the GPS satellite signals from a number of sites simultaneously around the world and on either side of earthquake fault lines. The double difference data between pairs of satellites and pairs of observing sites are processed to simultaneously estimate the GPS satellite orbits better than the broadcast ephemerides and the coordinates of the phase-tracking receivers relative to each other with accuracies approaching a millimeter. Continental drift and the motion across fault lines are easily seen.

20.6 Star sightings

The astronomic latitude and longitude of a site can be determined from star sightings with a telescope oriented relative to the local vertical, such as the telescope on a theodolite (see 20.5.1). Astronomically observed geographic coordinates are referred to the actual local vertical and the earth's rotation axis (*Supplement to Astronomical Almanac* [B4]). Knowing the geodetic coordinates referred to, for example, the WGS-84 ellipsoid from either a triangulation survey or GPS position determination, the deflection of the actual vertical from that of the reference ellipsoid can be determined (up to a minute of arc).

Observations in the northern hemisphere of the star Polaris can be used to determine the north direction pointing in the horizontal plane toward the earth's rotation axis. Published values by the national time services and the International Earth Rotation Service[13] of the position of the pole of rotation of the earth relative to the pole of figure (namely, the earth wobble, about 0.3 arcseconds in magnitude) can correct this north direction to point at the axis of figure, and vice versa.

For almost a century, the earth's wobble was determined from photographic zenith tube measurements, where star images are reflected off a pool of mercury (which defines the local vertical) as they cross the field of view of a vertically oriented telescope. The modern measurement of the earth's wobble is accomplished with long baseline radio interferometer observations of stellar radio sources and laser ranging observations of earth satellites and the laser corner reflectors that were placed on the moon.

The measurement of the north direction from telescope star observations can be transferred with a theodolite along a line of sight from where stars are visible to an inertial sensor test station. Interpretation of inertial sensor test data requires knowledge of the test table earth-centered coordinates, the test table orientation relative to the local vertical and the north direction, and the local value of the acceleration due to gravity.

Gyroscopes care about the horizontal north direction pointing toward the earth's rotation axis, which will vary by ± 0.3 arcsecond over time due to the earth's wobble compared to the north direction determined by a star sighting at a specific time or from a gyrocompass alignment of the test table at a specific time (see 9.3.1 and 20.4). This small correction is ignorable for the testing of many gyroscopes, but it can be corrected for from the published wobble values.

[13]See the Internet Web sites: http://maia.usno.navy.mil and http://www.iers.org.

21. Calibration of test equipment and instrumentation

21.1 Site coordinates, gravity, and components of earth's rotation rate

The geodetic latitude ϕ, longitude λ, and height h above the reference ellipsoid should be measured for each test station in an inertial instrument test laboratory (see 20.5). The plumb bob gravity acceleration at each test station should also be measured (see 20.1) because it is used as a reference for calibrating accelerometer scale factor.

The earth's rotation angular velocity is

$$\omega_e = 7.292115 \times 10^{-5} \text{ rad/s } (15.04106 \text{ °/h}) \quad (108)$$

where the difference between atomic time and universal mean solar time rates affects the value of the earth rate beyond the number of digits given. The earth precession, nutation, wobble, and seasonal variations in length of day affect the value of earth rate two or more places beyond the number of digits given.

The horizontal and vertical components of the earth's rotation angular velocity (used in analyzing gyroscope test data) are

$$\omega_{eh} = \omega_e \cos \phi \quad (109)$$

$$\omega_{ev} = \omega_e \sin \phi \quad (110)$$

21.2 Time and frequency references

All inertial sensor test stations need a frequency reference, which could be provided by a quartz crystal clock to perhaps a part in 10^8 or 10^9 accuracy. However, the best source for an absolute frequency reference is provided by a rubidium or cesium atomic clock with a part in 10^{11} or 10^{12} accuracy, where the SI second is defined to be 9 192 631 770 periods of the radiation from the transition between two hyperfine levels of the ground state of the cesium 133 atom.

The calibration laboratory at a facility could have a cesium or rubidium atomic clock from which a 10 MHz or other such square-wave timing signal could be sent throughout the facility on coaxial cables. This timing signal is used as a reference for timing of data acquisition interrupts, for running counters that measure time per event, and for the input reference to, for example, commercial frequency counters.

This laboratory-wide timing signal can also indicate absolute time of day to perhaps a millisecond by locking to the UTC timing signal broadcast by a national time service radio station. Coordinated universal time (UTC) runs at the atomic time rate. There is a leap second every six months or a year to keep UTC time within 0.9 s of the universal time one (UT1) Greenwich mean solar time determined by the rotation of the earth, where earth rate varies because of tidal friction, seasonal changes in moments of inertia, etc. The value of UT1 – UTC is published by the national time services and is determined by the same astronomical observations that determine the earth wobble (see 20.6).

The start of an inertial sensor test file should always be date and time tagged with a few seconds or even 1 min accuracy being adequate. The interrupt count to the computer then provides a very accurate time for a data point relative to the start of the data file. The time relative to the start plus the absolute time of start gives the absolute time of the data point for making geophysical corrections to the data (such as for the lunar-solar earth tide) and for correlating with events (such as disturbances in data occurring at the start of the work day). Inertial sensor test data are often quietest overnight and on weekends when cultural seismic and electrical disturbances are their smallest.

21.3 Calibration of electrical equipment

Voltmeters, decade resistor boxes, and other such electrical equipment at a test station should be periodically calibrated. The calibration laboratory at a facility would put a date sticker on a piece of equipment when it has been adjusted and calibrated. Management procedures could require, for example, that equipment be recalibrated at least once a year.

The traceability of the calibration of the equipment at a test station relative to absolute standards is important for verifying the quality of the data taken at the test station.

The units of the volt and ohm are defined by the superconducting Josephson junction effect and the quantum Hall effect, respectively. It is unlikely that any but the most sophisticated calibration laboratories would possess these primary standards. Rather, electrochemical cells or Zener diodes calibrated against the absolute voltage standard or resistances calibrated against the absolute resistance standard would be used to calibrate the test equipment in a facility.

21.4 Calibration of temperature-measuring instrumentation

Probes for measuring temperature, such as platinum resistors, thermistors, thermocouples, semiconductor devices, and crystal frequency devices (see 16.3), have manufacturer-supplied tables of the characteristic of the device versus temperature. These tables give resistance, output voltage, or output frequency as functions of temperature.

The determination of the calibration table of a temperature probe device by the manufacturer, or if necessary by the user, is accomplished by inserting the probe into a temperature-controlled environment, such as an oil bath, and measuring, by an accurate standard such as a platinum resistor, the output of the probe as the temperature is varied.

The calibration table will, in general, be a nonlinear function of temperature, although over a small temperature range, the output, such as voltage, can be assumed to be linearly related to temperature, but with a scale factor that varies at different temperature reference points.

21.5 Calibration of other equipment

A tilt meter can be calibrated by placing it on a dividing head, moving the dividing head small angles from horizontal, and comparing the dividing head output with the tilt meter voltage output. In some cases, the resolution of the dividing head input signal can be improved by tilting its axis of rotation until it is nearly vertical.

A dividing head or rate table is leveled relative to the local vertical using precision bubble levels (see 8.4, 9.2.1, and 9.3.1). A rate table is oriented relative to east-west and north-south by transfer of alignment from a star sighting or by use of a gyrocompass (see 9.3.1).

Accelerometer dividing heads and gyroscope rate tables are typically designed and manufactured to maintain accuracy and repeatability over long periods of time with little attention and no scheduled maintenance. However, they are not totally maintenance free and should be checked occasionally, especially if they are moved.

Dividing heads with meshing gear teeth can be degraded by the intrusion of dirt, corrosion, and mechanical dings. Optical dividing head or rotary table readouts can acquire large square-law errors by small shifts of optical discs so that they are no longer concentric; and electromagnetic sensing, which depends on a balance of in-phase and quadrature-phase signals, can degrade by an order of magnitude in repeatability and linearity if its electrical connections contain ground loops.

Detection and compensation of such errors are usually accomplished by autocollimator techniques, most often by the use of polygonal mirrors (see 4.19). Lacking such specialized equipment, useful measurements can often be made by the use of test fixtures with polygonal mounting surfaces.

For accelerometers with greater precision than the dividing head on which they are tested, dual orthogonal accelerometer testing can estimate tumble angles relative to the local vertical simultaneously with estimating accelerometer model coefficients and misalignments (see 8.4 and 19.13.2.1 of this recommended practice and Annex K of IEEE Std 1293-1998). For inertial navigation system testing, the magnitude-squared-of-*g* observable (sum-of-squares of accelerometer outputs) from three nearly orthogonal accelerometers can be used to calibrate accelerometer model coefficients and misalignments in a navigation system tumble test independently of the accuracy with which tumble angles are set by a navigation system's or rate table's gimbals (see 9.4.3 of this recommended practice and K.2.6 of IEEE Std 1293-1998).

Rotation rate tests to calibrate a gyroscope's scale factor can be made independent of the accuracy of a rate table's readout and the alignment of the gyroscope IA relative to the table rotation axis by utilizing integral revolution data where the gyroscope's output is read in synchronism with an integral revolution optical trigger (see 9.3.4).

See 10.5 for the calibration of shock and vibration monitors.

Annex A

(informative)

Bibliography

A.1 General bibliography

[B1] *The Astronomical Almanac,* Annex K. U.S. Naval Observatory, U.S. Government Printing Office, any recent year.

[B2] Bendat, J. S., and Piersol, A. G., *Random Data: Analysis and Measurement Procedures*. New York: Wiley-Interscience, 1971.

[B3] Cramer, H., *Mathematical Methods of Statistics*, ninth printing. Princeton, NJ: Princeton University Press, 1961.

[B4] *Explanatory Supplement to the Astronomical Almanac*. Sausalito, CA: University Science Books, 1992.

[B5] IEEE 100, *The Authoritative Dictionary of IEEE Standards Terms*, 7th ed.[14]

[B6] IEEE Std 488.1, IEEE Standard for Higher Performance Protocol for the Standard Digital Interface for Programmable Instrumentation.

[B7] Jazwinski, A. H., *Stochastic Processes and Filtering Theory*. San Diego, CA: Academic Press, 1970.

[B8] MIL-STD-1553B-1996, Digital Time Division Command/Response Multiplex Data Bus.

[B9] Press, et al., *Numerical Recipes in C; The Art of Scientific Computing*. Cambridge University Press, 1992.

[B10] Rabiner, L. B., and Gold, B., *Theory and Application of Digital Signal Processing.* Englewood Cliffs, NJ: Prentice-Hall, 1975.

[B11] Sargent, D., and Wyman, B. O, "Extraction of Stability Statistic from Integrated Rate Data," *Proceedings of the AIAA Guidance and Control Conference*, Aug. 11−13, 1980.

[B12] Wilkinson, R. H., "High-Fidelity Low-Pass Finite-Impulse-Response Filters," *Journal of Guidance, Control, and Dynamics*, vol. 12, pp. 412−420, 1989.

A.2 Nuclear radiation testing bibliography

[B13] Johnston, A. H., and Hughlock, B.W., "Latch-up in CMOS from Single Particles," *IEEE Trans. Nucl. Sci.*, **NS-38**(6), 1990.

[B14] Johnston, A. H., Lee, C. I., and Rax, B. G., "Enhanced Damage in Bipolar Devices at Low Dose Rates: Very Low Dose Rates," *IEEE Trans. Nucl. Sci.*, **NS-43**(6), 1996.

[14]IEEE publications are available from the Institute of Electrical and Electronic Engineers, 445 Hoes Lane, Piscataway, NJ 08854, USA (http://www.standards.ieee.org).

[B15] Ma, T. P., and Dressendorfer, P. V., eds., "Ionizing Radiation Effects in MOS Devices and Circuits," *Ionizing Radiation Effects in MOS Devices and Circuits*, New York: John Wiley & Sons, 1989.

[B16] Messenger, G. C., and Ash, M. S., *The Effects of Radiation on Electronic Systems*, 2nd ed. New York: Van Nostrand Reinhold, 1992, Chapter 5.

[B17] Shapiro, P., Petersen, E. L., and Adams, Jr., J. H., "Calculation of Cosmic Ray Induced Soft Upsets and Scaling in VLSI Devices," *IEEE Trans. Nucl. Sci.*, NS-29(6), Dec. 1982.